VIRION STIFFNESS AND HUMAN IMMUNODEFICIENCY VIRUS TYPE 1 ENTRY

by

Hongbo Pang

A dissertation submitted to the faculty of
The University of Utah
in partial fulfillment of the requirements for the degree of

Doctor of Philosophy

Department of Biochemistry

The University of Utah

December 2011

The University of Utah Graduate School

STATEMENT OF DISSERTATION APPROVAL

The dissertation of	**Hongbo Pang**	
has been approved by the following supervisory committee members:		
Michael S. Kay	, Chair	07/20/2011
		Date Approved
Sherwood Casjens	, Member	07/20/2011
		Date Approved
Christopher P. Hill	, Member	07/20/2011
		Date Approved
Vicente Planelles	, Member	07/20/2011
		Date Approved
Wesley I. Sundquist	, Member	07/20/2011
		Date Approved
and by	**Christopher P. Hill and Wesley I. Sundquist**	, Chairs of
the Department of	**Biochemistry**	
and by Charles A. Wight, Dean of The Graduate School.		

ABSTRACT

After budding from infected cells, Human Immunodeficiency Virus type 1 (HIV-1) undergoes a maturation process that is required for viral infectivity. In the immature state, the major structural protein of viral particles, Gag, forms a thick protein shell underneath the viral membrane. During maturation, Gag is cleaved by HIV-1 protease and the resulting mature particles have a much thinner membrane-bound protein layer surrounding a conical core (capsid), which is a dramatic morphological change from the immature state. Employing atomic force microscopy (AFM), Itay Rousso's group together with ours previously discovered a dramatic change in particle stiffness during HIV-1 maturation mediated by the cytoplasmic tail (CT) of HIV-1's envelope protein (Env). A correlation between high particle stiffness and weak viral entry activity led us to investigate whether viral particle stiffness directly regulates viral entry activity.

First, after observing that standard viral purification conditions perturb virion structure and stiffness, we determined new purification conditions that preserve both. Next, we showed that CT alone is sufficient to regulate viral particle stiffness. This observation allowed us to independently increase particle stiffness using a construct that lacks the Env ectodomain and thus has no entry ability itself. Using this system, we showed that particle stiffness directly regulates the entry activity of the Env proteins of both HIV-1 and the unrelated Vesicular Stomatatis Virus (VSV). These results suggest a general role for particle stiffness in the regulation of viral entry, linking viral physical properties and biological functions. Mutagenesis studies reveal the important domains within CT or Gag

that regulate viral entry activity. Employing an Env mutant with cleavable CT, we obtained preliminary data about the timing of CT's regulation of particle stiffness. Taken together, these studies improve our understanding of viral structure and function during the viral lifecycle and suggest potential novel inhibitory strategies.

TABLE OF CONTENTS

LIST OF FIGURES

ACKNOWLEDGEMENTS

Many individuals have extensively helped me achieve this important goal of my life, and I owe them a debt of gratitude.

First, I thank my parents for their unending support and love. They are my first and the greatest mentors that have shaped who I am today.

Second, I thank all my professors and friends in Peking University. Peking University provided me one of the best undergraduate educations in biology and many other fields, and instilled in me the confidence and the courage to explore the world of the unknown. Many people have generously helped me along the path, and thanks to their help, I could come abroad to pursue a scientific career.

Third, I thank Kay lab members. Especially, Dr. Debbie Eckert and two former Kay lab members, Brett Welch and Sunghwan Kim, have taught me almost all the basic research techniques, and extensively helped me through the beginning of graduate school. I also thank my friends from the biochemistry department and MB/BC program, who have helped me on experiments and shared happy moments with me.

Fourth, I thank my committee members, Sherwood Casjens, Chris Hill, Vicente Planelles and Wes Sundquist. They have been very responsible and supportive of me with helpful advice on my projects, the use of their personal connections to help my projects and postdoc application, and good letters for my application to fellowship and postdoc labs.

Fifth, I am very grateful to my mentor, Michael Kay. He is one of the nicest people I have ever known, and has always been patient, willing to help, inspiring and supportive. Thanks to his guidance, I can earn this Ph.D. degree from very limited experience and sense about biological research. I could have not received a better education in any other lab.

Finally, I thank my beautiful and loving fiancé, Yan Zhou (Zoe). She is my greatest accomplishment in the past six years. For her, I strive to be continually better.

CHAPTER 1

INTRODUCTION TO HIV-1 STRUCTURE AND ENTRY

The HIV Pandemic

Globally, an estimated 33 million people are currently living with Acquired Immunodeficiency Syndrome (AIDS), and approximately 2.6 million new infection cases and 2 million deaths were reported in 2009 (*1*). AIDS is caused by the human immunodeficiency virus (HIV), which spreads via blood or sexual transmission. After infection, HIV specifically attacks and destroys the host immune system and leaves patients vulnerable to various opportunistic infections.

Over the past 20+ years, increased HIV prevention efforts, new treatments and improved access to treatment have lowered the number of new HIV infection cases and AIDS-related deaths (*1*). The currently recommended treatment, known as highly active antiretroviral therapy (HAART), uses a "cocktail" of anti-HIV drugs to target multiple events in the HIV lifecycle (*8*). However, due to HIV's high mutation rate, strains with resistance to all available drugs are an emerging threat (*9, 10*). Meanwhile, due to the integration of the viral genome into host genome and viral latency, the patients whose disease is under control still require medication for the rest of their lives to suppress the

infection (*11*). Therefore, additional research on HIV is still urgently needed to develop new strategies for more effective prevention and treatment.

HIV-1 Virion and Lifecycle

HIV belongs to the family *Retroviridae* and the genus *Lentivirus*. HIV can be divided into two major types, HIV type 1 (HIV-1) and type 2 (HIV-2). HIV-1 is the most common and pathogenic group (*12, 13*), and is the focus of this thesis. The genetic material of each virion includes two copies of single-stranded, positive-sense, nonsegmented RNA, which is ~9 kilobases (kb). HIV-1's genome encodes nine open reading frames (Fig.1-1). The major structural component is the Gag polyprotein, which is proteolytically processed by HIV-1 protease (PR) during maturation into structural proteins MA (forms the matrix), CA (forms the capsid), NC (forms the nucleocapsid), and nonstructural proteins p1, p2, p6. Envelope (Env) polyprotein, which mediates viral entry, is initially synthesized as a precursor protein (gp160) and then proteolytically processed into gp120 (surface subunit) and gp41 (transmembrane subunit). The Pol polyprotein is another precursor protein which is cleaved into PR (protease), RT (reverse transcriptase) and IN (integrase). Other viral proteins include the regulatory proteins Tat and Rev, and the accessory proteins Nef, Vpr, Vif and Vpu (*14*).

The lifecycle of HIV-1 can be roughly divided into early and late events (Fig.1-2) (*15*). After recognizing the host cell surface receptors, Env mediates the fusion between the viral and host membranes. After entry into the cell, the virion undergoes an uncoating

process to release its genetic material and incorporated enzymes into the cytoplasm. The ssRNA genome is converted into dsDNA by RT, which then enters the nucleus and is integrated into the host genome by IN. Host cell machinery replicates the viral genome and translates viral genes. The viral RNA genome and proteins assemble at the plasma membrane and bud out as immature HIV-1 particles. In the extracellular environment, HIV-1 undergoes a maturation process to become infectious and then enters the next target cell.

HIV-1 Maturation

HIV-1, along with almost all other retroviruses (except spumaviruses), undergoes a maturation process after budding out of infected cells (*4, 15*). Maturation is characterized by PR cleavage of Gag into individual Gag proteins. The individual Gag proteins and their relative positions are shown in Fig. 1-3 A. Nascent HIV-1 particles bud out as immature virions (Fig. 1-3 B, left model) (*15*). The outer surface of the viral particle is a lipid bilayer membrane that is derived from the infected cell to anchor Env and Gag proteins. Gag polymerizes underneath the lipid membrane forming a protein shell. During maturation, the morphology of viral particles is changed dramatically by PR cleavage of Gag. After maturation, only MA still associates with the lipid membrane, and CA forms a conical capsid that houses NC-RNA complex (Fig. 1-3 B, right model). The detailed initial timing for PR cleavage of Gag is still unclear, but it is commonly accepted that the immature morphology remains at least until viral release (*15*).

The most striking feature of maturation is the dramatic morphological change of viral structure, which can be visualized by electron microscopy (EM) (Fig. 1-3 B, bottom images). The Gag shell of immature virions is roughly spherical and thick (~17-19 nm), surrounding an electron-lucent core (Fig. 1-3 B, left bottom EM image). In mature virions, the protein layer associated with viral membrane is composed of only MA and is much thinner (~5 nm). CA condenses to form an electron-dense, conical capsid core at the center of the virions, which houses NC-coated viral genome (Fig. 1-3 B, right bottom EM image) (*16*).

Maturation plays an essential role during the HIV-1 lifecycle. Defects in PR activity or PR cleavage sites block maturation and completely abolish HIV-1 infectivity (*15*). Several groups including ours have reported that immature viruses have much lower entry activity than mature ones (*4, 17, 18*). This feature may help prevent reentry into infected cells, but more detailed studies are needed to improve our understanding of the biological relevance of maturation in the viral lifecycle.

Gag and PR Cleavage

As the major structural protein, up to 5,000 Gag molecules are estimated to polymerize at the plasma membrane to form a single immature HIV-1 particle (*19*). Expression of Gag is sufficient to produce viral-like particles without other viral proteins or viral genome (*20-22*). MA, CA and NC are highly conserved across different strains (*23, 24*). p6 is a small Pro-rich domain located at the C-terminus of Gag and interacts

with host ESCRT (Endosomal Sorting Complex Required for Transportation) machinery to facilitate viral release (*23, 25-28*). The function of two spacer peptides, p1 and p2 (or sp2 and sp1, respectively), is relatively unknown, although they appear to help regulate the stepwise process of virion maturation and capsid assembly (*29-31*).

Due to a ribosomal frameshift that occurs at a frequency of 5-10% during Gag translation, each immature virion is estimated to contain ~250 molecules of Gag-Pol (*19*). Gag-Pol precursors are targeted to plasma membrane and multimerize together with Gag molecules to drive viral budding (*23, 28*). The exact mechanism to activate PR activity is poorly defined, but may be attributed to increasing concentration of Gag-Pol at assembly sites or a more active switch (*32*). Activated PR begins to process Gag-Pol and Gag polyproteins by transcleavage of each cleavage site. The cleavage rate at each site is different, resulting in a sequential order of cleavage. Sequential cleavage was observed in infected cells represented by the transient appearance of processed intermediates, and was also shown using an *in vitro* Gag processing assay (*29, 30, 33*). The *in vitro* assay at pH 7 showed the order of cleavage as p2/NC > p1/p6 ~ MA/CA > NC/p1 > CA/p2, with a maximal difference in cleavage rate of 400-fold (*30, 31*). In contrast, at pH 5 which is near the optimal condition for PR activity, only a ~15-fold difference in cleavage rate was observed. These results suggest that cleavage site sequences are optimized for the maximal cleavage rate difference at physiological pH. Gag mutants with one or more PR cleavage sites mutated have been constructed, but their effects on PR cleavage rate have not been investigated (*18*).

MA and Membrane Targeting of Gag

Located at the N-terminus of Gag, a major function of MA is to direct Gag to the assembly sites at the plasma membrane (*23*). During Gag translation, the N-terminal methionine of MA is replaced by the saturated, 14-carbon fatty acid (myristic acid), which is required for virus assembly and Gag targeting to plasma membrane (*16, 20, 34*). Meanwhile, a cluster of conserved basic residues near the N-terminus of MA is also implicated in membrane binding of Gag (*35, 36*). Therefore, it has been proposed that the membrane targeting of MA is fulfilled by insertion of the N-terminal myristyl group into the lipid bilayer and binding of the positively charged residues to acidic phospholipids at the inner face of the lipid bilayer (*24, 35-38*). This model is supported by structural study of the HIV-1 MA protein (*38*). Studies of other retroviral MA structures also showed that MA exposes positively charged side chains that may function to interact with the inner face of lipid bilayer (*39-41*).

Besides the N-terminal domain of MA, the rest of MA and other Gag proteins are also involved in modulation of Gag's membrane binding. Mutations in the middle or near the C-terminus of MA can recover the defect of Gag membrane binding caused by mutations at the N-terminus of MA (*42*). MA itself is found to bind with membrane less efficiently and exclusively than intact Gag, and deletions in the C-terminus of MA enhance membrane binding (*43, 44*). The myristyl group can adopt two conformations: exposed and hidden (*44, 45*). Based on these observations, a "myristyl switch" model of membrane binding has been proposed in which the myristyl moiety is highly exposed in

unprocessed Gag precursor and thus free to bind with the plasma membrane; after separation from downstream Gag proteins, the MA C-terminus sequesters its N-terminal myristyl group, which weakens membrane binding.

This "myristyl switch" model is further supported by a recent NMR (Nuclear Magnetic Resonance) study of MA bound to a plasma membrane component, phosphatidylinositol (PI) 4,5-bisphosphate ($PI(4,5)P_2$) (*46*). $PI(4,5)P_2$ usually concentrates in the inner face of the lipid raft, which is enriched in sphingolipids and cholesterol (*47, 48*). Several observations suggest that HIV-1 mainly assembles and buds at lipid rafts (*28, 49*), and the specific targeting of Gag at assembly sites depends on $PI(4,5)P_2$ (*50*). In an NMR study, Saad et al. show that $PI(4,5)P_2$ directly binds with myristoylated MA, inducing a conformational change that triggers myristate exposure (*46*). Repositioning of several residues within the myristyl group upon $PI(4,5)P_2$ binding makes additional hydrophobic and electrostatic interactions, which enhances the binding affinity between MA and $PI(4,5)P_2$. This study shows the triggered exposure of MA's myristyl group and the importance of myristyl exposure for membrane binding. It also provides a structural basis for specific targeting of Gag to the assembly sites.

Furthermore, the myristyl group may function to stabilize MA oligomerization, which may be related to the membrane binding. NMR studies show that nonmyristoylated MA adopts a monomeric structure at up to millimolar concentration, while x-ray diffraction study suggests that nonmyristoylated MA crystallizes as a trimer (*37, 38, 51*). Wu et al. show that at a concentration of >100 μM, nonmyristoylated MA stays as a monomer

while myristoylated MA predominately exists as a trimer (*52*). They further show that myristoylation promotes thermal stability of the MA oligomer in solution (*52*). Considering that the myristyl group may become partially hidden after maturation, one can speculate that PR cleavage of Gag weakens the matrix layer stability, which may lower the energy barrier for membrane fusion.

Another important function of MA is to interact with Env CT and facilitate Env's incorporation into virions, which will be discussed in more detail below.

CA, NC and Gag Assembly

CA is believed to be the major driving force of Gag polymerization during viral assembly and forms the conical protein shell (capsid) surrounding the viral RNA genome and associated proteins in mature virions. CA also plays an important role in early postentry events, such as uncoating (*23*). The CA protein contains two domains: an N-terminal domain (NTD) that is composed of seven α-helixes, two β-hairpins and an exposed loop; and a C-terminal domain (CTD) that is also highly helical (*23*).

Another Gag structural protein, NC, mainly functions in RNA binding and encapsidation (*23*). NC contains two zinc finger motifs similar to the motifs found in many DNA binding proteins, and these motifs are highly conserved among retroviruses (*53*). However, NC has been also implicated in other aspects of the viral lifecycle, including Gag-Gag interaction, RNA dimerization, and reverse transcription (*23*).

Once transported to assembly sites, Gag polymerizes to form a new viral particle. The

polymerization of Gag molecules is driven by lateral interactions throughout the whole Gag polyprotein, although some specific regions are particularly important. MA mainly functions to target Gag molecules to the assembly sites, which tethers Gag together and may provide the initial driving force for multimerization. MA may also play a role in Gag-Gag multimerization (*54*). However, Gag can assemble to form immature particles without MA, leading to the current idea that MA is largely dispensable for Gag-Gag interactions (*55*). MA and CA_{NTD} are connected by a flexible linker, and MA conformation does not change when tethered to CA_{NTD} (*56*). This observation supports the idea that MA is rather flexible and isolated from downstream Gag interactions. Similarly, p6 does not contribute much to Gag-Gag contacts (*24*). In contrast, CA, NC and the spacer peptide between them, p2, are believed to make critical contacts for Gag assembly (*24*).

Mutational studies on CA have defined specific sequences important for viral assembly. CA_{CTD} has been suggested by mutational and structural studies to play an important role in Gag-Gag multimerization and viral assembly (*57-60*). A minimal Gag construct containing only CA_{CTD} and p2 can support efficient particle production (*61*). CA_{CTD} contains the only region in Gag that is highly conserved among different genera of retroviruses: the major homology region (MHR) (*62*). CA dimerizes in solution, and CA_{CTD} constructs have been crystallized as dimmers (*57, 63*). Mutations disrupting these intermolecular interactions reduce Gag dimerization *in vitro* and inhibit formation of immature particles (*64, 65*). These results support that CA_{CTD} is the driving force for CA

dimerization and Gag assembly. CA is also required for incorporation of Gag-Pol precursor into virions (*66-68*). Biochemical studies also identify two regions in CA_{NTD} important for immature virion formation (*65, 69, 70*). A model has been proposed that CA_{NTD} provides symmetric intermolecular contacts to stabilize the Gag lattice, supported by structural and mutational studies (*71-73*).

Studies of HIV-1 NC mutants also show the important role of this domain in viral assembly. The N-terminal basic residues of NC seem to be particularly important in this regard (*74-76*), and these residues promote intracellular Gag assembly in an RNA-dependent way (*75*). These results suggest that NC may promote Gag assembly via its interaction with RNA to tether Gag molecules together, and its basic residues may also provide additional Gag-Gag contacts. Replacement of NC by a protein that can form interprotein contacts permits efficient viral assembly even without RNA (*76*). NC also appears to play a role in the tight packing of Gag in immature virions, based on the observation that deletions in NC lead to the production of viral particles with lighter density (*77*). This density alteration is not attributed to the basic residues (*78*).

Two recent electron cryo-microscopy (cryoEM) studies on immature HIV-1 provide more details on the organization of immature Gag lattice. In both studies, the Gag lattice is seen to be composed of close-packed, cup-shaped hexamers (*71, 79*). CA and p2 layers seem to form the walls and bottom of the cup-shaped hexamer, respectively (*71*). CA_{CTD} makes both inter- and intrahexamer interactions in the immature Gag lattice (*71*). This observation is consistent with previous reports that the region from the CA C-terminus to

p2 is essential for immature particle formation (*80, 81*). The N-terminal MA layer lacks the hexagonal order, although it has been shown that MA proteins can form both trimers (*38, 46*) and hexamers (*82*) *in vitro*. On the other end, NC and viral RNA form a disordered layer (*79*). Although incompleteness of Gag lattice is seen in both studies, we have shown that this incompleteness is exaggerated by pelleting of viral particles through a sucrose cushion (*83*) (Chapter 2).

Structural studies of the Gag lattice also reveal an interesting change of its packing pattern during maturation. CA protein can assemble *in vitro* into two distinct hexagonal arrangements: tightly and loosely packed (*84*). The tightly packed arrangement is similar to the Gag lattice in the immature virions, where the hexamer-to-hexamer spacing is in the range of 65-80 Å (*19*). On the other hand, the loosely packed arrangement corresponds more to the organization of the mature capsid core, where the interhexamer spacing is ~95-110 Å (*85, 86*). A more intact Gag construct, which includes MA, CA, p2 and NC, assembles *in vitro* into hexamer rings with a spacing of 79.7Å (*87*). These results suggest that the presence of other Gag domains in immature virions makes CA more compatible with a tightly packed arrangement, and PR processing of Gag during maturation yields a more loosely packed capsid core. The tight-to-loose packing change may represent a strategy of viral structure rearrangement to lower the energy barrier for better entry and fusion, and may be accompanied by changes in viral physical properties.

Env Ectodomain and HIV-1 Entry

After maturation in the extracellular environment, HIV-1 virions circulate until entry into the next target cell. HIV-1 is commonly thought to enter target cells by membrane fusion at the plasma membrane, though a recent study claims endocytosis as the main entry route (*88*). The viral envelope (Env) glycoproteins, gp120 and gp41, are necessary and sufficient to mediate viral entry (*89*). gp120 and gp41 are initially synthesized as a precursor protein, gp160. Following cotranslational glycosylation and oligomerization, gp160 is cleaved in the Golgi complex by a cellular protease, Furin, after Arg508-Glu-Lys-Arg511 to produce gp120 and gp41 (*90, 91*). This processing is necessary to activate Env for viral entry. HIV-1 Env has been reported to be transported to the plasma membrane via intracellular CTLA-4-mediated secretory granules, although the detailed mechanism is still unclear (*28*). The gp120-gp41 complex forms trimeric spikes on the viral surface (*92*). gp41 contains a transmembrane (TM) domain that anchor Env on the viral surface, and gp120 interacts noncovalently with gp41.

gp120 mediates target cell recognition by interacting with cellular receptor and coreceptors. CD4 and a seven-transmembrane, G protein-coupled chemokine receptor (typically CCR5 or CXCR4) on target cells, such as CD4+ T cells or macrophages, have been identified as the receptor and coreceptor, respectively (*89*). gp41 provides the driving force for membrane fusion via a series of conformational changes. The ectodomain of gp41 includes an N-terminal fusion peptide, which inserts into the host cell membrane during entry, and two helical heptad repeat regions termed the N- and

C-peptides (Fig. 1-4 A). There is a short linker region between the N- and C-peptide regions containing an intramolecular disulfide bond, which we refer to as the DSL (disulfide loop) region. Several groups have solved the structure of the gp41 ectodomain in its most stable postfusion state (*5, 93-95*). In this structure, three N-peptides form a trimeric coiled coil (N-trimer) and three C-peptides bind antiparallel into the grooves of the N-trimer to form the postfusion structure (six-helix bundle or trimer-of-hairpins).

The current model of HIV-1 entry is described as follows (Fig. 1-4 B). In the native state before entry, most of the gp41 ectodomain, including the fusion peptide, is covered by gp120. The first step of viral entry is the encounter of gp120 and CD4, which induces further conformational changes in gp120 that expose a coreceptor binding site. Moreover, CD4 binding also induces a conformational change in gp41 leading to the formation and partial exposure of the N-trimer region (prehairpin intermediate state). This model is supported by the fact that exogenous C-peptide can transiently access and bind to the gp41 N-trimer region after CD4 binding (*96, 97*). Subsequent coreceptor binding with gp120 may induce further exposure of the N-trimer region. Eventually, C-peptides bend over and bind with the N-trimer to form a six-helix bundle, which drives host cell and viral membranes together to achieve fusion.

The gp41 postfusion structure is its most stable state. The existence of the prehairpin intermediate state suggests that gp41 must have a metastable prefusogenic state in which N- and C-peptide are separated. This metastable structure is very likely to be stabilized by the gp41-gp120 interaction, which is eventually disrupted by CD4 and coreceptor binding,

leading to formation of the six-helix bundle structure. The prefusogenic intermediate state of gp41 has been an attractive target for HIV-1 entry inhibitor and neutralizing antibody development. A peptide derived from the C-peptide sequence has been approved for AIDS treatment (Fuzeon). Several D-peptide inhibitors specifically targeting a conserved hydrophobic pocket region on the N-trimer have been developed by the Kay lab (*7, 98*). Vaccine development targeting the N-trimer, on the other hand, has been challenging partly due to a steric restraint caused by associated gp120. Detailed structural information about the gp41-gp120 complex and the prefusogenic state is urgently needed. In the intermediate state, the N- and C-peptides must be separated from each other to prevent formation of a six-helix bundle, and separation is most likely attributed to gp120. We have identified the gp41 DSL plus the N-terminal C-peptide region (DSL49) as being the most critical for interaction with gp120, while the N-peptide region is dispensable (*99*) (Appendix A). DSL49, which cannot form a six-helix bundle, may provide an important tool for obtaining the gp41 prefusogenic structure (in complex with gp120).

Env CT

HIV-1 together with other lentiviruses has a relatively long CT including ~150 amino acids (aa), which extends into the interior of the virion and makes contacts with MA (*4, 100, 101*). In contrast, other retroviruses have a much shorter CT with ~20-30 aa (*100, 101*). CT has been shown to be critical for Env incorporation in primary cell types that serve as natural targets of HIV-1 (*100*). However, little is known about the detailed role of

CT in the viral lifecycle.

Currently, there is no high-resolution structural data available for the Env CT domain, but several structural features have been predicted and their functions implicated by mutagenesis studies (Fig. 1-5). Although CT has no typical membrane binding sequences, three highly conserved amphipathic α-helical secondary structures have been proposed to bind with the membrane (*102*). Peptides with these segment sequences have also been shown to decrease bilayer stability, alter membrane permeability, and cause cytolytic effects, leading to the naming of these segments as "lentivirus lytic peptides" (LLP-1, LLP-2 and LLP-3) (*103-105*). Among these, LLP-1 has been further shown to be important for lipid raft association of Env (*102*).

CT is responsible for rapid internalization of HIV-1 Env, which reduces the susceptibility of infected cells to the host immune system. A tyrosine-based YxxL endocytic motif at the N-terminus of CT interacts with the μ2 chain of the AP-2 clathrin complexes to induce Env internalization (*106-109*). A dileucine motif at the C-terminus of CT is also responsible for Env internalization through interacting with clathrin and AP-2 (*110*). This dileucine motif also interacts with AP-1 to affect Env expression level on the cell surface and subcellular localization (*111*). Two inhibitory sequences around one of CT's palmitylated Cys (C762, HXB2 numbering) are also reported to lower the surface Env level (*112*). A diaromatic motif (YW801) is involved in interactions with cellular protein TIP47, which may function to target Env to the Golgi network (*113*). HIV-1 Env is concentrated in lipid rafts on infected cell membranes. Two palmitylated

Cys residues have been shown to be important for Env localization to lipid raft regions and viral infectivity (*114-116*).

Env can interact with Gag intracellularly, but can only be assembled onto viral particles on the plasma membrane (*28*). Several lines of genetic and biochemical evidence have established that Env CT interacts with MA, and this interaction is important for Env incorporation. First, mutations in MA inhibit WT Env incorportion into virions, which can be restored by truncation of CT (*117-120*). Similarly, a single amino acid change in MA can reverse the incorporation defect caused by a small deletion in CT domain (*121*). Second, Env expression is essential to direct Gag assembly at the basolateral surface of polarized epithelial cells, and mutations in MA or truncation in CT eliminate this polarized budding (*107, 122, 123*). Third, coexpression with Gag inhibits the rapid internalization of Env mediated by endocytotic motif located within CT (*124*). Fourth, a detergent-resistant interaction was reported between Env and Gag, which is dependent on CT and MA (*125, 126*). Finally, a direct interaction between CT and MA was reported *in vitro* using recombinant CT and MA proteins (*127*).

Besides interacting with other viral components and host proteins, CT can also affect the Env ectodomain conformation ("inside-out" signaling). Identified from screening CD4-independent variants, an Env mutant bearing a 27 aa C-terminal CT truncation was shown to expose highly conserved gp120 domains involved in both CD4 and coreceptor binding, induce antigenic changes in the gp41 ectodomain and increase sensitivity to neutralizing antibodies (*128*). CT truncations proximal to LLP2, which is located near the

middle of CT, show a similar effect increasing fusion efficiency and exposing CD4-induced epitopes (*129*). In contrast, a point mutation in LLP2 can render viruses resistant to broadly neutralizing antibodies, while the receptor binding and viral infectivity remain unchanged (*130*). These results suggest that CT alteration can induce conformational changes in the gp41 ectodomain and gp120 that affect viral fusion and sensitivity to the host immune response, though the mechanism remains unclear.

Physical Properties of Viruses

During the viral lifecycle, several potentially conflicting demands must be met, such as spontaneous assembly during budding, durability in the extracellular environment, efficient membrane fusion and disassembly after entry into a target cell. Therefore, we speculate that the virus may have different physical properties at distinct phases of its lifecycle. During maturation of retroviruses, the internal structural organization changes dramatically while the overall size of viral particles does not. The molecular and morphological change during maturation has been well characterized by biochemical and various EM imaging techniques (*15*). However, little is known about the impact of maturation on viral physical properties.

AFM has been most commonly used in biology as a tool to obtain high-resolution topographical images in various samples including HIV-1. Recently, the Rousso group has measured the spring constants for two retroviruses, Murine Moloney Leukemia Virus (MLV) and HIV-1, to determine viral particle stiffness (*4, 131*). The uniqueness of these

studies is that compared to EM, which requires sample fixation, AFM can measure unfixed viral particles. Using AFM, several groups also reported mechanical property measurements on capsids of several other viruses, e.g. bacteriophage (*132*), cowpea chlorotic mottle virus (*133*) and minute virus (*134*). In MLV, AFM reveals a clear difference between mature and immature MLV particles, in which immature particles are two-fold stiffer than mature ones (*131*).

In contrast, for HIV-1, immature virions are ~14-fold stiffer than mature ones, a much more dramatic change than observed with MLV that we dubbed the "stiffness switch" (*4*). Further investigation of Env's role in this stiffness change reveals that deletion of Env, or only CT, dramatically softens immature particles to near the mature level, showing that Env CT is required for the stiffness switch. Since viral entry is the next step after maturation, we speculate that the stiffness switch may have a role in regulating viral entry activity. In agreement with previous reports, we observed that immature HIV-1 enters target cells ~10-fold less efficiently than mature HIV-1, and deletion of CT in immature virions largely restores their entry activity to the mature level. These results suggest an inverse correlation between particle stiffness and viral entry activity. However, truncation of CT can also induce conformational changes on the Env ectodomain, which could alter viral entry activity. Therefore, a cause and effect relationship between particle stiffness and viral entry cannot be proven by the above observation. Further studies are needed to elucidate the nature of viral particle stiffness, and its biological relevance during the HIV-1 lifecycle.

Summary of The Dissertation

Chapter 2

Recent cyroEM studies of the immature Gag lattice show incorporation defects in the forms of gaps of various sizes (~40%-70% of Gag lattice completeness) (*71*, *79*). All these immature virions were purified by pelleting through a sucrose cushion, which has been a standard method in HIV-1 studies. We asked whether sucrose purification is damaging the immature Gag shell by osmotic shock or the mechanical force during centrifugation, leading to large observed gaps. We previously reported that immature HIV-1 has much higher particle stiffness than mature ones, which argues against the idea that the immature Gag lattice has large gaps (*4*). Therefore, we wonder whether a gentler method of purification method would preserve the stiffness of immature HIV-1 to a higher degree. A comparison of morphology and stiffness was conducted between viruses purified by sucrose or Iodixanol, a nonionic density gradient media also known as OptiPrep. Viruses purified by OptiPrep were found to have a much higher degree of completeness in Gag lattice and particle stiffness, suggesting that purification method does affect the integrity of the immature Gag shell. I played a supporting role in this study, which was published in the Journal of Virological Methods in 2010.

Chapter 3

In this chapter, we aimed to prove the cause-effect relationship between particle stiffness and viral entry. To achieve this goal, it was necessary to separate the entry and

stiffness properties of HIV-1 Env. First, we showed that CT alone is sufficient to regulate the particle stiffness of immature HIV-1. Using a CT-containing construct that has no viral entry activity due to lack of the Env ectodomain, we were able to independently stiffen the immature particles. Increasing particle stiffness was shown to reduce viral entry mediated by the Env proteins of different HIV-1 strains and VSV (Vesicular Stomatitis Virus), which is unrelated to HIV-1 and enters the target cells via endocytosis. These results support the hypothesis that particle stiffness directly regulates viral entry, regardless of viral type or entry route. In this work, I did everything except for the AFM measurement, and it is nearly ready to be submitted pending AFM control measurements.

Chapter 4

In this chapter, we aimed to identify the critical factors that regulate viral particle stiffness and clarify how particle stiffness is regulated. Both CT and Gag processing have been suggested to affect the particle stiffness change during HIV-1 maturation (*4*). A series of CT truncation mutants and partially maturated Gag mutants were employed to identify the critical subdomains important for particle stiffness. So far, a region near the N-terminus of CT was shown to be important for suppression of immature viral entry. In agreement with a previous report, we also found that this region is critical for Env-Gag interaction (*6*). Studies with Gag mutants also showed that the integrity of Gag structural domains is essential to suppress viral entry.

We propose two models for how CT might regulate particle stiffness: first, CT

functions during viral assembly to seed the initial formation of the Gag shell; second, CT functions to stabilize the Gag shell by its interaction with Gag. To distinguish these two models, the timing of CT's effect on stiffening immature particles needed to be defined. Using an Env mutant with a CT that could be cleaved by HIV-1 PR, we were able to control the CT cleavage time so that it followed viral budding. Initial viral entry measurement showed that immature particles in which CT was cleaved after budding had similar entry activities that were similar to immature WT, suggesting that CT is only important for enhancing particle stiffness during assembly. I have finished the majority of work that I am responsible for, and AFM measurement of all these viruses is pending.

Appendix A

During HIV-1 entry, CD4 and coreceptor binding induce a series of conformational changes to gp120. gp120 then transmits these entry signals to gp41 via their interaction, leading to exposure of gp41 and eventually formation of the six-helix bundle structure that drives membrane fusion. However, the interface of the gp120-gp41 complex is poorly understood, slowing our understanding of the HIV-1 entry process and development of novel entry inhibitors. Here, we identified a critical interface of the gp120-gp41 complex that is required for stabilizing the prehairpin intermediate gp41 conformation. This interaction needs to be disrupted in order to form the six-helix bundle. This study identifies the critical regions in gp120 and gp41 that mediate activation of gp41 during entry. I played a supporting role in isolation of the minimal DSL region for

gp120 binding, which was published in the Journal of Molecular Biology in 2008.

Appendix B

After maturation, HIV-1 virions stay in the extracellular environment until entry into the next target cell. The durability of virions is little studied except for the fact that mature HIV-1 infectivity decays rapidly. In this study, we discovered that immature HIV-1 can preserve its entry activity much better than mature virions. Deletion of CT or PR cleavage of Gag disrupts this stability of immature viral entry activity. Stiffening of immature ΔCT virions does not restore extracellular stability. Preliminary studies reveal that neither gp120 incorporation level nor CD4 binding ability changes with deletion of CT in the immature state. The underlying mechanism for extracellular stability change of viral entry activity remains to be further defined.

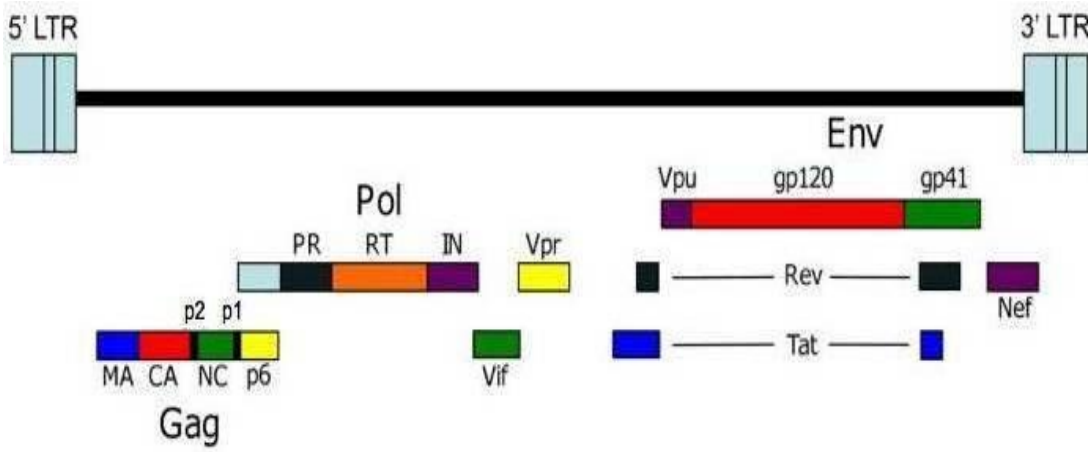

Fig 1-1. Organization of the HIV-1 genome.
Details are provided in the text. On the 5' and 3' ends of genome are two long terminal repeats (LTRs). Figure is adapted from (*2*).

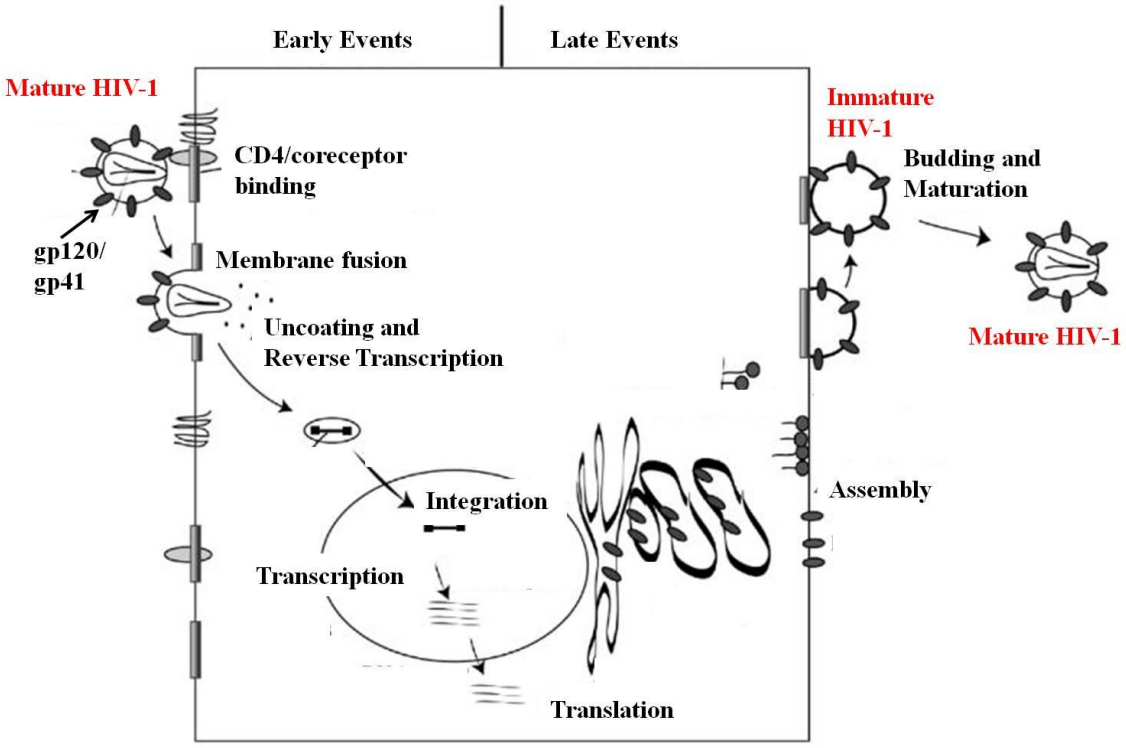

Fig 1-2. Schematic representation of the HIV-1 life cycle.
Details are provided in the text. The figure is adapted from (*3*)

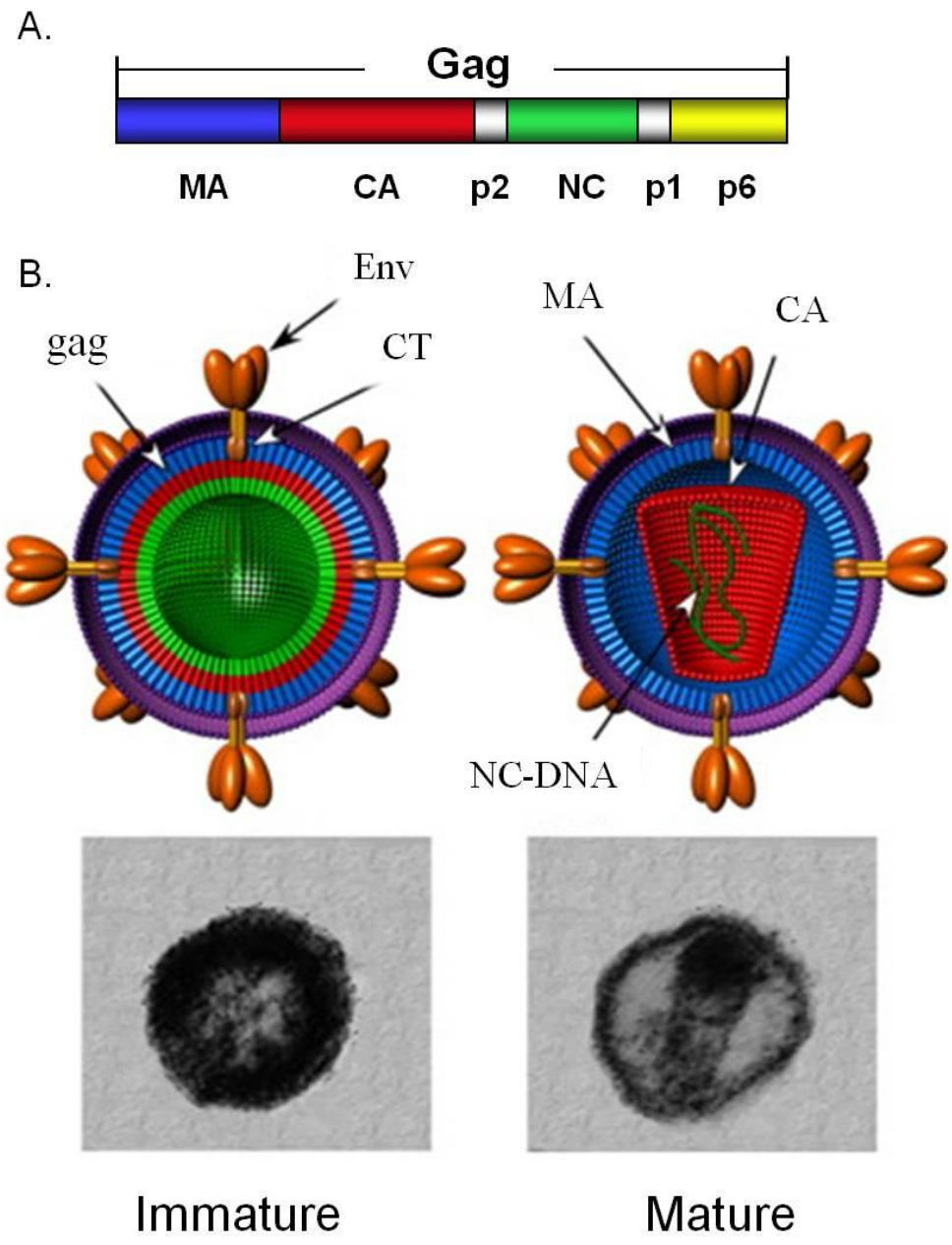

Fig 1-3. HIV-1 Gag and viral structure change during maturation
(A). Schematic representation of HIV-1 Gag domains.
(B). Schematic models (top) and EM images (bottom) of HIV-1 immature and mature virions. Viral lipid membrane is labeled in purple and HIV-1 Env trimer spikes are in brown. HIV-1 Env does not undergo proteolytic processing during maturation. For simplicity, the nonstructrual Gag proteins (p1, p2 and p6) are not included in the virion model. The models are adapted from (*4*) and the EM images are courtesy of Dr. Wes Sundquist.

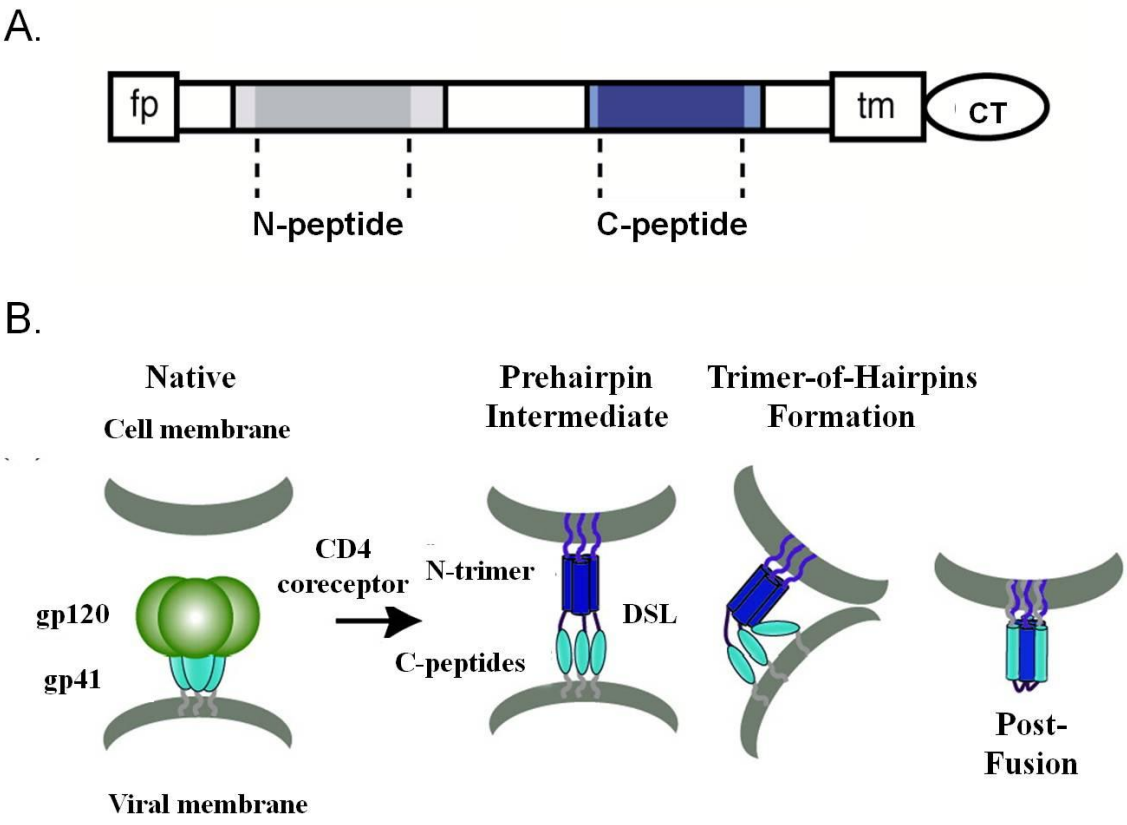

Fig 1-4. The organization of gp41 and HIV-1 entry model.
(A). Schematic representation of gp41 domains. On the N-terminus of gp41 is the fusion peptide (fp). The transmembrane (TM) and cytoplasmic tail (CT) domains are at the C-terminus. (B). Model of HIV-1 entry. The gp41 scheme is adapted from (*5*) and the entry model is adapted from (*99*).

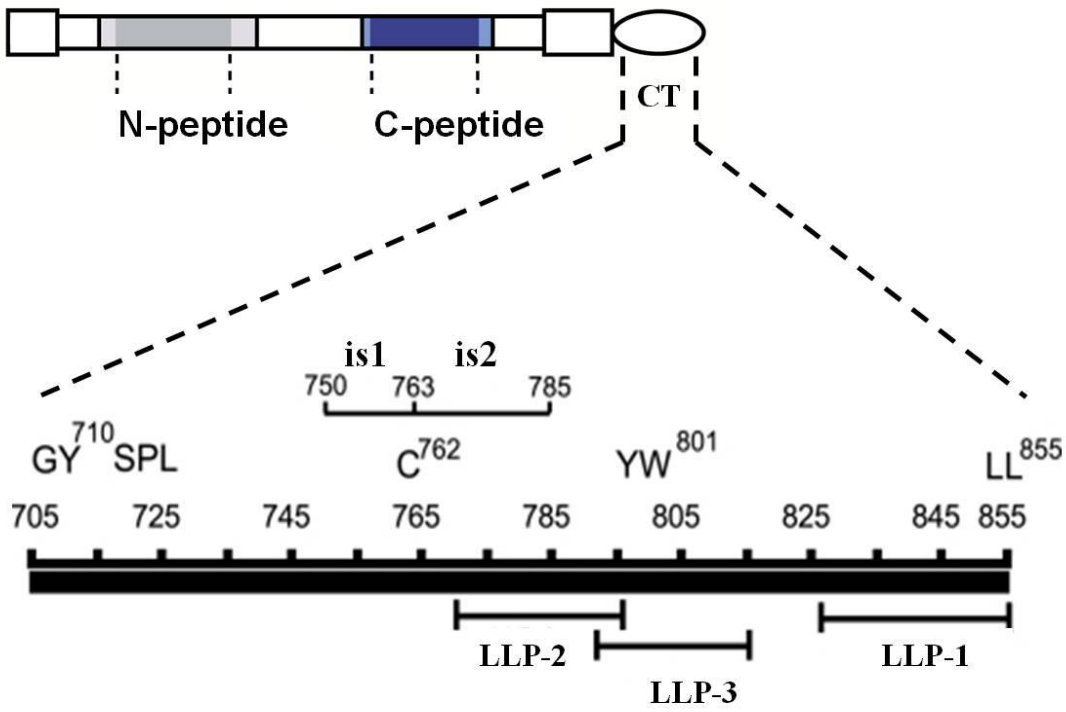

Fig 1-5. Schematic representation of CT sub-domains.
Numbering is based on HXB2 strain. Details about the N-terminal Y^{710}SPL, LLPs, LL^{855}, and two inhibitory sequences (is1 and is2) are in the text. The figure is adapted from (*6*).

References

1. UNAIDS/WHO. (2010) Annual report on global HIV/AIDS pandemic development. *http://www.unaids.org/globalreport/2010*.

2. Adamson, C. S., and Freed, E. O. (2010) Novel approaches to inhibiting HIV-1 replication, *Antiviral Res 85*, 119-141.

3. Freed, E. O. (2004) HIV-1 and the host cell: an intimate association, *Trends Microbiol 12*, 170-177.

4. Kol, N., Shi, Y., Tsvitov, M., Barlam, D., Shneck, R. Z., Kay, M. S., and Rousso, I. (2007) A stiffness switch in human immunodeficiency virus, *Biophys J 92*, 1777-1783.

5. Chan, D. C., Fass, D., Berger, J. M., and Kim, P. S. (1997) Core structure of gp41 from the HIV envelope glycoprotein, *Cell 89*, 263-273.

6. Jiang, J., and Aiken, C. (2007) Maturation-dependent human immunodeficiency virus type 1 particle fusion requires a carboxyl-terminal region of the gp41 cytoplasmic tail, *J Virol 81*, 9999-10008.

7. Welch, B. D., VanDemark, A. P., Heroux, A., Hill, C. P., and Kay, M. S. (2007) Potent D-peptide inhibitors of HIV-1 entry, *Proc Natl Acad Sci U S A 104*, 16828-16833.

8. NIH AIDS info. (2007) Federally approved HIV/AIDS treatment and prevention guidelines. *http://aidsinfo.nih.gov*.

9. D'Aquila, R. T., Schapiro, J. M., Brun-Vezinet, F., Clotet, B., Conway, B., Demeter, L. M., Grant, R. M., Johnson, V. A., Kuritzkes, D. R., Loveday, C., Shafer, R. W., and Richman, D. D. (2002) Drug Resistance Mutations in HIV-1, *Top HIV Med 10*, 21-25.

10. HIV Drug Resistance Database, Stanford University. (2007) HIV-1 resistant strains. *http://hivdb.stanford.edu*.

11. Blankson, J. N., Persaud, D., and Siliciano, R. F. (2002) The challenge of viral reservoirs in HIV-1 infection, *Annu Rev Med 53*, 557-593.

12. Weiss, R. A. (1993) How does HIV cause AIDS?, *Science (New York, N.Y 260*, 1273-1279.

13. Gilbert, P. B., McKeague, I. W., Eisen, G., Mullins, C., Gueye, N. A., Mboup, S.,

and Kanki, P. J. (2003) Comparison of HIV-1 and HIV-2 infectivity from a prospective cohort study in Senegal, *Stat Med 22*, 573-593.

14. Frankel, A. D., and Young, J. A. (1998) HIV-1: fifteen proteins and an RNA, *Annu Rev Biochem 67*, 1-25.

15. Coffin, J. M., S.H. Hughes, and H.E. Varmus. (1997) Retroviruses, *Cold Spring Harbor Laboratory Press, Plainview, NY.*

16. Gottlinger, H. G., Sodroski, J. G., and Haseltine, W. A. (1989) Role of capsid precursor processing and myristoylation in morphogenesis and infectivity of human immunodeficiency virus type 1, *Proc Natl Acad Sci U S A 86*, 5781-5785.

17. Murakami, T., Ablan, S., Freed, E. O., and Tanaka, Y. (2004) Regulation of human immunodeficiency virus type 1 Env-mediated membrane fusion by viral protease activity, *J Virol 78*, 1026-1031.

18. Wyma, D. J., Jiang, J., Shi, J., Zhou, J., Lineberger, J. E., Miller, M. D., and Aiken, C. (2004) Coupling of human immunodeficiency virus type 1 fusion to virion maturation: a novel role of the gp41 cytoplasmic tail, *J Virol 78*, 3429-3435.

19. Briggs, J. A., Simon, M. N., Gross, I., Krausslich, H. G., Fuller, S. D., Vogt, V. M., and Johnson, M. C. (2004) The stoichiometry of Gag protein in HIV-1, *Nat Struct Mol Biol 11*, 672-675.

20. Gheysen, D., Jacobs, E., de Foresta, F., Thiriart, C., Francotte, M., Thines, D., and De Wilde, M. (1989) Assembly and release of HIV-1 precursor Pr55gag virus-like particles from recombinant baculovirus-infected insect cells, *Cell 59*, 103-112.

21. Campbell, S., and Rein, A. (1999) *In vitro* assembly properties of human immunodeficiency virus type 1 Gag protein lacking the p6 domain, *J Virol 73*, 2270-2279.

22. Gross, I., Hohenberg, H., Wilk, T., Wiegers, K., Grattinger, M., Muller, B., Fuller, S., and Krausslich, H. G. (2000) A conformational switch controlling HIV-1 morphogenesis, *EMBO J 19*, 103-113.

23. Freed, E. O. (1998) HIV-1 gag proteins: diverse functions in the virus life cycle, *Virology 251*, 1-15.

24. Ganser-Pornillos, B. K., Yeager, M., and Sundquist, W. I. (2008) The structural biology of HIV assembly, *Curr Opin Struct Biol 18*, 203-217.

25. Gottlinger, H. G., Dorfman, T., Sodroski, J. G., and Haseltine, W. A. (1991) Effect

of mutations affecting the p6 gag protein on human immunodeficiency virus particle release, *Proc Natl Acad Sci U S A 88*, 3195-3199.

26. Strack, B., Calistri, A., Craig, S., Popova, E., and Gottlinger, H. G. (2003) AIP1/ALIX is a binding partner for HIV-1 p6 and EIAV p9 functioning in virus budding, *Cell 114*, 689-699.

27. von Schwedler, U. K., Stuchell, M., Muller, B., Ward, D. M., Chung, H. Y., Morita, E., Wang, H. E., Davis, T., He, G. P., Cimbora, D. M., Scott, A., Krausslich, H. G., Kaplan, J., Morham, S. G., and Sundquist, W. I. (2003) The protein network of HIV budding, *Cell 114*, 701-713.

28. Murakami, T. (2008) Roles of the interactions between Env and Gag proteins in the HIV-1 replication cycle, *Microbiol Immunol 52*, 287-295.

29. Krausslich, H. G., Ingraham, R. H., Skoog, M. T., Wimmer, E., Pallai, P. V., and Carter, C. A. (1989) Activity of purified biosynthetic proteinase of human immunodeficiency virus on natural substrates and synthetic peptides, *Proc Natl Acad Sci U S A 86*, 807-811.

30. Tritch, R. J., Cheng, Y. E., Yin, F. H., and Erickson-Viitanen, S. (1991) Mutagenesis of protease cleavage sites in the human immunodeficiency virus type 1 gag polyprotein, *J Virol 65*, 922-930.

31. Pettit, S. C., Moody, M. D., Wehbie, R. S., Kaplan, A. H., Nantermet, P. V., Klein, C. A., and Swanstrom, R. (1994) The p2 domain of human immunodeficiency virus type 1 Gag regulates sequential proteolytic processing and is required to produce fully infectious virions, *J Virol 68*, 8017-8027.

32. Parker, S. D., and Hunter, E. (2001) Activation of the Mason-Pfizer monkey virus protease within immature capsids *in vitro*, *Proc Natl Acad Sci U S A 98*, 14631-14636.

33. James, M. N. G. (1996) Aspartic proteinases: retroviral and cellular enzymes.

34. Bryant, M., and Ratner, L. (1990) Myristoylation-dependent replication and assembly of human immunodeficiency virus 1, *Proc Natl Acad Sci U S A 87*, 523-527.

35. Yuan, X., Yu, X., Lee, T. H., and Essex, M. (1993) Mutations in the N-terminal region of human immunodeficiency virus type 1 matrix protein block intracellular transport of the Gag precursor, *J Virol 67*, 6387-6394.

36. Zhou, W., Parent, L. J., Wills, J. W., and Resh, M. D. (1994) Identification of a

membrane-binding domain within the amino-terminal region of human immunodeficiency virus type 1 Gag protein which interacts with acidic phospholipids, *J Virol 68*, 2556-2569.

37. Massiah, M. A., Starich, M. R., Paschall, C., Summers, M. F., Christensen, A. M., and Sundquist, W. I. (1994) Three-dimensional structure of the human immunodeficiency virus type 1 matrix protein, *J Mol Biol 244*, 198-223.

38. Hill, C. P., Worthylake, D., Bancroft, D. P., Christensen, A. M., and Sundquist, W. I. (1996) Crystal structures of the trimeric human immunodeficiency virus type 1 matrix protein: implications for membrane association and assembly, *Proc Natl Acad Sci U S A 93*, 3099-3104.

39. Christensen, A. M., Massiah, M. A., Turner, B. G., Sundquist, W. I., and Summers, M. F. (1996) Three-dimensional structure of the HTLV-II matrix protein and comparative analysis of matrix proteins from the different classes of pathogenic human retroviruses, *J Mol Biol 264*, 1117-1131.

40. Conte, M. R., Klikova, M., Hunter, E., Ruml, T., and Matthews, S. (1997) The three-dimensional solution structure of the matrix protein from the type D retrovirus, the Mason-Pfizer monkey virus, and implications for the morphology of retroviral assembly, *EMBO J 16*, 5819-5826.

41. McDonnell, J. M., Fushman, D., Cahill, S. M., Zhou, W., Wolven, A., Wilson, C. B., Nelle, T. D., Resh, M. D., Wills, J., and Cowburn, D. (1998) Solution structure and dynamics of the bioactive retroviral M domain from Rous sarcoma virus, *J Mol Biol 279*, 921-928.

42. Ono, A., Huang, M., and Freed, E. O. (1997) Characterization of human immunodeficiency virus type 1 matrix revertants: effects on virus assembly, Gag processing, and Env incorporation into virions, *J Virol 71*, 4409-4418.

43. Zhou, W., and Resh, M. D. (1996) Differential membrane binding of the human immunodeficiency virus type 1 matrix protein, *J Virol 70*, 8540-8548.

44. Spearman, P., Horton, R., Ratner, L., and Kuli-Zade, I. (1997) Membrane binding of human immunodeficiency virus type 1 matrix protein in vivo supports a conformational myristyl switch mechanism, *J Virol 71*, 6582-6592.

45. Hermida-Matsumoto, L., and Resh, M. D. (1999) Human immunodeficiency virus type 1 protease triggers a myristoyl switch that modulates membrane binding of Pr55(gag) and p17MA, *J Virol 73*, 1902-1908.

46. Saad, J. S., Miller, J., Tai, J., Kim, A., Ghanam, R. H., and Summers, M. F. (2006) Structural basis for targeting HIV-1 Gag proteins to the plasma membrane for virus assembly, *Proc Natl Acad Sci U S A 103*, 11364-11369.

47. Caroni, P. (2001) New EMBO members' review: actin cytoskeleton regulation through modulation of PI(4,5)P(2) rafts, *EMBO J 20*, 4332-4336.

48. Pike, L. J., and Miller, J. M. (1998) Cholesterol depletion delocalizes phosphatidylinositol bisphosphate and inhibits hormone-stimulated phosphatidylinositol turnover, *J Biol Chem 273*, 22298-22304.

49. Ono, A., and Freed, E. O. (2005) Role of lipid rafts in virus replication, *Adv Virus Res 64*, 311-358.

50. Ono, A., Ablan, S. D., Lockett, S. J., Nagashima, K., and Freed, E. O. (2004) Phosphatidylinositol (4,5) bisphosphate regulates HIV-1 Gag targeting to the plasma membrane, *Proc Natl Acad Sci U S A 101*, 14889-14894.

51. Matthews, S., Barlow, P., Boyd, J., Barton, G., Russell, R., Mills, H., Cunningham, M., Meyers, N., Burns, N., Clark, N., and et al. (1994) Structural similarity between the p17 matrix protein of HIV-1 and interferon-gamma, *Nature 370*, 666-668.

52. Wu, Z., Alexandratos, J., Ericksen, B., Lubkowski, J., Gallo, R. C., and Lu, W. (2004) Total chemical synthesis of N-myristoylated HIV-1 matrix protein p17: structural and mechanistic implications of p17 myristoylation, *Proc Natl Acad Sci U S A 101*, 11587-11592.

53. Maurer, B., Bannert, H., Darai, G., and Flugel, R. M. (1988) Analysis of the primary structure of the long terminal repeat and the gag and pol genes of the human spumaretrovirus, *J Virol 62*, 1590-1597.

54. Li, H., Dou, J., Ding, L., and Spearman, P. (2007) Myristoylation is required for human immunodeficiency virus type 1 Gag-Gag multimerization in mammalian cells, *J Virol 81*, 12899-12910.

55. Reil, H., Bukovsky, A. A., Gelderblom, H. R., and Gottlinger, H. G. (1998) Efficient HIV-1 replication can occur in the absence of the viral matrix protein, *EMBO J 17*, 2699-2708.

56. Tang, C., Ndassa, Y., and Summers, M. F. (2002) Structure of the N-terminal 283-residue fragment of the immature HIV-1 Gag polyprotein, *Nat Struct Biol 9*, 537-543.

57. Gamble, T. R., Yoo, S., Vajdos, F. F., von Schwedler, U. K., Worthylake, D. K., Wang, H., McCutcheon, J. P., Sundquist, W. I., and Hill, C. P. (1997) Structure of the carboxyl-terminal dimerization domain of the HIV-1 capsid protein, *Science (New York, N.Y 278*, 849-853.

58. Kattenbeck, B., von Poblotzki, A., Rohrhofer, A., Wolf, H., and Modrow, S. (1997) Inhibition of human immunodeficiency virus type 1 particle formation by alterations of defined amino acids within the C terminus of the capsid protein, *J Gen Virol 78 (Pt 10)*, 2489-2496.

59. von Poblotzki, A., Wagner, R., Niedrig, M., Wanner, G., Wolf, H., and Modrow, S. (1993) Identification of a region in the Pr55gag-polyprotein essential for HIV-1 particle formation, *Virology 193*, 981-985.

60. Dorfman, T., Bukovsky, A., Ohagen, A., Hoglund, S., and Gottlinger, H. G. (1994) Functional domains of the capsid protein of human immunodeficiency virus type 1, *J Virol 68*, 8180-8187.

61. Accola, M. A., Strack, B., and Gottlinger, H. G. (2000) Efficient particle production by minimal Gag constructs which retain the carboxy-terminal domain of human immunodeficiency virus type 1 capsid-p2 and a late assembly domain, *J Virol 74*, 5395-5402.

62. Wills, J. W., and Craven, R. C. (1991) Form, function, and use of retroviral gag proteins, *AIDS 5*, 639-654.

63. Ivanov, D., Tsodikov, O. V., Kasanov, J., Ellenberger, T., Wagner, G., and Collins, T. (2007) Domain-swapped dimerization of the HIV-1 capsid C-terminal domain, *Proc Natl Acad Sci U S A 104*, 4353-4358.

64. Datta, S. A., Zhao, Z., Clark, P. K., Tarasov, S., Alexandratos, J. N., Campbell, S. J., Kvaratskhelia, M., Lebowitz, J., and Rein, A. (2007) Interactions between HIV-1 Gag molecules in solution: an inositol phosphate-mediated switch, *J Mol Biol 365*, 799-811.

65. von Schwedler, U. K., Stray, K. M., Garrus, J. E., and Sundquist, W. I. (2003) Functional surfaces of the human immunodeficiency virus type 1 capsid protein, *J Virol 77*, 5439-5450.

66. Srinivasakumar, N., Hammarskjold, M. L., and Rekosh, D. (1995) Characterization of deletion mutations in the capsid region of human immunodeficiency virus type 1 that affect particle formation and Gag-Pol precursor incorporation, *J Virol 69*, 6106-6114.

67. Smith, A. J., Srinivasakumar, N., Hammarskjold, M. L., and Rekosh, D. (1993) Requirements for incorporation of Pr160gag-pol from human immunodeficiency virus type 1 into virus-like particles, *J Virol 67*, 2266-2275.

68. Huang, M., and Martin, M. A. (1997) Incorporation of Pr160(gag-pol) into virus particles requires the presence of both the major homology region and adjacent C-terminal capsid sequences within the Gag-Pol polyprotein, *J Virol 71*, 4472-4478.

69. Lanman, J., Lam, T. T., Emmett, M. R., Marshall, A. G., Sakalian, M., and Prevelige, P. E., Jr. (2004) Key interactions in HIV-1 maturation identified by hydrogen-deuterium exchange, *Nat Struct Mol Biol 11*, 676-677.

70. Auerbach, M. R., Brown, K. R., and Singh, I. R. (2007) Mutational analysis of the N-terminal domain of Moloney murine leukemia virus capsid protein, *J Virol 81*, 12337-12347.

71. Wright, E. R., Schooler, J. B., Ding, H. J., Kieffer, C., Fillmore, C., Sundquist, W. I., and Jensen, G. J. (2007) Electron cryotomography of immature HIV-1 virions reveals the structure of the CA and SP1 Gag shells, *EMBO J 26*, 2218-2226.

72. Mortuza, G. B., Dodding, M. P., Goldstone, D. C., Haire, L. F., Stoye, J. P., and Taylor, I. A. (2008) Structure of B-MLV capsid amino-terminal domain reveals key features of viral tropism, gag assembly and core formation, *J Mol Biol 376*, 1493-1508.

73. Mortuza, G. B., Haire, L. F., Stevens, A., Smerdon, S. J., Stoye, J. P., and Taylor, I. A. (2004) High-resolution structure of a retroviral capsid hexameric amino-terminal domain, *Nature 431*, 481-485.

74. Jowett, J. B., Hockley, D. J., Nermut, M. V., and Jones, I. M. (1992) Distinct signals in human immunodeficiency virus type 1 Pr55 necessary for RNA binding and particle formation, *J Gen Virol 73 (Pt 12)*, 3079-3086.

75. Cimarelli, A., Sandin, S., Hoglund, S., and Luban, J. (2000) Basic residues in human immunodeficiency virus type 1 nucleocapsid promote virion assembly via interaction with RNA, *J Virol 74*, 3046-3057.

76. Zhang, Y., Qian, H., Love, Z., and Barklis, E. (1998) Analysis of the assembly function of the human immunodeficiency virus type 1 gag protein nucleocapsid domain, *J Virol 72*, 1782-1789.

77. Bennett, R. P., Nelle, T. D., and Wills, J. W. (1993) Functional chimeras of the

Rous sarcoma virus and human immunodeficiency virus gag proteins, *J Virol 67*, 6487-6498.

78. Cimarelli, A., and Luban, J. (2000) Human immunodeficiency virus type 1 virion density is not determined by nucleocapsid basic residues, *J Virol 74*, 6734-6740.

79. de Marco, A., Muller, B., Glass, B., Riches, J. D., Krausslich, H. G., and Briggs, J. A. (2010) Structural analysis of HIV-1 maturation using cryo-electron tomography, *PLoS Pathog 6*, e1001215.

80. Krausslich, H. G., Facke, M., Heuser, A. M., Konvalinka, J., and Zentgraf, H. (1995) The spacer peptide between human immunodeficiency virus capsid and nucleocapsid proteins is essential for ordered assembly and viral infectivity, *J Virol 69*, 3407-3419.

81. Accola, M. A., Hoglund, S., and Gottlinger, H. G. (1998) A putative alpha-helical structure which overlaps the capsid-p2 boundary in the human immunodeficiency virus type 1 Gag precursor is crucial for viral particle assembly, *J Virol 72*, 2072-2078.

82. Alfadhli, A., Huseby, D., Kapit, E., Colman, D., and Barklis, E. (2007) Human immunodeficiency virus type 1 matrix protein assembles on membranes as a hexamer, *J Virol 81*, 1472-1478.

83. Kol, N., Tsvitov, M., Hevroni, L., Wolf, S. G., Pang, H. B., Kay, M. S., and Rousso, I. (2010) The effect of purification method on the completeness of the immature HIV-1 Gag shell, *J Virol Methods 169*, 244-247.

84. Mayo, K., Huseby, D., McDermott, J., Arvidson, B., Finlay, L., and Barklis, E. (2003) Retrovirus capsid protein assembly arrangements, *J Mol Biol 325*, 225-237.

85. Li, S., Hill, C. P., Sundquist, W. I., and Finch, J. T. (2000) Image reconstructions of helical assemblies of the HIV-1 CA protein, *Nature 407*, 409-413.

86. Briggs, J. A., Wilk, T., Welker, R., Krausslich, H. G., and Fuller, S. D. (2003) Structural organization of authentic, mature HIV-1 virions and cores, *EMBO J 22*, 1707-1715.

87. Huseby, D., Barklis, R. L., Alfadhli, A., and Barklis, E. (2005) Assembly of human immunodeficiency virus precursor gag proteins, *J Biol Chem 280*, 17664-17670.

88. Miyauchi, K., Kim, Y., Latinovic, O., Morozov, V., and Melikyan, G. B. (2009)

HIV enters cells via endocytosis and dynamin-dependent fusion with endosomes, *Cell 137*, 433-444.

89. Chan, D. C., and Kim, P. S. (1998) HIV entry and its inhibition, *Cell 93*, 681-684.

90. Oliva, R., Leone, M., Falcigno, L., D'Auria, G., Dettin, M., Scarinci, C., Di Bello, C., and Paolillo, L. (2002) Structural investigation of the HIV-1 envelope glycoprotein gp160 cleavage site, *Chemistry 8*, 1467-1473.

91. Veronese, F. D., Joseph, B., Copeland, T. D., Oroszlan, S., Gallo, R. C., and Sarngadharan, M. G. (1989) Identification of simian immunodeficiency virus SIVMAC env gene products, *J Virol 63*, 1416-1419.

92. Zhu, P., Liu, J., Bess, J., Jr., Chertova, E., Lifson, J. D., Grise, H., Ofek, G. A., Taylor, K. A., and Roux, K. H. (2006) Distribution and three-dimensional structure of AIDS virus envelope spikes, *Nature 441*, 847-852.

93. Tan, K., Liu, J., Wang, J., Shen, S., and Lu, M. (1997) Atomic structure of a thermostable subdomain of HIV-1 gp41, *Proc Natl Acad Sci U S A 94*, 12303-12308.

94. Caffrey, M., Cai, M., Kaufman, J., Stahl, S. J., Wingfield, P. T., Covell, D. G., Gronenborn, A. M., and Clore, G. M. (1998) Three-dimensional solution structure of the 44 kDa ectodomain of SIV gp41, *EMBO J 17*, 4572-4584.

95. Weissenhorn, W., Dessen, A., Harrison, S. C., Skehel, J. J., and Wiley, D. C. (1997) Atomic structure of the ectodomain from HIV-1 gp41, *Nature 387*, 426-430.

96. Furuta, R. A., Wild, C. T., Weng, Y., and Weiss, C. D. (1998) Capture of an early fusion-active conformation of HIV-1 gp41, *Nat Struct Biol 5*, 276-279.

97. Si, Z., Madani, N., Cox, J. M., Chruma, J. J., Klein, J. C., Schon, A., Phan, N., Wang, L., Biorn, A. C., Cocklin, S., Chaiken, I., Freire, E., Smith, A. B., 3rd, and Sodroski, J. G. (2004) Small-molecule inhibitors of HIV-1 entry block receptor-induced conformational changes in the viral envelope glycoproteins, *Proc Natl Acad Sci U S A 101*, 5036-5041.

98. Welch, B. D., Francis, J. N., Redman, J. S., Paul, S., Weinstock, M. T., Reeves, J. D., Lie, Y. S., Whitby, F. G., Eckert, D. M., Hill, C. P., Root, M. J., and Kay, M. S. (2010) Design of a potent D-peptide HIV-1 entry inhibitor with a strong barrier to resistance, *J Virol 84*, 11235-11244.

99. Kim, S., Pang, H. B., and Kay, M. S. (2008) Peptide mimic of the HIV envelope gp120-gp41 interface, *J Mol Biol 376*, 786-797.

100. Murakami, T., and Freed, E. O. (2000) The long cytoplasmic tail of gp41 is required in a cell type-dependent manner for HIV-1 envelope glycoprotein incorporation into virions, *Proc Natl Acad Sci U S A 97*, 343-348.

101. Hunter, E., and Swanstrom, R. (1990) Retrovirus envelope glycoproteins, *Curr Top Microbiol Immunol 157*, 187-253.

102. Yang, P., Ai, L. S., Huang, S. C., Li, H. F., Chan, W. E., Chang, C. W., Ko, C. Y., and Chen, S. S. (2010) The cytoplasmic domain of human immunodeficiency virus type 1 transmembrane protein gp41 harbors lipid raft association determinants, *J Virol 84*, 59-75.

103. Miller, M. A., Cloyd, M. W., Liebmann, J., Rinaldo, C. R., Jr., Islam, K. R., Wang, S. Z., Mietzner, T. A., and Montelaro, R. C. (1993) Alterations in cell membrane permeability by the lentivirus lytic peptide (LLP-1) of HIV-1 transmembrane protein, *Virology 196*, 89-100.

104. Miller, M. A., Garry, R. F., Jaynes, J. M., and Montelaro, R. C. (1991) A structural correlation between lentivirus transmembrane proteins and natural cytolytic peptides, *AIDS Res Hum Retroviruses 7*, 511-519.

105. Xu, Y., Lu, H., Kennedy, J. P., Yan, X., McAllister, L. A., Yamamoto, N., Moss, J. A., Boldt, G. E., Jiang, S., and Janda, K. D. (2006) Evaluation of "credit card" libraries for inhibition of HIV-1 gp41 fusogenic core formation, *J Comb Chem 8*, 531-539.

106. West, J. T., Weldon, S. K., Wyss, S., Lin, X., Yu, Q., Thali, M., and Hunter, E. (2002) Mutation of the dominant endocytosis motif in human immunodeficiency virus type 1 gp41 can complement matrix mutations without increasing Env incorporation, *J Virol 76*, 3338-3349.

107. Lodge, R., Lalonde, J. P., Lemay, G., and Cohen, E. A. (1997) The membrane-proximal intracytoplasmic tyrosine residue of HIV-1 envelope glycoprotein is critical for basolateral targeting of viral budding in MDCK cells, *EMBO J 16*, 695-705.

108. Boge, M., Wyss, S., Bonifacino, J. S., and Thali, M. (1998) A membrane-proximal tyrosine-based signal mediates internalization of the HIV-1 envelope glycoprotein via interaction with the AP-2 clathrin adaptor, *J Biol Chem 273*, 15773-15778.

109. Berlioz-Torrent, C., Shacklett, B. L., Erdtmann, L., Delamarre, L., Bouchaert, I., Sonigo, P., Dokhelar, M. C., and Benarous, R. (1999) Interactions of the cytoplasmic domains of human and simian retroviral transmembrane proteins

with components of the clathrin adaptor complexes modulate intracellular and cell surface expression of envelope glycoproteins, *J Virol 73*, 1350-1361.

110. Byland, R., Vance, P. J., Hoxie, J. A., and Marsh, M. (2007) A conserved dileucine motif mediates clathrin and AP-2-dependent endocytosis of the HIV-1 envelope protein, *Mol Biol Cell 18*, 414-425.

111. Wyss, S., Berlioz-Torrent, C., Boge, M., Blot, G., Honing, S., Benarous, R., and Thali, M. (2001) The highly conserved C-terminal dileucine motif in the cytosolic domain of the human immunodeficiency virus type 1 envelope glycoprotein is critical for its association with the AP-1 clathrin adaptor [correction of adapter], *J Virol 75*, 2982-2992.

112. Bultmann, A., Muranyi, W., Seed, B., and Haas, J. (2001) Identification of two sequences in the cytoplasmic tail of the human immunodeficiency virus type 1 envelope glycoprotein that inhibit cell surface expression, *J Virol 75*, 5263-5276.

113. Lopez-Verges, S., Camus, G., Blot, G., Beauvoir, R., Benarous, R., and Berlioz-Torrent, C. (2006) Tail-interacting protein TIP47 is a connector between Gag and Env and is required for Env incorporation into HIV-1 virions, *Proc Natl Acad Sci U S A 103*, 14947-14952.

114. Bhattacharya, J., Peters, P. J., and Clapham, P. R. (2004) Human immunodeficiency virus type 1 envelope glycoproteins that lack cytoplasmic domain cysteines: impact on association with membrane lipid rafts and incorporation onto budding virus particles, *J Virol 78*, 5500-5506.

115. Yang, C., Spies, C. P., and Compans, R. W. (1995) The human and simian immunodeficiency virus envelope glycoprotein transmembrane subunits are palmitoylated, *Proc Natl Acad Sci U S A 92*, 9871-9875.

116. Rousso, I., Mixon, M. B., Chen, B. K., and Kim, P. S. (2000) Palmitoylation of the HIV-1 envelope glycoprotein is critical for viral infectivity, *Proc Natl Acad Sci U S A 97*, 13523-13525.

117. Dorfman, T., Mammano, F., Haseltine, W. A., and Gottlinger, H. G. (1994) Role of the matrix protein in the virion association of the human immunodeficiency virus type 1 envelope glycoprotein, *J Virol 68*, 1689-1696.

118. Freed, E. O., and Martin, M. A. (1995) Virion incorporation of envelope glycoproteins with long but not short cytoplasmic tails is blocked by specific, single amino acid substitutions in the human immunodeficiency virus type 1 matrix, *J Virol 69*, 1984-1989.

119. Yu, X., Yuan, X., Matsuda, Z., Lee, T. H., and Essex, M. (1992) The matrix protein of human immunodeficiency virus type 1 is required for incorporation of viral envelope protein into mature virions, *J Virol 66*, 4966-4971.

120. Mammano, F., Kondo, E., Sodroski, J., Bukovsky, A., and Gottlinger, H. G. (1995) Rescue of human immunodeficiency virus type 1 matrix protein mutants by envelope glycoproteins with short cytoplasmic domains, *J Virol 69*, 3824-3830.

121. Murakami, T., and Freed, E. O. (2000) Genetic evidence for an interaction between human immunodeficiency virus type 1 matrix and alpha-helix 2 of the gp41 cytoplasmic tail, *J Virol 74*, 3548-3554.

122. Lodge, R., Gottlinger, H., Gabuzda, D., Cohen, E. A., and Lemay, G. (1994) The intracytoplasmic domain of gp41 mediates polarized budding of human immunodeficiency virus type 1 in MDCK cells, *J Virol 68*, 4857-4861.

123. Owens, R. J., Dubay, J. W., Hunter, E., and Compans, R. W. (1991) Human immunodeficiency virus envelope protein determines the site of virus release in polarized epithelial cells, *Proc Natl Acad Sci U S A 88*, 3987-3991.

124. Egan, M. A., Carruth, L. M., Rowell, J. F., Yu, X., and Siliciano, R. F. (1996) Human immunodeficiency virus type 1 envelope protein endocytosis mediated by a highly conserved intrinsic internalization signal in the cytoplasmic domain of gp41 is suppressed in the presence of the Pr55gag precursor protein, *J Virol 70*, 6547-6556.

125. Bhattacharya, J., Repik, A., and Clapham, P. R. (2006) Gag regulates association of human immunodeficiency virus type 1 envelope with detergent-resistant membranes, *J Virol 80*, 5292-5300.

126. Wyma, D. J., Kotov, A., and Aiken, C. (2000) Evidence for a stable interaction of gp41 with Pr55(Gag) in immature human immunodeficiency virus type 1 particles, *J Virol 74*, 9381-9387.

127. Cosson, P. (1996) Direct interaction between the envelope and matrix proteins of HIV-1, *EMBO J 15*, 5783-5788.

128. Edwards, T. G., Wyss, S., Reeves, J. D., Zolla-Pazner, S., Hoxie, J. A., Doms, R. W., and Baribaud, F. (2002) Truncation of the cytoplasmic domain induces exposure of conserved regions in the ectodomain of human immunodeficiency virus type 1 envelope protein, *J Virol 76*, 2683-2691.

129. Wyss, S., Dimitrov, A. S., Baribaud, F., Edwards, T. G., Blumenthal, R., and

Hoxie, J. A. (2005) Regulation of human immunodeficiency virus type 1 envelope glycoprotein fusion by a membrane-interactive domain in the gp41 cytoplasmic tail, *J Virol 79*, 12231-12241.

130. Kalia, V., Sarkar, S., Gupta, P., and Montelaro, R. C. (2005) Antibody neutralization escape mediated by point mutations in the intracytoplasmic tail of human immunodeficiency virus type 1 gp41, *J Virol 79*, 2097-2107.

131. Kol, N., Gladnikoff, M., Barlam, D., Shneck, R. Z., Rein, A., and Rousso, I. (2006) Mechanical properties of murine leukemia virus particles: effect of maturation, *Biophys J 91*, 767-774.

132. Ivanovska, I. L., de Pablo, P. J., Ibarra, B., Sgalari, G., MacKintosh, F. C., Carrascosa, J. L., Schmidt, C. F., and Wuite, G. J. (2004) Bacteriophage capsids: tough nanoshells with complex elastic properties, *Proc Natl Acad Sci U S A 101*, 7600-7605.

133. Michel, J. P., Ivanovska, I. L., Gibbons, M. M., Klug, W. S., Knobler, C. M., Wuite, G. J., and Schmidt, C. F. (2006) Nanoindentation studies of full and empty viral capsids and the effects of capsid protein mutations on elasticity and strength, *Proc Natl Acad Sci U S A 103*, 6184-6189.

134. Carrasco, C., Carreira, A., Schaap, I. A., Serena, P. A., Gomez-Herrero, J., Mateu, M. G., and de Pablo, P. J. (2006) DNA-mediated anisotropic mechanical reinforcement of a virus, *Proc Natl Acad Sci U S A 103*, 13706-13711.

CHAPTER 2

THE EFFECT OF PURIFICATION METHOD ON THE COMPLETENESS OF THE IMMATURE HIV-1 GAG SHELL

Nitzan Kol, Marianna Tsvitov, Liron Hevroni, Sharon G. Wolf, Hong-Bo Pang

Michael S. Kay, and Itay Rousso

Reproduced with permission from:

Kol N, Tsvitov M, Hevroni L, Wolf SG, Pang HB, Kay MS and Rousso I.

The Journal of Virological Methods

Volume 169, Issue 1, Oct 2010, Pages 244-247

Journal of Virological Methods 169 (2010) 244–247

Contents lists available at ScienceDirect

Journal of Virological Methods

journal homepage: www.elsevier.com/locate/jviromet

Short communication

The effect of purification method on the completeness of the immature HIV-1 Gag shell

Nitzan Kol[a], Marianna Tsvitov[a], Liron Hevroni[a], Sharon G. Wolf[b], Hong-Bo Pang[c], Michael S. Kay[c], Itay Rousso[a,*]

[a] Department of Structural Biology, Weizmann Institute of Science, Rehovot 76100, Israel
[b] Electron Microscopy Center, Weizmann Institute of Science, Rehovot 76100, Israel
[c] Department of Biochemistry, University of Utah School of Medicine, Salt Lake City, UT 84112-5650, USA

Article history:
Received 15 April 2010
Received in revised form 27 July 2010
Accepted 29 July 2010
Available online 4 August 2010

Keywords:
HIV-1
Structure
Immature
Gag
Purification
Sucrose
OptiPrep
Iodixanol

A B S T R A C T

Elucidating the structure of the immature HIV-1 Gag core is an important aspect of understanding the biology of this virus. In doing so, preservation of the fragile Gag lattice is essential. In this study, the effects of purification methods on the structural and mechanical integrity of immature HIV-1 are examined. The results show that the morphological and mechanical properties of the virion are preserved to a significantly higher degree by Iodixanol (OptiPrep) purification compared to the standard sucrose method. In conclusion, these results indicate that OptiPrep instead of sucrose purification should be employed when conducting structural studies on the HIV-1 virion.

Gag is the structural protein of HIV-1, which comprises the core of the virion and drives its assembly and budding at the plasma membrane. HIV-1 buds as a non-infectious immature particle, composed of a dense doughnut-like shell consisting of Gag, located directly underneath the viral membrane. The Gag polyprotein includes three main structural domains – MA, CA, and NC, which are cleaved after budding by the viral protease to form the mature infectious virion. The mature virus particle has a distinctly different morphology and contains a conical capsid.

Elucidating the structure of the immature virion's Gag shell has been the focus of several studies, as it may resolve important questions associated with the assembly, budding, and maturation processes of HIV-1. Initially Gag was assumed to generally form a complete lattice beneath the viral lipid bilayer membrane. Later it was shown that the lattice is hexagonal (Briggs et al., 2006, 2004; Mayo et al., 2003; Nermut et al., 1998), the closure of which requires the presence of defects. Defects can either be in form of pentamers at each of the 12 vertices yielding an icosohedral virion, like in the case of many viruses such as HSV, adenovirus, and bacteriophage, or gaps in the hexagonal lattice. In the last decade, several studies suggested that closure of the HIV shell is accomplished by the incorporation of defects in the form of gaps of various sizes (Briggs et al., 2009; Carlson et al., 2008; Fuller et al., 1997; Wilk et al., 2001; Wright et al., 2007). The most recent studies used electron cryotomography to estimate the size and nature of these gaps (Briggs et al., 2009; Carlson et al., 2008; Wright et al., 2007). The first study found the Gag shell to be ~40% complete on average and to consist of several patches of Gag lattice (Wright et al., 2007). Two recent studies from the Krausslich group showed that the Gag shell has an average completeness of ~70% and consists of one continuous lattice that contains small gaps throughout (Briggs et al., 2009; Carlson et al., 2008). All of these studies were carried out on viruses that were purified by pelleting through a sucrose cushion, a method that is used commonly in the HIV field. In the past, concerns were raised about the use of sucrose solutions to purify retroviruses due to possible damage by osmotic shock and the need for pelleting by ultracentrifugation. In fact, extensive damage to virus glycoproteins was indeed demonstrated using this method (McGrath et al., 1978; Moennig et al., 1974). Therefore the structure of the Gag shell of the immature HIV-1 virion in its native state remains unknown.

It has previously been reported that the Gag shell of the immature HIV-1 particle is mechanically rigid (Kol et al., 2007). This finding is difficult to reconcile with the idea that the Gag shell is discontinuous and has large gaps. In this study, the impact on virus

* Corresponding author. Tel.: +972 8 9343479; fax: +972 8 9344136.
E-mail address: itay.rousso@weizmann.ac.il (I. Rousso).

0166-0934/$ – see front matter © 2010 Elsevier B.V. All rights reserved.
doi:10.1016/j.jviromet.2010.07.035

structure by the virus purification method is investigated. More specifically, it was asked if a gentler method of purification would preserve the completeness of the immature HIV-1 shell to a higher degree.

A comparison of the morphology and stiffness of virus particles purified using sucrose or Iodixanol, a non-ionic density gradient media also known as OptiPrep was conducted. 293T cells were transfected with the pNL-MA/p6 vector, which produces immature HIV-1 particles (Wyma et al., 2004), using the PEI protocol (Boussif et al., 1995). 18–20 h post-transfection, media was exchanged, and 60 ml of viral supernatant was collected after 6 h. The filtered supernatant was split into two parts. One half was pelleted through a 5-ml cushion of 20% sucrose in TNE buffer (0.15 M NaCl, 1 mM EDTA, 10 mM Tris, pH 7.6) in a SW-28 rotor (25,000 rpm, 1 h). The virus pellet was resuspended in TNE by gentle pipetting and stored at 4 °C. The other half of the filtered supernatant was pelleted onto a 5-ml cushion of OptiPrep in a SW-28 rotor (21,000 rpm, 1.5 h). The supernatant was then aspirated, leaving 2–3 ml of media above the cushion, containing the concentrated virus, and the cushion was then removed with a syringe. The remaining supernatant was combined with TNE and concentrated by centrifugal ultrafiltration with a MWCO of 100,000 (Vivaspin 20, Sartorius, Goettingen, Germany). Virus was concentrated from 20 to 1 ml at 3000 × *g* and then washed with TNE by repeating this procedure three times. The final volume of approximately 500 μl was removed and stored at 4 °C for up to 3 weeks, during which time no changes in virus structure and mechanical properties were observed.

1. Effects on virus morphology

The morphology of the purified virions was studied by examining the projections of virions using Cryo-TEM. 4 μl of virus was deposited on a microscope grid, either Quantifoil or lacey (Electron Microscopy Sciences, Hatfield, PA), which was soaked previously in chloroform, and rendered hydrophilic using glow discharge. The grids were immediately inserted into liquid ethane. Images were acquired on a Tecnai T12 electron microscope (FEI, Hillsboro, OR) under low dose regime. Fig. 1A and B show representative images from the sucrose and OptiPrep-purified samples, respectively. At a qualitative level, it is clear that while the viruses purified using the sucrose method typically display only a partial Gag layer, those purified using the OptiPrep method show a much more complete layer, which usually runs along most, if not all of the interior of the viral membrane.

In order to quantify the extent of this difference, the portion of the virus circumference that had a Gag layer underneath was analyzed by identifying the boundaries of the shell manually (Fig. 1 arrowheads) and calculating the percentage of completeness by dividing this length by the overall virus circumference. The results show that the Gag shell of viruses purified with the sucrose method (Fig. 2A) is significantly more incomplete than that of the viruses purified using OptiPrep (Fig. 2B). While the mean coverage of the sucrose-purified viruses was only 60 ± 18%, that of the viruses purified using the OptiPrep method was 82 ± 16% (64 particles were analyzed in each group with the standard deviation indicated). Moreover, there were three times as many viruses that displayed a complete shell using the OptiPrep vs. the sucrose method (33% vs. 9%). Student's *t*-test showed the difference between the two populations to be highly significant ($P < 0.0001$).

2. Effects on virus stiffness

To complement the structural analysis, the stiffness of immature virus particles purified with the sucrose or the OptiPrep methods was measured. Virus particles were attached to glass slides that

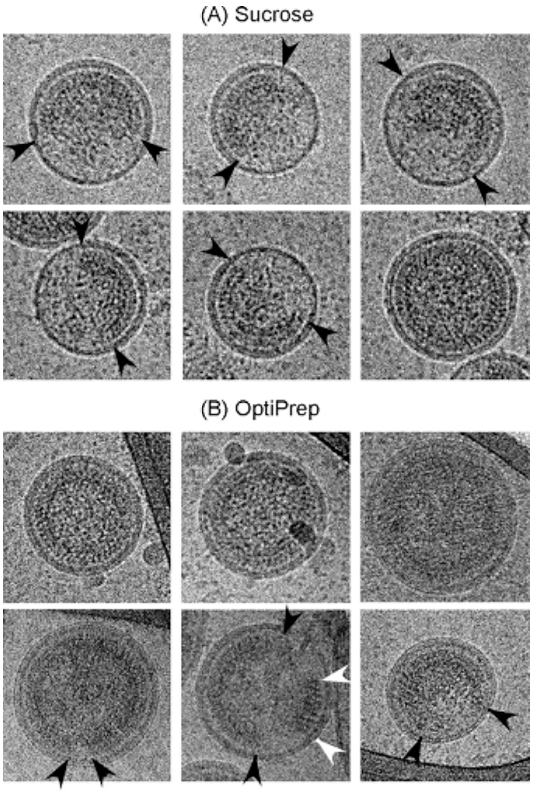

Fig. 1. Cryo-TEM images of immature HIV-1 particles. The Gag shell in the projections of viruses purified with the sucrose method (A) is less complete than that of viruses purified using OptiPrep (B). The black arrowheads mark the beginning and end of the continuous shell. White arrowheads mark a second Gag segment. Absence of arrowheads indicates a virion with a complete shell.

were rendered hydrophobic with HMDS, and the surface of the slide was scanned with a Bioscope AFM (Veeco, Santa-Barbara, CA) until particles were located. The tip of the AFM was then positioned in the center of the virion and used to compress the particle. The response of the particle to the applied force of the AFM tip is recorded in the form of a force–distance curve, from which the stiffness of the particle is derived according to a previously described method (Kol et al., 2006, 2007). Pyramidal silicon nitride probes, either DNP ($K = 0.1$ N/m, Veeco, Santa-Barbara) or NSC35 ($K = 3–7$ N/m, Micromasch, Tallinn, Estonia) were used. The spring constants of the DNP probes were determined by measuring the thermal fluctuations (Hutter and Bechhoefer, 1993) and of the NSC35 probes by the method developed by Sader et al. (1999). The use of different methods was necessary due to the low amplitude of the thermal fluctuations of the NSC35 probes. While viruses purified using the two methods appeared identical when imaged by the AFM, their response to the applied force varied greatly. Virions purified using the sucrose method were significantly softer than particles purified using OptiPrep (0.3 ± 0.01 N/m ($n = 23$) and 15 ± 0.7 N/m ($n = 19$), respectively). In a previous study, the stiffness of immature virus particles was significantly reduced by removal of the viral envelope protein (gp160). It is therefore possible that lower gp160 levels in sucrose-purified virus particles contribute to their reduced stiffness. However, Western-blot analysis of virus particles purified

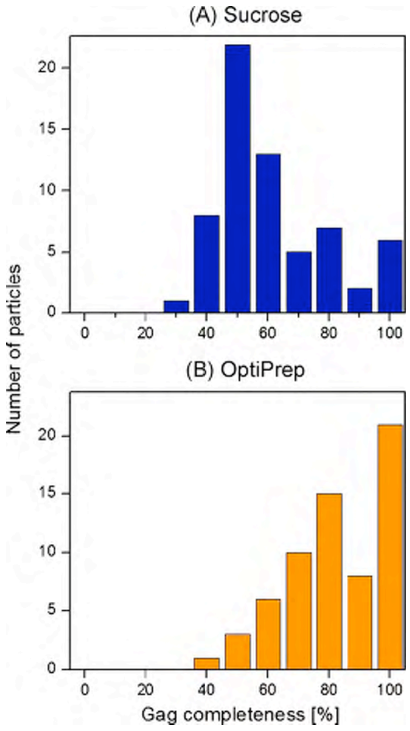

Fig. 2. The distribution of Gag shell completeness derived from Cryo-TEM images. Virus particles purified with (A) the sucrose method had an average completeness of 60% and those purified with (B) the OptiPrep method had an average completeness of 82% (64 images of virions prepared by each method were analyzed).

using the two methods revealed similar levels of gp160 incorporation (Fig. 3C).

Further insights into the structure of the Gag shell can be obtained from the shape of the force–distance curves. When a structured protein layer exists beneath the membrane, the resistance of the particle to the force is approximately linear. In contrast, in the absence of a structured layer, the particle behaves much like a vesicle, the stiffness of which increases monotonically as it is compressed. In this manner, the AFM can be used as a complementary method to the cryo-EM analysis to probe the completeness of the Gag shell. All the force–distance curves obtained from virus particles purified by the OptiPrep method were nearly linear (Fig. 3A), indicating the presence of a structured Gag layer beneath the viral envelope. However, nearly 30% of the virus particles that were purified with the sucrose method lacked an ordered layer, as evident by the non-linearity of their force–distance curves (Fig. 3B). Thus, the mechanical results correlate with the cryo-EM analysis.

It should be emphasized that the variability in the amount of damage done to the virus particles using the sucrose purification methods is significantly larger than that of the OptiPrep method. In a previous study (Kol et al., 2007), sucrose was used to purify viruses and the average stiffness of the immature virion was found to be 3.15 N/m. Those viruses presumably had a more complete shell than the sucrose-purified viruses in the current study (0.3 N/m). Nevertheless, the damage to the Gag shell in all sucrose-purified virus particles is significantly higher than that of the OptiPrep-purified viruses, the stiffness of which is on the average 15 N/m.

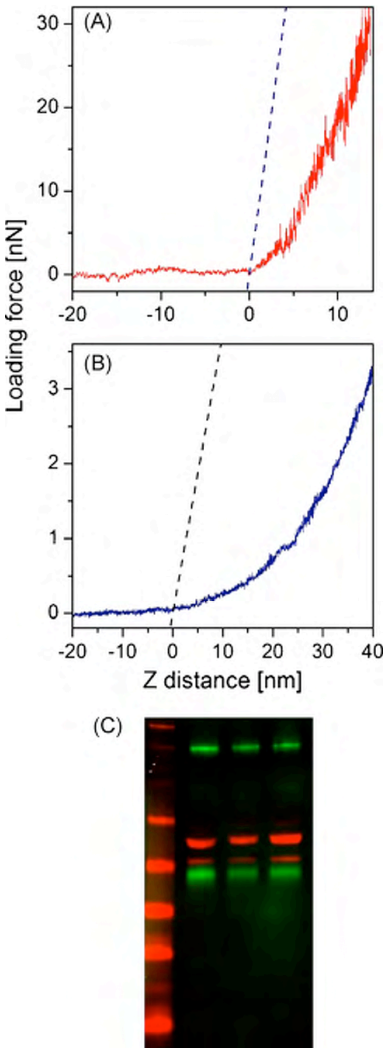

Fig. 3. Measuring the point stiffness of the Gag shell of immature HIV. A typical force–distance curve of an immature virus purified using the OptiPrep method (A) compared to that of a virus purified using sucrose (B). For reference, the cantilever deflection is plotted (dashed black line). The response of the virus Gag shell in A is linear whereas the stiffness of the shell in B gradually increases. (C) Western-blot analysis of gp160 levels (green, Chessie-8 Ab) and capsid levels (red, anti-p24 Ab). Unpurified virus particles are shown in lane 1 while sucrose- and OptiPrep-purified virus particles are shown in lanes 2 and 3, respectively. Unpurified and OptiPrep-purified virus particles were concentrated via centrifugation. (For interpretation of the references to color in the figure caption, the reader is referred to the web version of the article.)

These results demonstrate that the purification method has a great impact on the mechanical stiffness and the completeness of the immature HIV-1 Gag shell. Currently it is not known which aspect of the sucrose purification method is damaging to the virus – osmotic pressure caused by sucrose or mechanical stress imposed on them by pelleting onto a hard surface under high centrifugal forces. However it is clear that the OptiPrep purification method presented in this report preserves the integrity of the immature

HIV-1 virion to a much higher degree than the conventional sucrose purification method, and should be the method of choice for the purpose of conducting structural studies on this virus.

Conflict of interest

None.

Acknowledgments

We thank Alan Rein for helpful discussions and comments on this work. This work was supported in part by NIH grant AI076735 to I.R. and M.K. I.R. holds the Robert Edwards and Roselyn Rich Manson Career Development Chair. The electron microscopy studies were conducted at the Irving and Cherna Moskowitz Center for Nano and Bio-Nano Imaging at the Weizmann Institute of Science.

References

Boussif, O., Lezoualćh, F., Zanta, M.A., Mergny, M.D., Scherman, D., Demeneix, B., Behr, J.P., 1995. A versatile vector for gene and oligonucleotide transfer into cells in culture and in vivo: polyethylenimine. Proc. Natl. Acad. Sci. U.S.A. 92, 7297–7301.

Briggs, J.A., Johnson, M.C., Simon, M.N., Fuller, S.D., Vogt, V.M., 2006. Cryo-electron microscopy reveals conserved and divergent features of gag packing in immature particles of Rous sarcoma virus and human immunodeficiency virus. J. Mol. Biol. 355, 157–168.

Briggs, J.A., Riches, J.D., Glass, B., Bartonova, V., Zanetti, G., Krausslich, H.G., 2009. Structure and assembly of immature HIV. Proc. Natl. Acad. Sci. U.S.A. 106, 11090–11095.

Briggs, J.A., Simon, M.N., Gross, I., Krausslich, H.G., Fuller, S.D., Vogt, V.M., Johnson, M.C., 2004. The stoichiometry of Gag protein in HIV-1. Nat. Struct. Mol. Biol. 11, 672–675.

Carlson, L.A., Briggs, J.A., Glass, B., Riches, J.D., Simon, M.N., Johnson, M.C., Muller, B., Grunewald, K., Krausslich, H.G., 2008. Three-dimensional analysis of budding sites and released virus suggests a revised model for HIV-1 morphogenesis. Cell Host Microbe 4, 592–599.

Fuller, S.D., Wilk, T., Gowen, B.E., Krausslich, H.G., Vogt, V.M., 1997. Cryo-electron microscopy reveals ordered domains in the immature HIV-1 particle. Curr. Biol. 7, 729–738.

Hutter, J.L., Bechhoefer, J., 1993. Calibration of atomic-force microscope tips. Rev. Sci. Instrum. 64, 1868–1873.

Kol, N., Gladnikoff, M., Barlam, D., Shneck, R.Z., Rein, A., Rousso, I., 2006. Mechanical properties of murine leukemia virus particles: effect of maturation. Biophys. J. 91, 767–774.

Kol, N., Shi, Y., Tsvitov, M., Barlam, D., Shneck, R.Z., Kay, M.S., Rousso, I., 2007. A stiffness switch in human immunodeficiency virus. Biophys. J. 92, 1777–1783.

Mayo, K., Huseby, D., McDermott, J., Arvidson, B., Finlay, L., Barklis, E., 2003. Retrovirus capsid protein assembly arrangements. J. Mol. Biol. 325, 225–237.

McGrath, M., Witte, O., Pincus, T., Weissman, I.L., 1978. Retrovirus purification: method that conserves envelope glycoprotein and maximizes infectivity. J. Virol. 25, 923–927.

Moennig, V., Frank, H., Hunsmann, G., Schneider, I., Schafer, W., 1974. Properties of mouse leukemia viruses. VII. The major viral glycoprotein of friend leukemia virus. Isolation and physicochemical properties. Virology 61, 100–111.

Nermut, M.V., Hockley, D.J., Bron, P., Thomas, D., Zhang, W.H., Jones, I.M., 1998. Further evidence for hexagonal organization of HIV gag protein in prebudding assemblies and immature virus-like particles. J. Struct. Biol. 123, 143–149.

Sader, J.E., Chon, J.W.M., Mulvaney, P., 1999. Calibration of rectangular atomic force microscope cantilevers. Rev. Sci. Instrum. 70, 3967–3969.

Wilk, T., Gross, I., Gowen, B.E., Rutten, T., de Haas, F., Welker, R., Krausslich, H.G., Boulanger, P., Fuller, S.D., 2001. Organization of immature human immunodeficiency virus type 1. J. Virol. 75, 759–771.

Wright, E.R., Schooler, J.B., Ding, H.J., Kieffer, C., Fillmore, C., Sundquist, W.I., Jensen, G.J., 2007. Electron cryotomography of immature HIV-1 virions reveals the structure of the CA and SP1 Gag shells. EMBO J. 26, 2218–2226.

Wyma, D.J., Jiang, J.Y., Shi, J., Zhou, J., Lineberger, J.E., Miller, M.D., Aiken, C., 2004. Coupling of human immunodeficiency virus type 1 fusion to virion maturation: a novel role of the gp41 cytoplasmic tail. J. Virol. 78, 3429–3435.

CHAPTER 3

VIRION STIFFNESS REGULATES IMMATURE HIV-1 ENTRY

Hong-Bo Pang*, Liron Hevroni*, Debra M. Eckert, Marianna Tsvitov,

Itay Rousso and Michael S. Kay

*These authors contributed equally to this work.

Abstract

Human immunodeficiency virus type 1 (HIV-1) undergoes a protease-mediated maturation process that is required for its infectivity. Little is known about how the physical properties of viral particles change during this process. Using Atomic Force Microscopy (AFM), we previously reported a dramatic reduction in HIV-1 particle stiffness during maturation. In this study, we show that transmembrane anchored Envelope (Env) cytoplasmic tail (CT) domain is sufficient to produce stiff immature particles. Using this construct coexpressed with viral Env lacking the CT domain (ΔCT), we show that particle stiffness is inversely related to viral entry activity. A similar effect was also observed for vesicular stomatitis virus Env (VSVg) pseudovirions. This linkage between particle stiffness and viral entry activity illustrates a new level of regulation for viral replication and defines a new inhibitory target.

Introduction

The main structural components of an HIV-1 particle are its protein shell, composed of the viral Gag polyprotein and a surrounding lipid membrane. Expression of Gag alone is necessary and sufficient for viral particle assembly and budding (*1*). The viral surface contains the envelope protein (Env), which is synthesized as a precursor (gp160) that is cleaved by a cellular protease into two subunits: a receptor-binding subunit (gp120) and a transmembrane subunit (gp41). gp120 and gp41 form a noncovalent complex that mediates viral entry (*2, 3*). The Env transmembrane subunit of HIV-1 (and other lentiviruses) has an unusually long (~150 amino acids) cytoplasmic tail (CT) domain compared to other retroviruses. Gag interacts with Env via CT, which is essential for Env localization to its budding sites and efficient incorporation into virions (*4-6*).

New virions initially emerge from infected cells as immature particles. These particles undergo a maturation process in the extracellular environment induced by HIV protease cleavage of Gag into several products including three structural proteins: MA, CA and NC (*7*). Electron Microscopy (EM) shows that HIV particles undergo a dramatic morphological change from a roughly spherically symmetric immature particle with a thick protein shell to a mature particle with a prominent conical core (capsid) formed by CA (*8*). In mature virions, only MA remains associated with the viral membrane, creating a thin protein shell underlying the membrane. With such a striking morphological change, we hypothesized that the physical properties of viral particles would also change during maturation.

During the viral lifecycle, a virion needs to meet several distinct demands—efficient membrane fusion during entry, particle disassembly to release genetic material, assembly during budding and stability in the extracellular environment before the next entry. We speculate that the virion may adopt different physical properties at different stages of its lifecycle, but the link between physical properties and viral biological activity remain poorly understood. To study the physical properties of viral particles, atomic force microscopy (AFM) has proven to be uniquely informative. In contrast to EM, AFM can be performed on unfixed viruses under native conditions and does not require freezing or fixation, which can irreversibly damage viral particles. AFM has been successfully applied for measuring the physical properties of several viruses (*9-12*).

We previously reported that immature particles are ~14-fold stiffer than mature ones, a dramatic change in physical properties that we call the “stiffness switch” (*13*). Further studies determined that Env CT is required for the stiffness switch, as deletion of CT

softens immature HIV-1 particles almost to the mature level (*13*). Viral entry is the next event after maturation, and maturation is required for HIV infectivity. Immature HIV-1 virions are noninfectious due to postentry deficiencies (e.g. integration) and also fuse with target cells with ~10-fold lower efficiency than mature virions (*14, 15*). We also verified that deletion of CT restores the entry activity of immature HIV-1 to the mature level, in agreement with previous studies (*14, 15*). Although these results suggest a strong inverse correlation between viral particle stiffness and entry activity, a cause and effect relationship has not yet been demonstrated.

In this study, we ask whether particle stiffness of a virion directly regulates its entry activity. To rule out other possibilities and solely investigate the effect of particle stiffness on viral entry, we designed constructs that separate Env's fusion and stiffness-mediating activities. Using these constructs, we show that membrane-anchored CT alone can mediate particle stiffness and that stiffness directly regulates viral entry. We also show that stiffness can regulate entry activity mediated by an unrelated viral envelope protein (VSVg, Env of *Vesicular Stomatitis Virus*). This study, to the best of our knowledge, provides the first direct evidence to prove that particle stiffness regulates viral entry activity, linking a virion's physical and biological properties. Furthermore, our results suggest that particle stiffness has a fundamental effect on viral fusion independent of viral type or entry route. Our studies define a new regulatory level for viral replication and may provide a new strategy for the development of novel HIV-1 inhibitors.

Materials and Methods

Plasmids

Plasmids were obtained or constructed as follows: ΔEnv HIV-1 genome containing an inactivating integrase mutant (DHIV3-GFP-D116G (*16*), provided by V. Planelles), HIV-1 Env expression vector (pEBB-HXB2 (*17*), provided by B. Chen), VSVg expression vector (phCMV-VSV-G (*18, 19*), provided by W. Sundquist), Env expression plasmid for JRFL strain (pCAGGS-JRFL-Env WT and ΔCT, provided by Dr. James Binley) and vector expressing Vpr-β-lactamase (BlaM-Vpr) fusion protein, pMM310 (*14*). Human placental alkaline phosphatase (PLAP) expressing vector (pCMV-SPORT6) was from ATCC. Immature particles were generated by cloning Gag with all PR cleavage sites mutated (pNL-MA/p6 (*14*), provided by C. Aiken) into the ΔEnv Int− HIV-1 genome, while mature particles were produced using an HIV-1 genome vector with wild-type (WT) cleavage sites. ΔCT HXB2 Env (Δ147 (*20*)) was provided by E. Hunter and cloned into pEBB-HXB2.

To construct GFP-TM1, the open reading frame (ORF) encoding GFP (green fluorescent protein) was obtained from pET9a-GFP-C37 (*21*) by PCR using 5' KpnI-containing primer (5'-tctgggtacctagctctggcatggtgagcaagggcgagg) and 3' SacI-containing primer (5'-ctcgaggagctcttgtacag). The ORF for TM and CT fragments was obtained from pEBB-HXB2 by PCR using 5' SacI-containing primer (5'-caatgagctctggcggttggaattggtttaacataacaaattgg) and 3' BamHI-containing primer (5'-gtcccagataagtgctaaggatc). These two PCR products are annealed at the SacI digestion site. The generated GFP-TM1 fusion fragment was inserted into pEBB-HXB2 to replace the corresponding KpnI-BamHI fragment, which includes the residues from V44 to L681

of Env ectodomain (HXB2 numbering).

Viral preparation and analysis

Pseudovirion particles were produced by cotransfection of 293T cells with ΔEnv int-HIV-1 genome vector, an Env-expressing vector, varying amounts of pEBB-GFP-TM1 and pMM310. For example, to generate immature or mature WT virus, 2.5 μg of total DNA (1.23 μg genome vector, 0.819 μg Env expressing vector, and 0.45 μg pMM310) was transfected into ~10^6 cells using 10 μg polyethylenimine (PEI, Sigma). The amount of Env expressing plasmid input for immature WT has been defined as 100% for plasmid input. Media was changed at 6 h after transfection to avoid PEI's toxicity. Supernatants containing secreted viral particles were collected 30 h posttransfection and filtered through 0.2 μm Acrodisc syringe filters (Pall). Each series of viruses prepared on the same day is defined as one "batch".

For western blot (WB) analysis of viral concentration and Env incorporation level, virus supernatants were purified by centrifugation through a sucrose cushion (20% sucrose in 1 X TNE buffer: 0.1 M NaCl, 1 mM EDTA, 10 mM Tris, pH 7.6) at 20,000 X g for 90 min at 4℃. The pellet was resuspended in SDS-PAGE reducing sample buffer and resolved by SDS-PAGE. WB was developed using rabbit polyclonal anti-CA and anti-VSVg (provided by W. Sundquist), mouse monoclonal anti-gp41 Chessie 8 antibody (obtained from Chessie 8 hybridoma provided by NIH AIDS Research and References Reagent Program (ARRRP)), sheep polyclonal anti-gp120 (contributed by M. Phelan, ARRRP) and rabbit polyclonal anti-BlaM (Chemicon/Millpore). Blots were quantified using Li-Cor's Odyssey instrument.

AFM measurement and analysis

For AFM measurement, virus-containing supernatant was first concentrated as previously described (*22*). Briefly, the filtered viral supernatnant was pelleted onto a 1-ml cushion of OPTI-PREP (Iodixanol, Sigma) in a SW-41 rotor (21,000 rpm, 90 min, 4℃). ~90% of upper layer supernatant was then aspirated, and the cushion was removed with a syringe. The remaining supernatant was combined with 1 X TNE buffer and concentrated by centrifugal ultrafiltration with a MWCO of 100,000 (Vivaspin 20, Sartorius, Germany) for three times at 3,000 X g.

For AFM imaging and force measurements, virus particles were attached to HMDS-coated microscope glass slides using a previously described method (*13, 22*). All AFM experiments were carried out using a Bioscope with a Nanoscope IV controller (Veeco) equipped with a dimension XY closed loop scanner mounted on an inverted optical microscope (Axiovert 200M, Carl Zeiss AG). Images of virus particles were acquired in AFM tapping mode in a fluid environment. Pyramidal silicone nitride probes either XXX (K=1 N/m, Veeco) or NSC35 (K=3-7 N/m, Micromasch, Tallin, Estonia) were used. The spring constants of the DNP probes were determined experimentally by measuring thermal fluctuations (*23*). Since the amplitude of the NSC35 thermal fluctuations was too low, we used the method of Sadata et al. to determine their spring constant.

Virus stiffness was determined based on indentation type experiments, as previously described (*13*). Briefly, for each indentation measurement, ~100 force-distance curves were performed at a scan rate of 0.5 Hz. Viral stiffness was derived mathematically from the slope of the FD curve. The stiffness of the virus was computed according to Hooke’s

law on the assumption that our experimental system can be modeled as two springs (the virus and the cantilever) arranged in series.

β-lactamase (BlaM) assay for viral entry measurement

The viral entry assay was performed as described (*13*). Briefly, HIV-1 particles mixed with DEAE-Dextran (4 μg/ml) were added onto HOS-CD4-CXCR4 cells (provided by B.Chen), followed by centrifugation at 1,800 X g for 30 min at 4℃ and then incubation at 37℃ for 2 h. After removal of unbound viruses, 1 μM β-lactamase substrate solution (CCF2-AM, Invitrogen) was incubated with cells at 13℃ for 17 h. Uncleaved and cleaved CCF2-AM have emission peaks of 520 nm (green) and 447 nm (blue), respectively, under 409 nm excitation. Fluorescent signals from both channels were detected using an Olympus MVX10 fluorescent microscope and quantified using ImageJ software. For the same virus, BlaM signal increases proportionally to amount of virus added (data not shown). BlaM signal also increases proportionally with amount of processed Env, as measured by anti-gp120 Western blot (supplemental Fig. 3-1 A).

Therefore, viral entry signals were normalized to their corresponding gp120 concentration for viruses bearing different amount of GFP-TM1 and HIV-1 ΔCT. Hence, the specific entry activity we report here represents the viral entry activity per processed Env. BlaM assay signal also increases proportionally to VSVg incorporation level (supplemental Fig. 3-1 B), so VSV-specific entry activity was also normalized to VSVg concentration.

Similarly, a varying amount of pMM310 was used during transfection to create a series of viruses bearing titrating amount of BlaM-Vpr. 2-fold variation of BlaM incorporation level only slightly changed BlaM assay signal (supplemental Fig. 3-1 C).

Since anti-BlaM Western blots showed less than 2-fold variation in BlaM incorporation levels for all our GFP-TM1 titrating viruses (data not shown), BlaM incorporation level has not been considered during normalization.

To investigate whether we can compare the entry activity of viruses from different batches, normalized entry activities of ΔCT viruses without GFP-TM1 were measured and found to be very similar between different batches (supplemental Fig. 3-2). Therefore, the entry activity of viruses is reported as relative value to that of ΔCT virus within one series.

Triton X-100 (TX100) treatment

TX100 treatment of HIV-1 particles was performed as described previously (*6*). Briefly, virus-containing supernatant was first concentrated using sucrose cushion method as described above. The pellet was then resuspended into 0.5% TX100 in 1 X TNE buffer, and incubated at 4℃ for 30 min before centrifugation in a Beckman TLA-55 rotor at 45,000 rpm for 30 min. After centrifugation, the pellet was resuspended with SDS-PAGE reducing sample buffer and resolved by SDS-PAGE. WB was developed to detect proteins of interest.

Results

CT alone is sufficient to regulate immature viral particle stiffness

As previously reported (*3*, *13*), HIV-1 Env, specifically the CT domain, is necessary for maintaining stiff viral particles. To discern whether CT alone can stiffen the viral particles, we first deleted the entire Env ectodomain (all of gp120 and most of gp41), leaving the gp41 TM and CT. This construct was poorly incorporated into virions (data

not shown). Introduction of a trimerization domain to replace the ectodomian did not improve incorporation (data not shown). Next, we used GFP to replace the ectodomain leaving TM and CT intact (GFP-TM1). GFP-TM1 incorporates into virions efficiently (data not shown).

Increasing WT Env incorporation gradually increases viral particle stiffness (Fig. 3-1 A). To investigate whether GFP-TM1 can stiffen the viral particles similarly to WT Env, we generated immature particles with escalating amounts of GFP-TM1. GFP-TM1 incorporation level, measured by anti-CT western blot (WB), was normalized to Gag level and reported as a CT:Gag ratio. Increasing GFP-TM1 incorporation progressively stiffens immature particles to or beyond the WT immature level (Fig. 3-1 B). These data show that CT alone is sufficient to stiffen the immature viral particles in a similar manner to WT Env.

Particle stiffness regulates the immature HIV-1 entry

Both stiffness and viral entry are controlled by Env. Therefore, to investigate whether particle stiffness directly regulates viral entry, we need to separate the stiffness and entry-mediating properties of WT Env. GFP-TM1 stiffens viral particles without introducing entry activity (due to its missing ectodomain). ΔCT Env can mediate efficient entry, but contributes little to particle stiffness (*13*). These constructs allow us to modulate stiffness to determine its effect on viral entry activity.

We cotransfected varying amounts of GFP-TM1 plasmid (to modulate stiffness) and a fixed amount of ΔCT Env (to provide entry activity) together with an immature ΔEnv HIV genome. WB was used to quantify CT and ΔCT Env (represented by gp120) incorporation levels. Coexpression with ΔCT mildly increases GFP-TM1 incorporation

level relative to GFP-TM1 alone (supplemental Fig. 3-3). As with GFP-TM1 alone, increasing GFP-TM1 incorporation in the presence of ΔCT Env gradually increases immature particle stiffness (Fig. 3-2 A).

As previously reported, Env with intact CT has minimal effects on mature particle stiffness (*13*). Therefore, as a control, the same series of mature HIV-1 particles with coexpression of GFP-TM1 and ΔCT Env was produced as described for immature ones. AFM measurement confirmed that CT incorporation does not stiffen the mature virions (Fig. 3-2 A). Therefore, the mature series isolates effects of GFP-TM1 incorporation on viral entry independent of changing particle stiffness.

As shown in Fig. 3-2 B, increasing GFP-TM1 incorporation greatly impairs viral entry activity in immature ΔCT particles, while causing only modest reduction in the corresponding mature particles. This result, together with the observation that GFP-TM1 only stiffens the ΔCT viral particles in the immature state, strongly suggests that GFP-TM1 incorporation affects viral entry activity by changing particle stiffness.

Besides viral entry activity, we also observed that increasing GFP-TM1 incorporation reduces viral yield and gp160 processing (protease cleavage of gp160 to gp120 and gp41) (supplemental Fig. 3-4 A, B). Since gp160 processing is required for HIV-1 entry (*7*), this change could provide another explanation for GFP-TM1's effect on viral entry. However, gp160 processing declines similarly in both the immature and mature states, suggesting that the immature-specific changes in entry activity are not due to changes in gp160 processing (supplemental Fig. 3-4 B), although these changes may contribute to the modest decrease in mature particle entry activity. Nevertheless, poor gp160 processing does hamper the quantification of gp120 incorporation level and thus the entry activity

for viruses with high GFP-TM1 incorporation. As a result, normalized entry activity for viruses with 200% GFP-TM1 plasmid input could not be calculated.

In all of the above studies, we used HXB2, a commonly studied CXCR4-tropic laboratory HIV-1 strain (*9, 13*). Next we investigated whether our conclusion also applies for JRFL, a primary CCR5-tropic strain. We coexpressed GFP-TM1 with JRFL ΔCT Env on mature or immature virions. An immature-specific loss of viral entry activity was observed with increasing GFP-TM1 incorporation, as seen with HXB2 ΔCT Env (supplemental Fig. 3-5). Intriguingly, in contrast to HXB2 ΔCT, increasing GFP-TM1 incorporation reduces JRFL ΔCT Env incorporation but not gp160 processing (data not shown). This observation further suggests that neither incorporation nor processing of Env contributes significantly to the immature-specific effect on viral entry induced by GFP-TM1 incorporation.

Particle stiffness regulates viral entry of VSVg pseudovirions

HIV-1 is generally thought to enter target cells at the plasma membrane, though a recent report suggests endocytosis as an entry route (*24*). VSV, as a member of the *Rhabdoviridae* family, is unrelated to HIV-1 and is known to enter target cells via endocytosis mediated by its Env, VSVg (*24-26*). Compared to HIV-1 Env, VSVg incorporates at much higher levels, requires no protease cleavage to mediate entry and is unlikely to interact with GFP-TM1. Investigating the effect of GFP-TM1 incorporation on entry activity of VSVg pseudovirions therefore provides an independent test of the relationship between viral particle stiffness and entry.

As with HIV-1 ΔCT Env, GFP-TM1 and VSVg were coexpressed onto mature or immature HIV-1 virions. WB was used to quantify CT and VSVg incorporation level.

Increasing CT incorporation increases particle stiffness in immature viruses (Fig. 3-3 A). Similarly to the effect on HIV-1 entry, increasing CT incorporation greatly reduces VSVg-mediated entry in immature virions with much less effect on mature virions (Fig. 3-3 B). VSVg incorporation level changes little with increasing GFP-TM1 incorporation (supplemental Fig. 3-6). These results further support our hypothesis that increasing particle stiffness induced by CT incorporation inversely regulates viral entry and shows that it may be a general effect regardless of viral type, entry route and Env incorporation/processing level.

GFP-TM1 does not interact with viral Env

An important assumption of our study is that GFP-TM1 incorporation does not affect viral entry mediated by ΔCT Env or VSVg except by changing particle stiffness. As discussed earlier, GFP-TM1 cannot mediate viral entry itself, and loss of the ectodomain prevents trimer formation between GFP-TM1 and ΔCT Env. Nevertheless, there is still the possibility that GFP-TM1 physically interacts with ΔCT Env or VSVg.

To rule out this possibility fully, we used a nonionic detergent, Triton X-100 (TX100), to dissociate Env from the immature Gag shell. Under Triton X-100 treatment, WT Env associates with the Gag shell due to the CT-Gag interaction, while truncation of CT causes Env dissociation from the Gag shell (*5, 6*). Treating immature virions bearing both GFP-TM1 and JRFL ΔCT Env with TX100, we observed that GFP-TM1 remains associated with the Gag shell while almost all JRFL ΔCT Env dissociates (Fig. 3-4). This result suggests that there is no specific interaction between GFP-TM1 and ΔCT Env to keep ΔCT Env associated with the Gag shell. A similar result was observed for HXB2 ΔCT or VSVg pseudovirions expressing GFP-TM1 (data not shown). These data suggest

that GFP-TM1 does not interact with coexpressed viral Env.

Mild reduction of mature viral entry is likely due to overexpression of exogenous protein on the viral membrane

Although relatively immature-specific, GFP-TM1 does cause modest loss of viral entry activity in the mature state as shown above. We hypothesize that this reduction is due to overexpression of exogeneous protein (i.e. GFP-TM1) on the viral membrane. To test this hypothesis, we employ another membrane protein, PLAP (human placental alkaline phosphatase), to see whether overexpression of PLAP will cause similar modest reduction of viral entry. PLAP is a cell surface, glycosylphosphatidylinositol anchored protein, and does not normally exist on the lymphoid cell surface (*27*). As with GFP-TM1, we cotransfected ΔCT Env (HXB2 strain) with titrating PLAP plasmid levels to produce immature and mature HIV-1 virions. Increasing PLAP incorporation induces modest reduction of viral entry in both mature and immature state, similar to the effect of GFP-TM1 incorporation on mature viral entry (supplemental Fig. 3-7). Therefore, mild reduction of mature viral entry activity is, at least partially, due to the overexpression of exogenous proteins on the viral surface.

Discussion

In this study, we aimed to test whether HIV-1 employs particle stiffness as a novel regulatory mechanism for viral entry. We showed that increasing particle stiffness reduces viral entry activity in two HIV-1 strains and the unrelated VSV. Regulation of particle stiffness (e.g. by interfering with the stiffness switch during viral maturation), may represent a novel inhibitory strategy for HIV-1 entry. To achieve this goal, it is important

next to understand the mechanism by which viral particle stiffness is regulated.

Gag is the major structural protein of viral particles, and we speculate that the stiffness switch during HIV-1 maturation originates from the change of the Gag shell organization. In the immature state, the overall structure of the Gag shell is considered to be maintained mainly by three layers of interaction: NC-RNA interaction in the center, CA-CA multerization in the middle, and MA-membrane interaction (*28-30*). These interactions are greatly altered by PR cleavage. Besides the obvious morphological change, the CA layer transits from a tightly packed hexagonal arrangement (interring distance ~65-80 Å) in the immature state to a loosely packed form (interring distance ~95-110 Å) in the mature state (*31, 32*). MA relies on its N-terminal myristoyl group for membrane binding, and separation of downstream Gag components from MA was shown to partially bury its myristoyl group, which destabilizes the membrane binding and oligomer structure of MA (*29, 33*). A series of Gag mutants in which PR cleavage sites are selectively mutated will be employed to address the important layer(s) of interaction for particle stiffness (*14*).

To address how CT regulates particle stiffness, we will employ truncation mutagenesis to identify the important CT subdomain for immature particle stiffness. Meanwhile, current estimates of the number of HIV-1 Env spikes present on the viral surface are very low (~10 trimers per virion), compared to up to 5,000 Gag molecules in the immature virion Gag shell (*34-37*). An interesting mechanical question is how so few CT domains can dramatically alter a global property, like particle stiffness, in ~100 nm particles. We propose two potential models: first, CT functions during assembly to affect the initial formation of Gag shell in a templating role (analogous to seeding a crystal); second, CT functions via its interaction with Gag to stabilize the whole Gag shell. To distinguish

these two models, the timing of when CT functions to regulate particle stiffness needs to be identified. Waheed et al. previously reported an Env mutant in which a new HIV-1 protease cleavage site was created at the N-terminus of CT (*38*). Using this Env mutant, one could artificially control when CT is cleaved, and then identify the stage during which CT presence is critical to regulate particle stiffness.

Moreover, mature HIV-1 bearing this mutant is resistant to inhibition of viral entry by a cholesterol-binding compound, AME (*38*). HIV-1 virions are enriched in cholesterol as a consequence of their budding from lipid rafts (*39, 40*). This observation raises the question whether lipid membrane components, especially cholestoral, are also important for particle stiffness. It is therefore tempting to speculate that AME may inhibit viral entry by stiffening mature particles, and AME resistance might emerge by severing of the link between Env CT and Gag (via CT truncation). AFM measurement of AME-bound mature HIV-1 and those depleted of cholesterol will help us address this possibility.

Ultimately, structural studies of the Gag/CT interaction will be required to reveal how CT affects the overall Gag shell organization. Studies on other lentiviruses will show us whether the stiffness switch is general phenomenon during lentiviral maturation. A more detailed mechanistic and functional understanding of viral particle stiffness may enable the design of novel entry inhibitors.

Fig 3-1. CT is sufficient to regulate immature HIV-1 particle stiffness.

Different amounts of WT Env (A) or GFP-TM1 (B) were incorporated into immature HIV-1, and the particle stiffness of these viruses was measured using AFM as described in Materials and Methods. Anti-CT and anti-CA antibodies were used in WB to detect CT-containing proteins (WT Env or GFP-TM1) and Gag, respectively. GFP-TM1 or WT Env incorporation levels per virion were calculated in the resulting viruses as CT:Gag ratios. Error bars indicate the stand error of the mean (SEM).

(A). Increasing Env levels stiffen immature HIV-1. Viruses bearding different amount of WT Env are shown (orange diamond). X-axis values represent the Env incorporation levels of viruses normalized to that of virus with 100% Env plasmid input, and Y-axis values represent viral particle stiffness. The relationship between Env incorporation levels and particle stiffness is fit into a linear equation as shown in the figure.
(B). Increasing GFP-TM1 levels stiffen immature HIV-1. Viruses bearing different amounts of GFP-TM1 (orange diamond) are shown together with immature WT HIV (blue diamond). X-axis values represent the CT (representing GFP-TM1) incorporation levels normalized to that of immature WT, and Y-axis values represent particle stiffness. The relationship between CT incorporation levels and particle stiffness is fit into a linear equation as shown in the figure.

A.

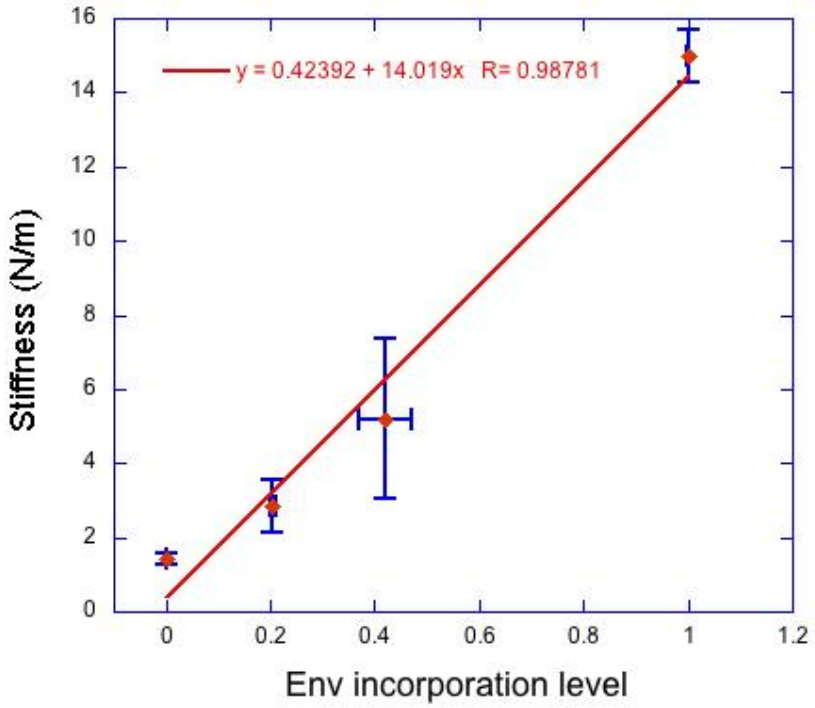
y = 0.42392 + 14.019x R= 0.98781
Stiffness (N/m)
Env incorporation level
0
2
4
6
8
10
12
14
16
0
0.2
0.4
0.6
0.8
1
1.2

B.

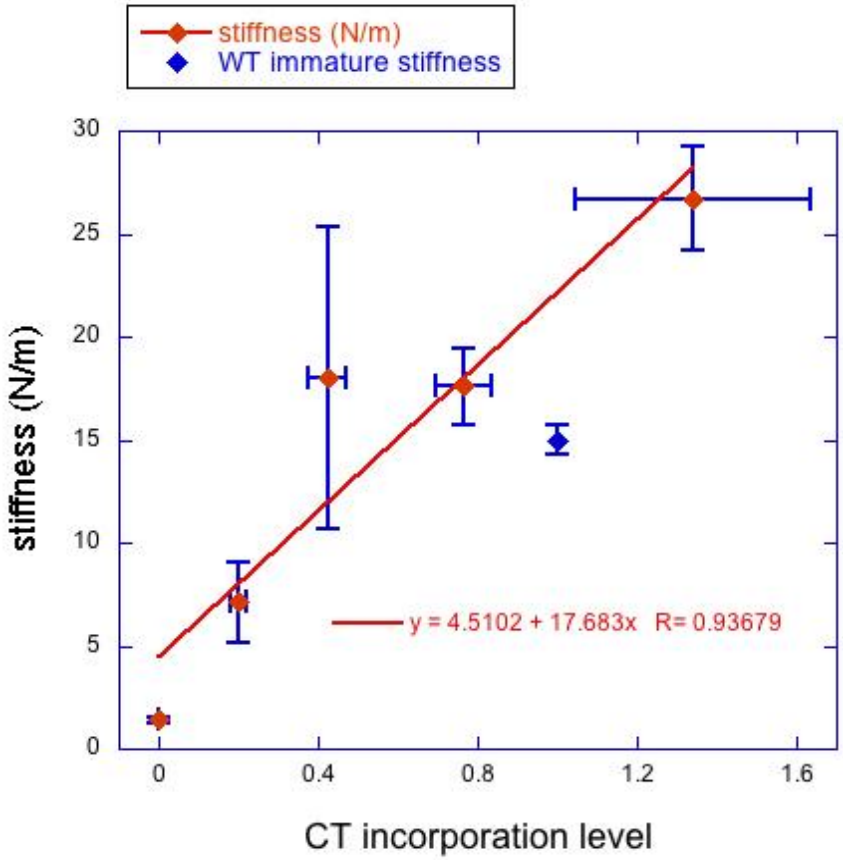
stiffness (N/m)
WT immature stiffness
y = 4.5102 + 17.683x R= 0.93679
stiffness (N/m)
CT incorporation level
0
5
10
15
20
25
30
0
0.4
0.8
1.2
1.6

Fig 3-2. Particle stiffness regulates immature HIV-1 entry.

Different amounts of GFP-TM1 were incorporated into immature or mature HIV-1 bearing ΔCT Env (HXB2). Anti-CT, anti-CA and anti-gp120 antibodies were used in WB to detect CT-containing proteins (GFP-TM1 or WT Env), Gag and ΔCT Env, respectively. As with Figure 3-1, GFP-TM1 amount per virion is represented by CT incorporation level as CT:Gag ratio. The gp120 amount represents all the Env capable of viral entry (ΔCT or WT Env). BlaM assay signals were normalized by gp120 concentration (gp120 per ml) for each virus to obtain its entry ability per Env. Error bars indicate the SEM.

(A). GFP-TM1 stiffens immature HIV-1 when coexpressed with ΔCT Env. Immature (orange dash) viruses bearing different amounts of GFP-TM1 are shown together with immature WT (blue diamond). X-axis values represent CT incorporation levels normalized to that of virus with 100% GFP-TM1 plasmid input. Y-axis values represent the stiffness values.
(B). GFP-TM1 specifically reduces immature viral entry. Immature (orange dash) or mature (blue solid) viruses bearing different amounts of GFP-TM1 are shown together with immature (orange solid diamond) or mature (blue solid circle) WT viruses. X-axis shows CT incorporation levels normalized to those of the corresponding mature or immature viruses with 100% GFP-TM1 plasmid input. Y-axis shows the viral entry activities per Env normalized to those of the corresponding mature or immature ΔCT viruses.

A.

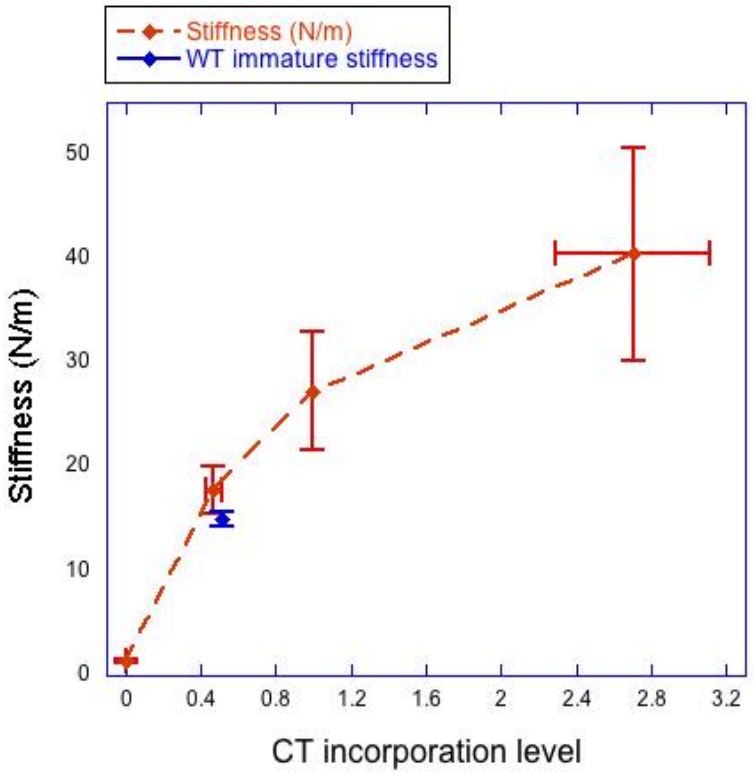
Stiffness (N/m)
WT immature stiffness
Stiffness (N/m)
0
10
20
30
40
50
0
0.4
0.8
1.2
1.6
2
2.4
2.8
3.2
CT incorporation level

B.

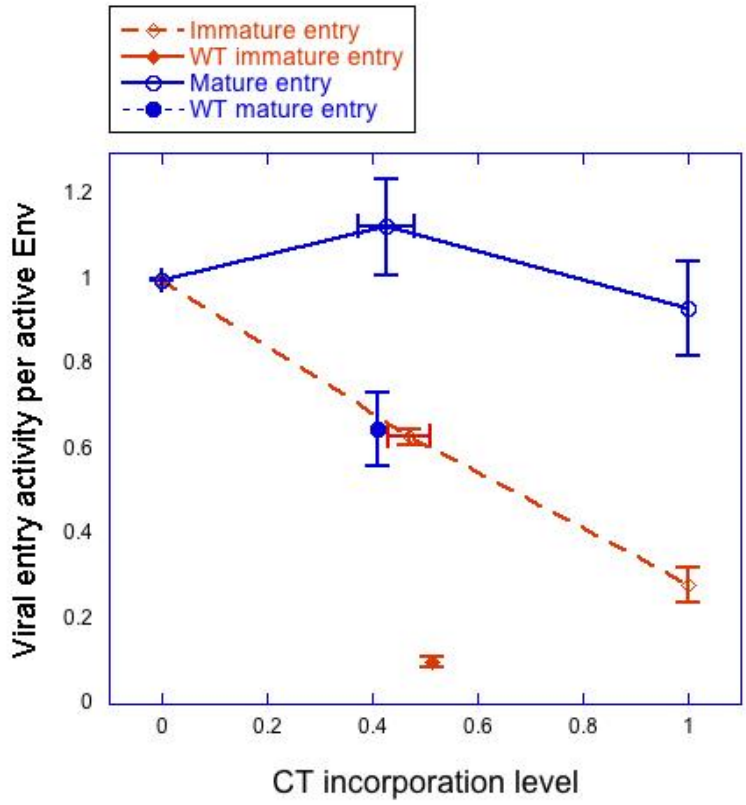
Immature entry
WT immature entry
Mature entry
WT mature entry
Viral entry activity per active Env
0
0.2
0.4
0.6
0.8
1
1.2
0
0.2
0.4
0.6
0.8
1
CT incorporation level

Fig 3-3. Particle stiffness regulates immature entry mediated by VSVg.

Different amounts of GFP-TM1 were incorporated into immature or mature HIV-1 bearing VSVg. GFP-TM1 levels per virion were determined as with Figure 3-2. Anti-VSVg antibody was used in WB to detect VSVg, and quantify VSVg concentration (VSVg per ml). BlaM assay signals were normalized by VSVg concentration for each virus to obtain its entry activity per VSVg. Error bars indicate the SEM.

(A). GFP-TM1 stiffens immature HIV-1 when coexpressed with VSVg. Immature HIV-1 bearing different amounts of GFP-TM1 are shown (orange empty diamonds). X-axis values represent the CT incorporation levels of viruses normalized to that of virus with 100% GFP-TM1 plasmid input. Y-axis shows the stiffness values.
(B). GFP-TM1 specifically reduces the entry of immature viruses bearing VSVg. Immature (orange empty diamonds) and mature (blue empty circles) HIV-1 bearing VSVg and GFP-TM1 are shown. X-axis values represent the CT (GFP-TM1) incorporation levels of immature and mature viruses as with (A). Y-axis shows the entry activities per VSVg normalized to those of the corresponding immature or mature viruses with no GFP-TM1.

A.

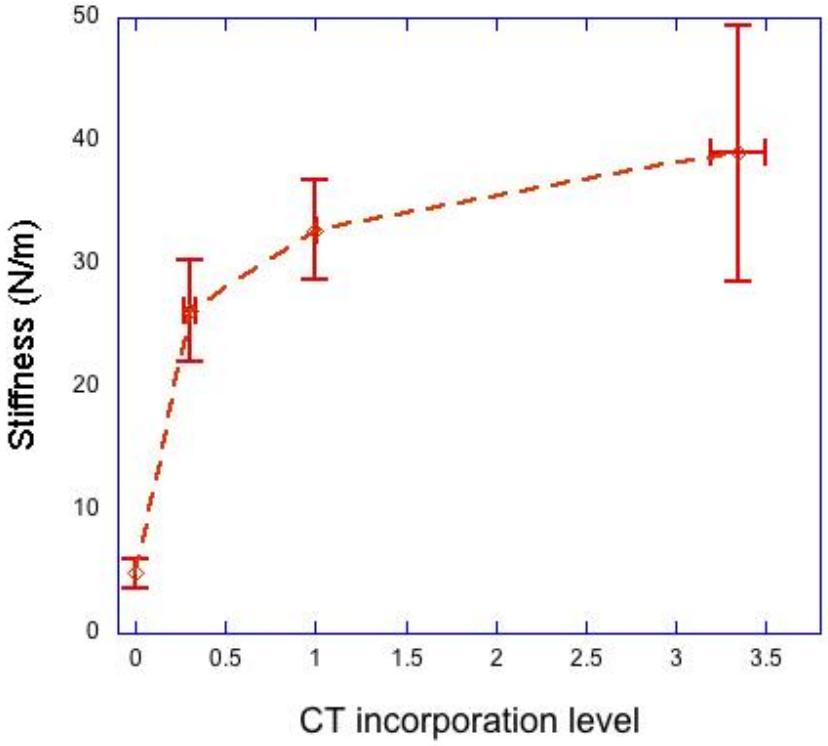
Stiffness (N/m)
50
40
30
20
10
0
0
0.5
1
1.5
2
2.5
3
3.5
CT incorporation level

B.

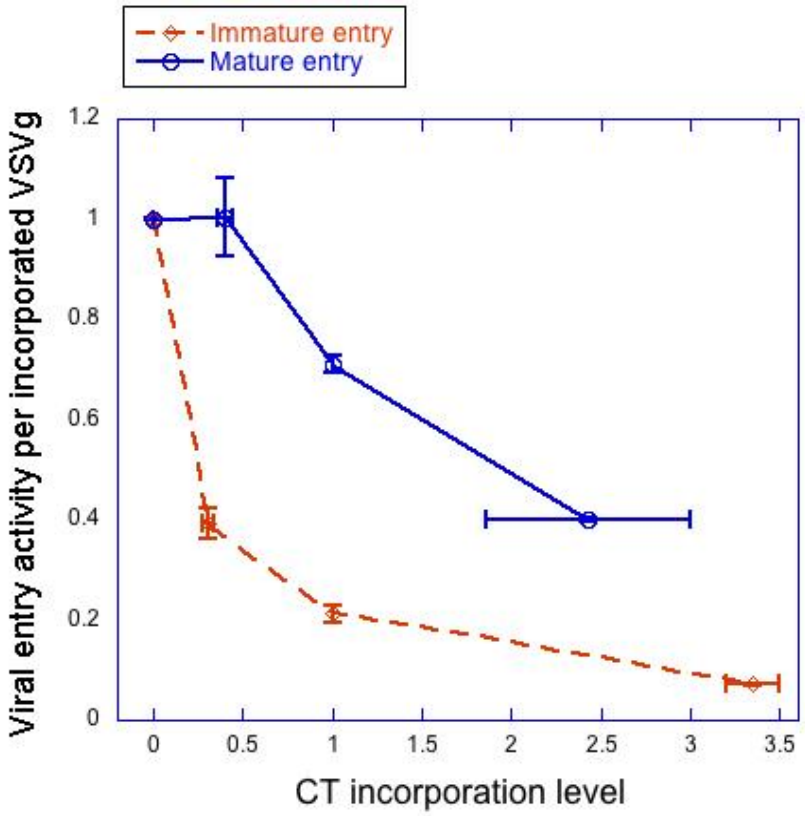
Immature entry
Mature entry
Viral entry activity per incorporated VSVg
1.2
1
0.8
0.6
0.4
0.2
0
0
0.5
1
1.5
2
2.5
3
3.5
CT incorporation level

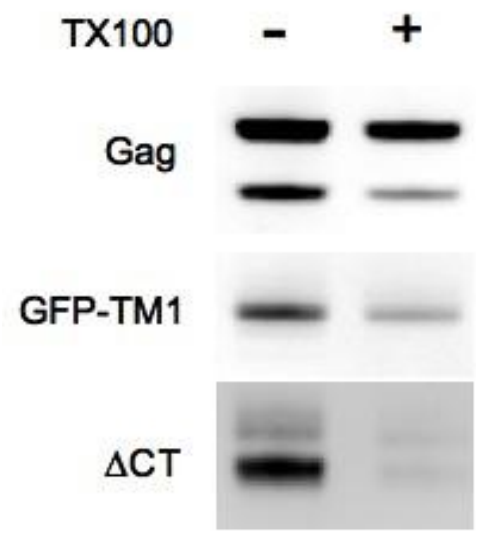

Fig 3-4. GFP-TM1 does not interact with coexpressed viral Env.

Immature HIV-1 bearing both GFP-TM1 and JRFL ΔCT Env was treated with or without 0.5% TX100 as described in Materials and Methods. As for no TX100 control, the viruses were resuspended in 1X TNE buffer instead. Gag, GFP-TM1 and ΔCT Env were detected by WB using anti-CA, anti-CT and anti-gp120 antibodies, respectively.

References

1. Wills, J. W., and Craven, R. C. (1991) Form, function, and use of retroviral gag proteins, *AIDS 5*, 639-654.

2. Berger, E. A., Murphy, P. M., and Farber, J. M. (1999) Chemokine receptors as HIV-1 coreceptors: roles in viral entry, tropism, and disease, *Annu Rev Immunol 17*, 657-700.

3. Chan, D. C., and Kim, P. S. (1998) HIV entry and its inhibition, *Cell 93*, 681-684.

4. Wyma, D. J., Kotov, A., and Aiken, C. (2000) Evidence for a stable interaction of gp41 with Pr55(Gag) in immature human immunodeficiency virus type 1 particles, *Journal of virology 74*, 9381-9387.

5. Cosson, P. (1996) Direct interaction between the envelope and matrix proteins of HIV-1, *EMBO J 15*, 5783-5788.

6. Jiang, J., and Aiken, C. (2007) Maturation-dependent human immunodeficiency virus type 1 particle fusion requires a carboxyl-terminal region of the gp41 cytoplasmic tail, *Journal of virology 81*, 9999-10008.

7. Swanstrom, R., and J.W. Wills. (1997) Synthesis, assembly, and processing of viral proteins in retrovirus, *Cold Spring Harbor Laboratory Press, Plainview, NY.*, 263-334.

8. Coffin, J. M., S.H. Hughes, and H.E. Varmus. (1997) Retroviruses, *Cold Spring Harbor Laboratory Press, Plainview, NY.*

9. Kol, N., Gladnikoff, M., Barlam, D., Shneck, R. Z., Rein, A., and Rousso, I. (2006) Mechanical properties of murine leukemia virus particles: effect of maturation, *Biophysical journal 91*, 767-774.

10. Ivanovska, I. L., de Pablo, P. J., Ibarra, B., Sgalari, G., MacKintosh, F. C., Carrascosa, J. L., Schmidt, C. F., and Wuite, G. J. (2004) Bacteriophage capsids: tough nanoshells with complex elastic properties, *Proc Natl Acad Sci U S A 101*, 7600-7605.

11. Michel, J. P., Ivanovska, I. L., Gibbons, M. M., Klug, W. S., Knobler, C. M., Wuite, G. J., and Schmidt, C. F. (2006) Nanoindentation studies of full and empty viral capsids and the effects of capsid protein mutations on elasticity and strength, *Proc Natl Acad Sci U S A 103*, 6184-6189.

12. Carrasco, C., Carreira, A., Schaap, I. A., Serena, P. A., Gomez-Herrero, J., Mateu, M. G., and de Pablo, P. J. (2006) DNA-mediated anisotropic mechanical reinforcement of a virus, *Proc Natl Acad Sci U S A 103*, 13706-13711.

13. Kol, N., Shi, Y., Tsvitov, M., Barlam, D., Shneck, R. Z., Kay, M. S., and Rousso, I.

(2007) A stiffness switch in human immunodeficiency virus, *Biophysical journal 92*, 1777-1783.

14. Wyma, D. J., Jiang, J., Shi, J., Zhou, J., Lineberger, J. E., Miller, M. D., and Aiken, C. (2004) Coupling of human immunodeficiency virus type 1 fusion to virion maturation: a novel role of the gp41 cytoplasmic tail, *J Virol 78*, 3429-3435.

15. Murakami, T., Ablan, S., Freed, E. O., and Tanaka, Y. (2004) Regulation of human immunodeficiency virus type 1 Env-mediated membrane fusion by viral protease activity, *J Virol 78*, 1026-1031.

16. Dehart, J. L., Andersen, J. L., Zimmerman, E. S., Ardon, O., An, D. S., Blackett, J., Kim, B., and Planelles, V. (2005) The ataxia telangiectasia-mutated and Rad3-related protein is dispensable for retroviral integration, *Journal of virology 79*, 1389-1396.

17. Chen, B. K., Saksela, K., Andino, R., and Baltimore, D. (1994) Distinct modes of human immunodeficiency virus type 1 proviral latency revealed by superinfection of nonproductively infected cell lines with recombinant luciferase-encoding viruses, *Journal of virology 68*, 654-660.

18. Yee, J. K., Miyanohara, A., LaPorte, P., Bouic, K., Burns, J. C., and Friedmann, T. (1994) A general method for the generation of high-titer, pantropic retroviral vectors: highly efficient infection of primary hepatocytes, *Proceedings of the National Academy of Sciences of the United States of America 91*, 9564-9568.

19. O'Rourke, J. P., Olsen, J. C., and Bunnell, B. A. (2005) Optimization of equine infectious anemia derived vectors for hematopoietic cell lineage gene transfer, *Gene Ther 12*, 22-29.

20. Dubay, J. W., Roberts, S. J., Hahn, B. H., and Hunter, E. (1992) Truncation of the human immunodeficiency virus type 1 transmembrane glycoprotein cytoplasmic domain blocks virus infectivity, *Journal of virology 66*, 6616-6625.

21. Hamburger, A. E., Kim, S., Welch, B. D., and Kay, M. S. (2005) Steric accessibility of the HIV-1 gp41 N-trimer region, *J Biol Chem 280*, 12567-12572.

22. Kol, N., Tsvitov, M., Hevroni, L., Wolf, S. G., Pang, H. B., Kay, M. S., and Rousso, I. (2010) The effect of purification method on the completeness of the immature HIV-1 Gag shell, *J Virol Methods 169*, 244-247.

23. Bechhoefer, J. L. H. a. J. (1993) Calibration of atomic-force microscopy tips, *Rev. Sci. Instrum. 64*, 1868-1873.

24. Miyauchi, K., Kim, Y., Latinovic, O., Morozov, V., and Melikyan, G. B. (2009) HIV enters cells via endocytosis and dynamin-dependent fusion with endosomes, *Cell 137*, 433-444.

25. Superti, F., Seganti, L., Ruggeri, F. M., Tinari, A., Donelli, G., and Orsi, N. (1987) Entry pathway of vesicular stomatitis virus into different host cells, *J Gen Virol 68 (Pt 2)*, 387-399.

26. Marsh, M., and Helenius, A. (2006) Virus entry: open sesame, *Cell 124*, 729-740.

27. Chen, B. K., Gandhi, R. T., and Baltimore, D. (1996) CD4 down-modulation during infection of human T cells with human immunodeficiency virus type 1 involves independent activities of vpu, env, and nef, *Journal of virology 70*, 6044-6053.

28. Briggs, J. A., Johnson, M. C., Simon, M. N., Fuller, S. D., and Vogt, V. M. (2006) Cryo-electron microscopy reveals conserved and divergent features of gag packing in immature particles of Rous sarcoma virus and human immunodeficiency virus, *J Mol Biol 355*, 157-168.

29. Ganser-Pornillos, B. K., Yeager, M., and Sundquist, W. I. (2008) The structural biology of HIV assembly, *Curr Opin Struct Biol 18*, 203-217.

30. Cimarelli, A., Sandin, S., Hoglund, S., and Luban, J. (2000) Basic residues in human immunodeficiency virus type 1 nucleocapsid promote virion assembly via interaction with RNA, *J Virol 74*, 3046-3057.

31. Huseby, D., Barklis, R. L., Alfadhli, A., and Barklis, E. (2005) Assembly of human immunodeficiency virus precursor gag proteins, *J Biol Chem 280*, 17664-17670.

32. Mayo, K., Huseby, D., McDermott, J., Arvidson, B., Finlay, L., and Barklis, E. (2003) Retrovirus capsid protein assembly arrangements, *J Mol Biol 325*, 225-237.

33. Wu, Z., Alexandratos, J., Ericksen, B., Lubkowski, J., Gallo, R. C., and Lu, W. (2004) Total chemical synthesis of N-myristoylated HIV-1 matrix protein p17: structural and mechanistic implications of p17 myristoylation, *Proc Natl Acad Sci U S A 101*, 11587-11592.

34. Zhu, P., Liu, J., Bess, J., Jr., Chertova, E., Lifson, J. D., Grise, H., Ofek, G. A., Taylor, K. A., and Roux, K. H. (2006) Distribution and three-dimensional structure of AIDS virus envelope spikes, *Nature 441*, 847-852.

35. Cimarelli, A., and Darlix, J. L. (2002) Assembling the human immunodeficiency virus type 1, *Cell Mol Life Sci 59*, 1166-1184.

36. Frankel, A. D., and Young, J. A. (1998) HIV-1: fifteen proteins and an RNA, *Annu Rev Biochem 67*, 1-25.

37. Turner, B. G., and Summers, M. F. (1999) Structural biology of HIV, *J Mol Biol 285*, 1-32.

38. Waheed, A. A., Ablan, S. D., Roser, J. D., Sowder, R. C., Schaffner, C. P., Chertova, E., and Freed, E. O. (2007) HIV-1 escape from the entry-inhibiting effects of a cholesterol-binding compound via cleavage of gp41 by the viral protease, *Proceedings of the National Academy of Sciences of the United States of America 104*, 8467-8471.

39. Brugger, B., Glass, B., Haberkant, P., Leibrecht, I., Wieland, F. T., and Krausslich, H. G. (2006) The HIV lipidome: a raft with an unusual composition, *Proceedings of the National Academy of Sciences of the United States of America 103*, 2641-2646.

40. Aloia, R. C., Tian, H., and Jensen, F. C. (1993) Lipid composition and fluidity of the human immunodeficiency virus envelope and host cell plasma membranes, *Proceedings of the National Academy of Sciences of the United States of America 90*, 5181-5185.

Supplemental Figures

A.

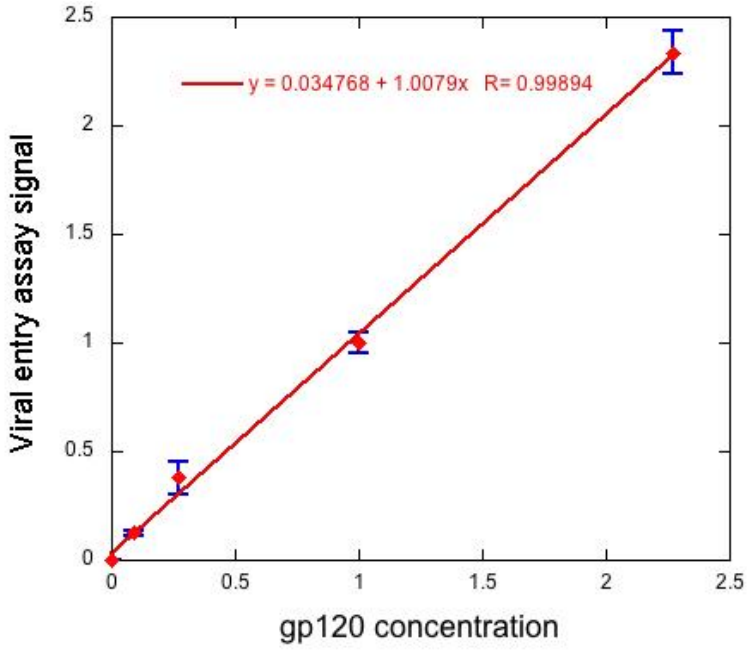

Supplemental Fig 3-1. Optimization of viral entry assay (BlaM assay)
A). gp120 represents active HIV-1 Env that is cleaved by cellular protease and capable of viral entry. To investigate the relationship between gp120 concentration and BlaM assay signal, immature viruses bearing different amounts of HIV-1 ΔCT Env was created and measured for their entry activities. X-axis values represent gp120 concentration (gp120 per ml) for each virus normalized to that of virus bearing 100% ΔCT plasmid input. Y-axis values represent the entry signal for each virus normalized to that of virus bearing 100% ΔCT plasmid input. Error bars (blue) represent the standard error of the mean (SEM). As shown in the fitting equation, y-axis value is proportional to x-axis value at a slope of 1, meaning that BlaM assay signal increases proportionally to gp120 concentration.
B). To investigate the relationship between VSVg concentration and BlaM assay signal, immature particles bearing titrating amount of VSVg was created similarly as immature ΔCT. X-axis values represent VSVg concentration (VSVg per ml) for each virus normalized to that of virus bearing 100% VSVg plasmid input. Y-axis values represent the entry signal for each virus normalized to that of virus bearing 100% VSVg plasmid input. Error bars indicate the SEM. The equation shows that BlaM assay signal also increases proportionally to VSVg concentration.
C). To investigate the relationship between BlaM enzyme incorporation level and BlaM assay signal, immature ΔCT particles were created with different amounts of BlaM incorporated. X-axis values represent BlaM concentration for each virus normalized to that of immature ΔCT with usual BlaM plasmid input. Y-axis values represent the BlaM assay signal for each virus normalized to that of virus with usual BlaM plamsid input. Error bars indicate the SEM. 2-fold variation of BlaM concentration does not cause significant change in BlaM assay signal.

B.

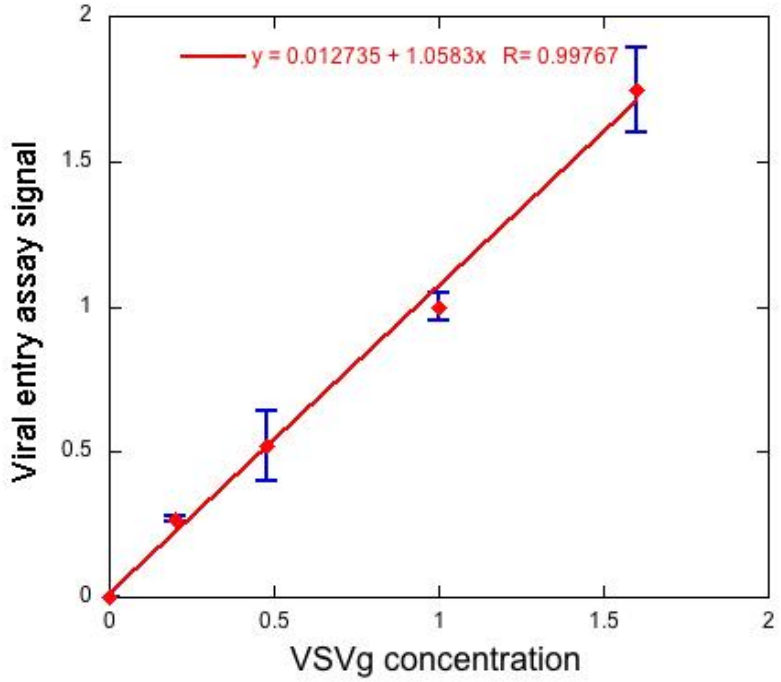

C.

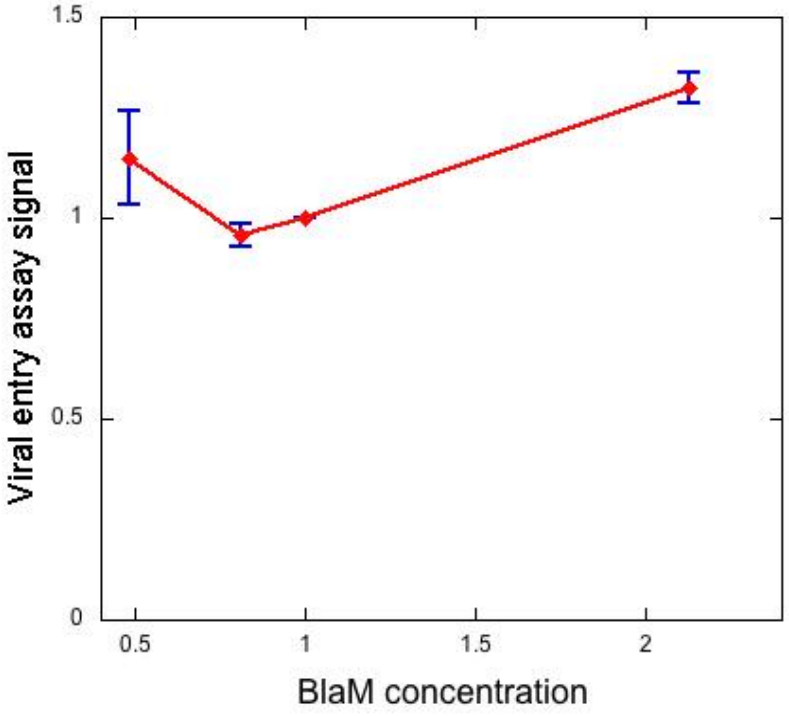

Supplemental Fig 3-1. Optimization of viral entry assay (Continued)

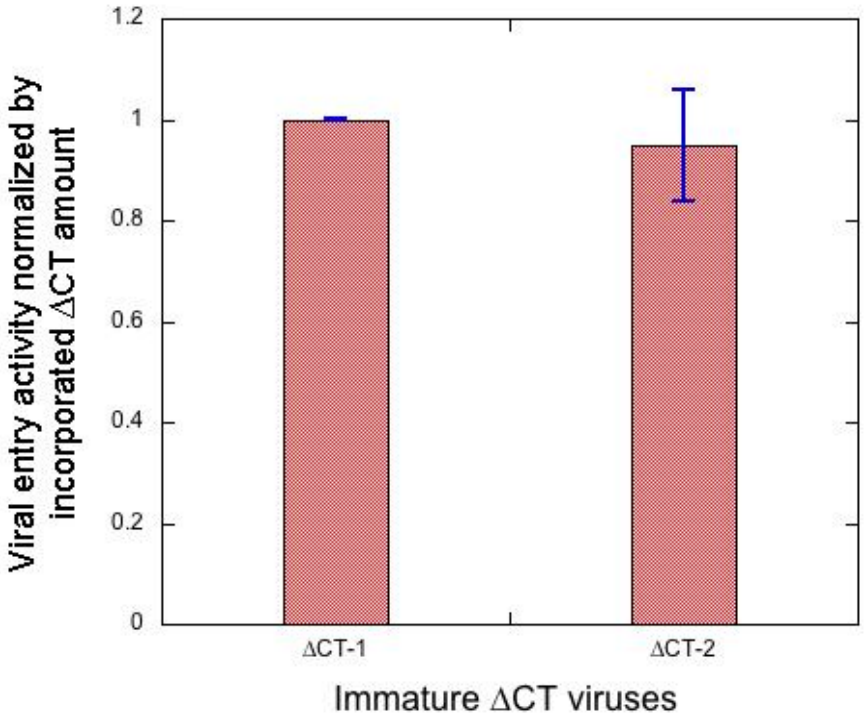

Supplemental Fig 3-2. ΔCT viruses from different batches display similar entry activity.

Immature ΔCT viruses from different batches (generated in different days) were analyzed for their gp120 concentration (gp120 per ml) using anti-gp120 antibody on the same WB and their entry activities in the same BlaM assay. X-axis represents ΔCT viruses from different days, and Y-axis values represent their viral entry activities per Env normalized to one of them. Error bars indicate the SEM.

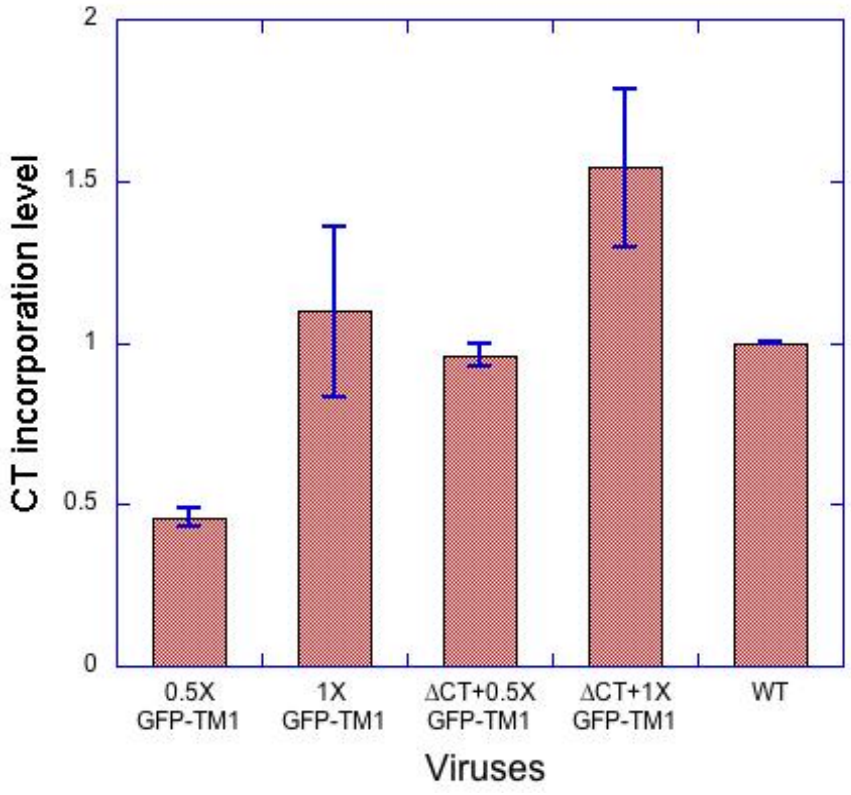

Supplemental Fig 3-3. ΔCT slightly increases GFP-TM1 incorporation level. Different amounts of GFP-TM1 were expressed in immature HIV-1 bearing ΔCT Env. 1X means 100% plamsid input amount. For 0.5X or 1X GFP-TM1, ΔCT plasmid input was replaced by the same amount of pCDF-BS, which is a mammalian-inert expressing vector used to balance plasmid input during transfection. Input amount of all other plasmids (i.e. genome and GFP-TM1) remain the same with the corresponding viruses bearing ΔCT. CT incorporation levels were determined as described in Figure 3-2. X-axis shows different viruses, and Y-axis shows their CT incorporation levels normalized to that of immature WT. Error bars indicate the SEM.

Supplemental Fig 3-4. The effect of GFP-TM1 incorporation on viral yield and gp160 processing.

Immature (orange) and mature (blue) HIV-1 bearing different amounts of GFP-TM1 and ΔCT were generated together with WT viruses. Error bars indicate the SEM.

A). Viral yield. Gag was detected by anti-CA antibody and its concentration (Gag per ml) was quantified as described in Materials and Methods. X-axis values represent CT incorporation levels normalized to those of the corresponding WT viruses. Y-axis values represent viral yield (Gag per ml) normalized to those of the corresponding ΔCT viruses.

B). gp160 processing. Processed Env (gp120) and unprocessed Env (gp160 for WT Env; gp140 for ΔCT Env) were detected by anti-gp120 antibody and quantified as described in Materials and Methods. X-axis values represent CT incorporation levels normalized to those of the corresponding WT viruses. Y-axis values represent gp160 processing efficiency for ΔCT Env (gp120:gp140 ratio) or WT Env (gp120:gp160 ratio).

A.

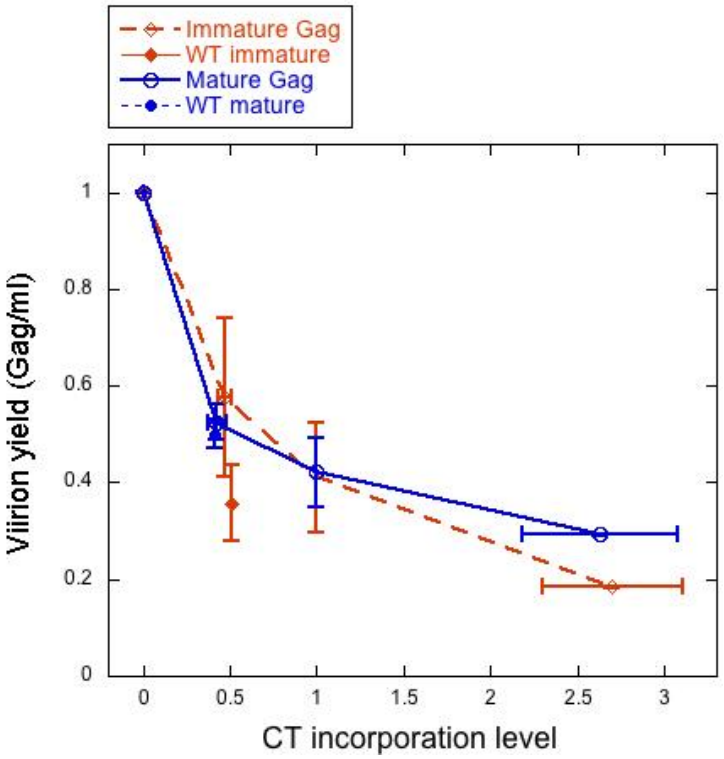
Immature Gag
WT immature
Mature Gag
WT mature
Virion yield (Gag/ml)
1
0.8
0.6
0.4
0.2
0
0
0.5
1
1.5
2
2.5
3
CT incorporation level

B.

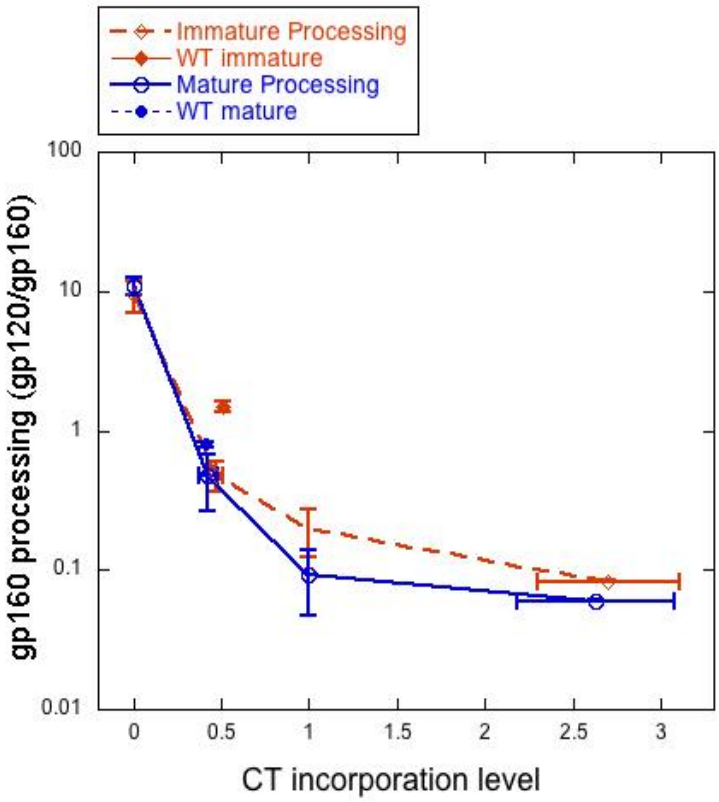
Immature Processing
WT immature
Mature Processing
WT mature
gp160 processing (gp120/gp160)
100
10
1
0.1
0.01
0
0.5
1
1.5
2
2.5
3
CT incorporation level

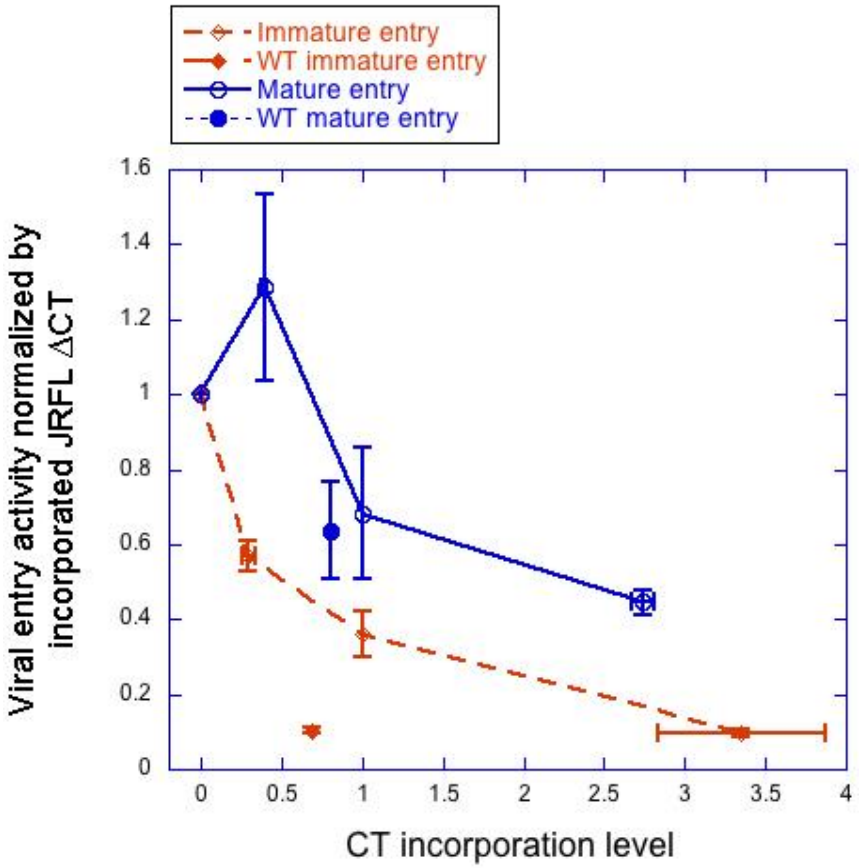

Supplemental Fig 3-5. GFP-TM1 incorporation induces an immature-specific reducing effect on viral entry mediated by HIV-1 JRFL ΔCT Env.
Different amounts of GFP-TM1 were incorporated in the immature (orange diamond) or mature (blue circle) HIV-1 bearing JRFL ΔCT Env. Immature (orange solid diamond) or mature (blue solid circle) JRFL WT viruses were also generated as control. Their GFP-TM1 levels per virion and entry activities were measured as with HXB2 viruses (Figure 3-2). X-axis shows CT incorporation levels (representing CT-containing GFP-TM1 or WT Env) normalized to those of the corresponding immature or mature viruses with 100% GFP-TM1 plasmid input. Y-axis shows the viral entry activities per Env normalized to those of the corresponding immature or mature ΔCT viruses with no GFP-TM1. Error bars indicate the SEM.

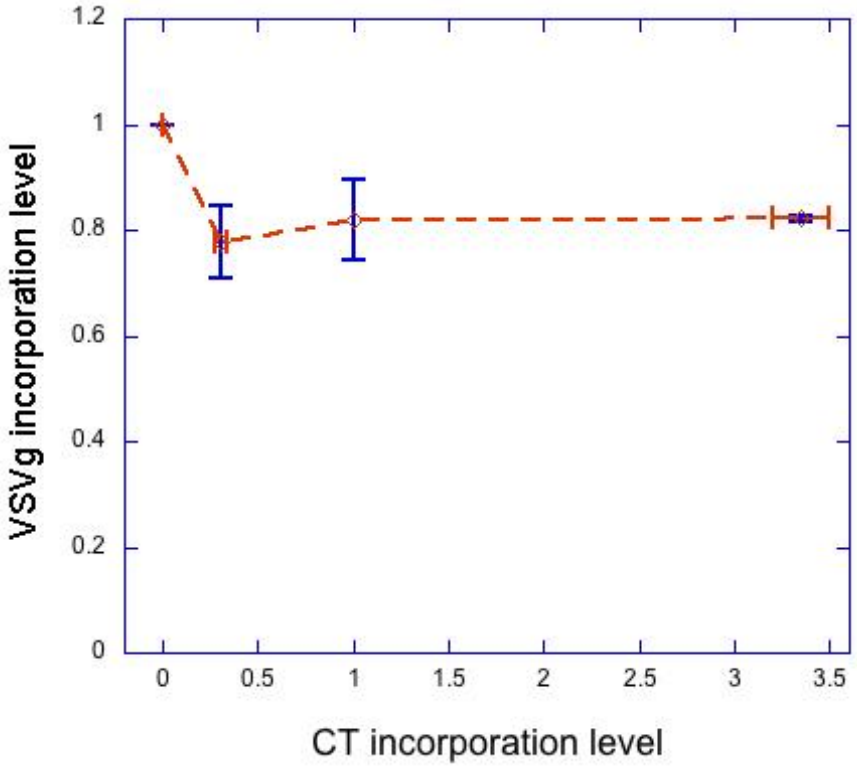

Supplemental Fig 3-6. GFP-TM1 incorporation has little effect on VSVg incorporation into virions.

Different amounts of GFP-TM1 were incorporated in immature viruses bearing VSVg. Anti-CA, anti-CT and anti-VSVg antibodies were used in WB to detect Gag, GFP-TM1 and VSVg, respectively. CT (representing GFP-TM1) and VSVg incorporation levels were calculated as CT:Gag and VSVg:Gag ratio, respectively. X-axis shows CT incorporation levels normalized to that of virus with 100% GFP-TM1 plasmid input, and Y-axis shows VSVg incorporation levels normalized to that of virus with no GFP-TM1. Error bars indicate the SEM.

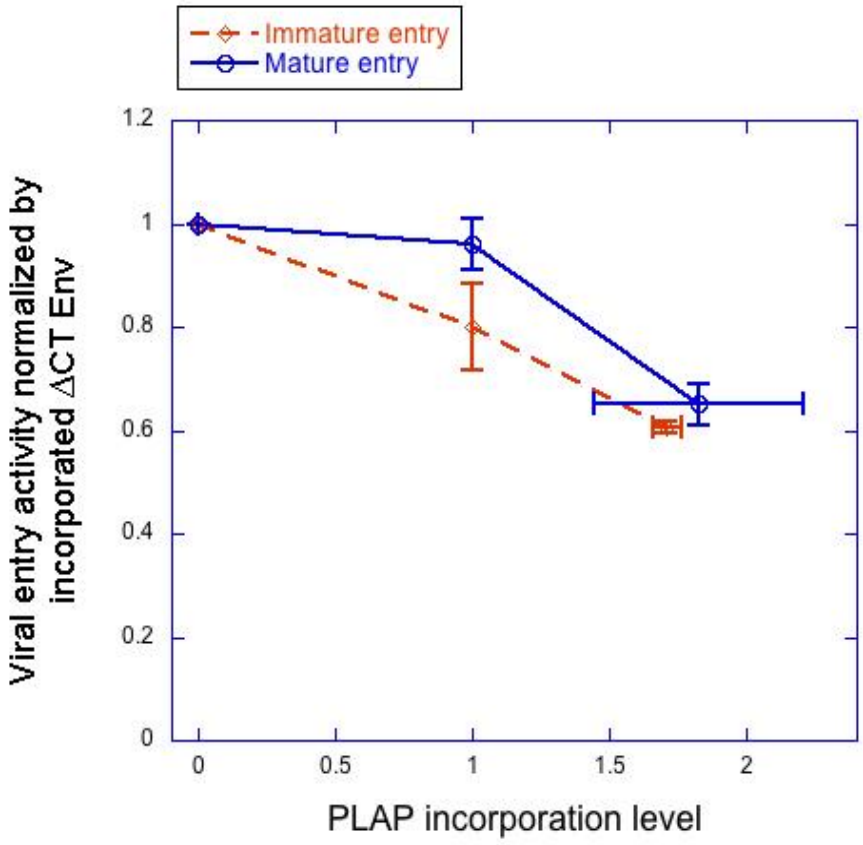

Supplemental Fig 3-7. PLAP incorporation causes mild reduction of viral entry activities in both mature and immature state.

Different amounts of PLAP were incorporated in the immature (orange diamond) or mature (blue circle) HIV-1 particles bearing ΔCT Env. PLAP was detected by anti-PLAP antibody and its incorporation level was calculated as PLAP:Gag ratios. X-axis values represent the PLAP incorporation levels normalized to that of virus with 100% PLAP plasmid input, and Y-axis values represent the viral entry activities per Env normalized to that of virus with no PLAP input. Error bars indicate the SEM.

CHAPTER 4

HIV-1 PARTICLE STIFFNESS AND ITS REGULATION

Hong-Bo Pang and Michael S. Kay

Abstract

After budding out of infected cells, Human Immunodeficiency Virus type 1 (HIV-1) undergoes a maturation process that is required for its infectivity. During maturation, Gag, the major structural protein of HIV-1 particles, is cleaved by HIV-1 protease. This cleavage induces a significant change in viral structure. We previously discovered a dramatic change in viral particle stiffness during maturation, which is further attributed to the cytoplasmic tail (CT) domain of HIV-1 Envelope proteins (Env). Viral particle stiffness was later characterized as a novel regulatory level for viral entry activity. In this study, we aimed to identify the critical factors that regulate viral particle stiffness and clarify how particle stiffness is regulated. A region near the N-terminus of the CT domain and the integrity of Gag structural components were shown to be likely important for particle stiffness regulation. Using an Env mutant with cleavable CT, we obtained preliminary data about the timing of CT's regulation of particle stiffness. Our studies might reveal the nature of viral particle stiffness and its regulation mechanism.

Introduction

During the viral lifecycle, several potentially conflicting demands must be met, including spontaneous assembly during budding, durability in the extracellular environment, efficient membrane fusion and disassembly after entry into a target cell (*4*). Therefore, it is reasonable to speculate that the virus may have different physical properties at distinct phases of its lifecycle. Although much progress has been made in understanding the morphology and molecular machinery of viruses, studies of viral physical properties have been technically challenging and largely neglected until recent studies of particle stiffness using atomic force microscopy (AFM) in several viruses (*2, 4,*

5). Of these, the biggest stiffness change occurs during the maturation process for human immunodeficiency virus type 1 (HIV-1), the causative agent of AIDS (Acquired Immunodeficiency Syndrome) (*2*).

HIV-1, along with almost all other retroviruses (except spumaviruses), undergoes a maturation process required for its infectivity (*6*). Nascent HIV-1 buds out of infected cells as immature virions, and Gag is its major structural protein. The organization of Gag domains is shown in Fig. 4-1 A. Electron microscopy (EM) imaging has long been used to visualize the morphology of viral particles (Fig. 4-1 B). In the immature state, Gag forms a thick spherical protein shell (~17-19 nm) underneath the viral membrane surrounding an electron-lucent center (*7*). Maturation is induced by HIV-1 protease (PR) cleavage of Gag into several products, including three structural proteins, MA (forming the matrix), CA (forming the capsid) and NC (forming the nucleocapsid). After maturation, only MA remains associated with the viral membrane forming a thin matrix layer (~5 nm), while CA forms an electron-dense, conical capsid core housing the viral genome and associated proteins (*7*). Consistent with this striking morphological change, we observed using AFM that immature HIV-1 is ~14-fold stiffer than mature HIV-1, a dramatic change that we dubbed the "stiffness switch" (*2*).

Considering the essential role of Gag in viral structure, it is reasonable to speculate that the stiffness switch is due to reorganization of the Gag shell. To form a single immature HIV-1 particle, up to 5,000 Gag molecules polymerize at the plasma membrane (*8*). Gag preferentially assembles at specific membrane microdomains enriched with sphingolipids and cholesterol (lipid rafts) (*9*). Hence, the viral membrane, which is derived from assembly sites of host cells, is similarly enriched. Expression of Gag alone

is sufficient to generate virus-like particles without other viral proteins or the genome (*10-12*). MA mainly functions to target Gag to the assembly sites at the plasma membrane, while it is largely dispensable for Gag-Gag interactions (*13-15*). CA is the major driving force for Gag polymerization and has been shown by EM to form a hexagonal array in the immature state (*13, 16, 17*). Structural studies show that the hexagonal arrangement of CA might change from a tight packing form (~65-80 Å hexamer-to-hexamer distance (*8, 16, 18*)) to a loosely packed state (~95-110 Å hexamer-to-hexamer distance (*19, 20*)) during maturation. NC mainly functions to bind the viral RNA genome and direct its incorporation into virions (*14*). Although they do not follow the regular hexagonal lattice symmetry, both MA and NC are thought to help initiate and stabilize Gag assembly, probably via their lipid and RNA interactions (*21, 22*). Additionally, Gag contains two spacer peptides, p1 and p2 (or SP2 and SP1, respectively), whose function is relatively unknown. At the C-terminus of Gag, p6 is a Pro-rich domain that interacts with host ESCRT complexes to facilitate viral budding (*23-25*). Deletion of p6 does not change the organization and thickness of Gag shell in immature HIV-1 (*26*).

A rather surprising regulator for viral physical properties is the HIV-1 envelope (Env) protein. Env is initially synthesized as a precursor protein, gp160. In the Golgi complex, gp160 is further cleaved by a cellular protease, furin, into gp120 and gp41 (*27, 28*). With a transmembrane domain, gp41 anchors the whole Env complex in the membrane, and gp120 interacts noncovalently with gp41 on the viral surface. HIV-1 together with other lentiviruses has a long cytoplamic tail on gp41 compared to other retroviruses (~150 vs. 20-30 amino acids) (*29, 30*). Our studies showed that Env CT is necessary and sufficient to stiffen the immature HIV-1 particles. It was previously shown that Murine Moloney

Leukemia virus (MLV), which is not a lentivirus and has a much shorter CT, has a much milder stiffness change (~2-fold) during its maturation (*4*). These studies suggest a correlation between CT length and the extent of stiffness change. Moreover, HIV-1 contains much less Env (~7-14 trimers per particle (*31*)) compared to Gag (up to 5,000 copies per particle). An interesting mechanical question is how so few CT can regulate the stiffness of the whole viral particle.

Although there is no detailed structural information about CT, several important functional domains of CT have been identified (Fig. 4-3 A): three lentivirus lytic peptides (LLP-1, LLP-2 and LLP-3), which are predicted to be amphipathic α-helixes and have cytolytic effects on cell membranes (*32, 33*); a membrane-proximal tyrosine-based YxxL endocytic motif, which is responsible for rapid Env internalization (*34*); a C-terminal dileucine motif, which also mediates Env internalization through its interactions with cellular proteins, AP-2 and AP-1 (*35, 36*); and two palmitoylated Cys residues, which are important for Env incorporation into lipid rafts (*37, 38*). One interesting property of CT is its interaction with MA. Several lines of evidence suggest that CT binds with MA, which is important for Env localization and incorporation into virions (*3, 9*). The region between L751 and C762 (HXB2 numbering) has been shown to be critical for the CT-MA interaction in the presence of nonionic detergent (*3*).

Viral particle stiffness has an important role in viral entry activity. Several groups including ours have shown that mature HIV-1 enters target cells ~10-fold more efficiently than immature HIV-1 (*1, 2, 39*). Entry activity is inversely correlated with the stiffness change during maturation (*2*). We further showed that independently increasing particle stiffness greatly lowers viral entry activity, suggesting that particle stiffness has a

direct novel regulatory role for viral replication. We aim here to decipher how HIV-1 particle stiffness is regulated. Mutagenesis analysis was used to isolate the important sub-domains within CT or Gag that are important for regulating particle stiffness and viral entry. Furthermore, an Env mutant with cleavable CT was used to identify the timing of CT's role in producing stiff particles. Preliminary results indicate that CT is only important for particle stiffness during viral assembly. AFM measurements are currently pending to confirm these conclusions. This study will improve our understanding of viral assembly, Env-Gag interactions, and inform the development of novel HIV-1 entry inhibitors.

Methods and Materials

Plasmids

Plasmids were obtained or constructed as follows: ΔEnv HIV-1 genome containing an inactivating integrase mutant (DHIV3-GFP-D116G (*40*), provided by V. Planelles), HIV-1 wild type (WT) Env expression vector (pEBB-HXB2 (*41*), provided by B. Chen), vector expressing Vpr-β-lactamase (BlaM-Vpr) fusion protein (pMM310 (*1*)), and partial maturation Gag mutants (provided by C. Aiken (*1*)). Immature particles were generated by cloning Gag with all PR cleavage sites mutated (pNL-MA/p6, provided by C. Aiken (*1*)) into the ΔEnv Int− HIV-1 genome, while mature particles were produced using a ΔEnv Int− HIV-1 genome with wild-type (WT) cleavage sites. ΔCT HXB2 Env (Δ147 (*42*)) was provided by E. Hunter and cloned into pEBB-HXB2. CT truncation mutants were obtained from C. Aiken (*3*), and cloned into pEBB-HXB2. Env mutant with cleavable CT (P203L) was obtained from E. Freed (*43*).

Viral preparation and analysis

Pseudovirion particles were produced by cotransfection of 293T cells with ΔEnv int-HIV-1 genome, an Env-expressing vector and pMM310. For example, to generate immature or mature WT virus, 2.5 μg of total DNA (1.23 μg genome vector, 0.819 μg WT Env expressing vector and 0.45 μg pMM310) was transfected into ~1 X 10^6 cells using 10 μg polyethylenimine (PEI, Sigma). The amount of Env-expressing plasmid input for immature WT has been defined as 100%. Media was changed at 6 h after transfection to avoid PEI's toxicity. Supernatants containing secreted viral particles were collected 30 h posttransfection and filtered through 0.2 μm Acrodisc syringe filters (Pall). A series of viruses prepared on the same day is defined as one batch of viruses.

For western blot (WB) analysis of viral concentration and Env incorporation level, virus supernatants were purified by centrifugation through a sucrose cushion (20% sucrose in 1 X TNE buffer: 0.1 M NaCl, 1 mM EDTA, 10 mM Tris, pH 7.6) at 20,000 X g for 90 min at 4℃. The pellet was resuspended in SDS-PAGE reducing sample buffer and resolved by SDS-PAGE. WB was developed using rabbit polyclonal anti-CA (provided by W. Sundquist), mouse monoclonal anti-gp41 Chessie 8 antibody (supernatant from Chessie 8 hybridoma provided by NIH AIDS Research and Reference Reagent Program, ARRRP), sheep polyclonal anti-gp120 (contributed by M. Phelan, ARRRP) and rabbit polyclonal anti-BlaM (Chemicon/Millpore). Blots were quantified using Li-Cor's Odyssey scanner.

Viral entry assay

The viral entry assay was performed as described (*2*). Briefly, HIV-1 particles mixed with DEAE-Dextran (4 μg/ml) were added onto HOS-CD4-CXCR4 cells (provided by B.

Chen), followed by centrifugation at 1,800 X g for 30 min at 4 ℃ and incubation at 37 ℃ for 2 h. After removal of unbound viruses, 1 μM CCF2-AM solution (β-lactamase substrate, Invitrogen) was incubated with cells at 13 ℃ for 17 h. Uncleaved and cleaved CCF2-AM have emission peaks of 520 nm (green) and 447 nm (blue), respectively, under 409 nm excitation. Fluorescent signals from both channels were detected using an Olympus MVX10 fluorescent microscope and quantified using ImageJ software (NIH). Viral entry activity is calculated as described in Chapter 3.

Triton X-100 (TX100) treatment

TX100 treatment of HIV-1 particles was performed as described previously (*3*). Briefly, supernatant containing viruses was first concentrated using the sucrose cushion method as described above. The pellet was resuspended in 0.5% TX100 in 1 X TNE buffer and incubated at 4 ℃ for 30 min before centrifugation in a Beckman TLA-55 rotor at 45,000 rpm for 30 min. After centrifugation, the pellet was resuspended in SDS-PAGE reducing sample buffer and resolved by SDS-PAGE.

DTT recovery of PR activity

When generating immature HIV-1 bearing Env mutant P203L, transfection was conducted as described above and 1 μM PR inhibitor (indinavir, contributed by ARRRP) was added during the media change 6 h after transfection. Cells were grown in the presence of indinavir until viral supernatant collection. The removal of PR inhibitor and the recovery of PR activity were performed as described previously (*44*). Briefly, virus-containing supernatant was centrifuged onto an OptiPrep cushion at 4 ℃, 21,000 X g for 90 min, immediately followed by removing ~90% of the supernatant upper layer. The

remaining supernatant was collected and DTT was added to a final concentration of 1 mM. After 1 h incubation at room temperature, the supernatant was centrifuged again onto an OptiPrep cushion as above, and ~90% of the upper layer supernatant was discarded. The rest of the solution was recovered, adjusted to pH~6.0 and incubated at 37 ℃ for 20 h to allow the reactivated PR to cleave Gag and CT.

Results

Structural integrity of Gag is important to suppress immature entry

The structure of immature HIV-1 is mainly composed of a Gag shell, which contains thousands of Gag molecules tethered together by interactions throughout the whole polyprotein. To isolate the most important layer of interactions for particle stiffness, we employed a series of partial maturation Gag mutants, in which selective PR cleavage sites are mutated (Fig. 4-2 A) (*1*). Using these mutants, we generated viral particles having different Gag layer thickness ranging from mature (thinnest) to immature (thickest). For example, in MA/CA all other Gag domains are cleaved from MA except CA, since the PR cleavage site between MA and CA is mutated. These mutants were coexpressed with WT HIV-1 Env and their entry activities were measured (Fig. 4-2 B). MA/CA and MA/p2 retain similar entry activities to WT mature HIV-1 (pNL4-3). In contrast, the entry activity of MA/NC drops to near the level of immature HIV-1 (MA/p6). This result suggests that any cleavage between MA, CA, p2 and NC releases the inhibitory effect of immature particles on viral entry. In CA6, Gag domains from CA through p6 remain intact, but dissociated from MA. This mutant also showed similar entry activity to mature virions, further supporting the idea that HIV-1 requires the integrity of all Gag structural domains to suppress viral entry in the immature state. AFM measurement of these viruses

is pending and will determine if viral particle stiffness is affected as predicted by the entry data (high stiffness causing low entry activity).

Important CT regions for regulating immature viral entry

To isolate important CT regions for regulating particle stiffness and viral entry, we employed a series of CT truncation and point mutants (Fig. 4-3 A) (*3*). The truncation mutants are named after the number of residues removed from CT's C-terminus. Immature HIV-1 particles bearing these mutants were generated and their entry activities were measured (Fig. 4-3 B). When 104 or more residues were deleted from the C-terminus of CT, the immature virions showed robust viral entry that is similar to immature ΔCT. Inclusion of more C-terminal residues decreases viral entry activity with the biggest drop occurring between CT104 and CT93. This result suggests that the region between L751 and C762 (HXB2 numbering) is important to suppress the immature viral entry. This conclusion differs from a previous report, which claimed that the C-terminal 28 residues of CT are important to suppress immature viral entry (*3*).

To investigate the importance of the CT-Gag interaction for viral entry and particle stiffness, we employed a nonionic detergent, Triton X-100 (TX100), to treat immature HIV-1 bearing different CT truncation mutations. In agreement with a previous report (*3*), we found that the region from L751 to C762 is important for Env-Gag association in the presence of TX100 (Fig. 4-4). This result builds up a correlation between the Env-Gag interaction and immature viral entry, and likely viral particle stiffness. Particle stiffness measurements of these CT truncation mutants are pending.

Timing of CT's regulation of viral particle stiffness and entry

We previously proposed two models for how CT might regulate viral particle stiffness: (1) CT functions as a templating seed during Gag assembly to affect the initial formation of Gag shell; (2) CT stabilizes the stiff Gag shell via its interaction with MA. To distinguish these two models, it is important to identify whether CT regulates particle stiffness during or after viral assembly. An Env mutant (P203L) was previously reported in which a novel PR cleavage site is created at the N-terminus of CT (*43*). Using this Env mutant, we performed the following experiments to specifically cleave CT off Env after viral budding (Fig. 4-5). In the presence of a PR inhibitor, indinavir, immature virions bearing this Env mutant still contain intact CT, showing that PR is inactive. The stiffness of these virions should be similar to that of immature WT HIV-1. Irreversible inactivation of PR by PI was shown to be due to oxidization of Cys in PR to form a disulfide bond, but recovery of PR activity is possible by treatment with a reducing reagent, such as DTT (*44*). Using a similar method, PR activity was recovered after viral budding, resulting in almost all CT being cleaved off Env by reactivated PR. Using this construct, we created immature viruses in which CT is present during assembly but later cleaved after budding.

The DTT treatment itself impairs viral entry activity. Immature WT HIV-1 had lower entry activity after DTT treatment compared to virions without DTT treatment (data not shown). Therefore, immature P203L and WT HIV-1 were produced in parallel in the presence of PI and their PR activities were recovered as described in Materials and Methods. The recovery protocol caused similar reduction for the viral entry activities of immature WT and P203L viruses (before vs. after DTT recovery) (data not shown). This result suggests that immature viruses with CT cleaved after budding have similar entry

activity with immature WT, indicating that CT may only function during viral assembly to regulate the viral particle stiffness. AFM measurements are pending.

Discussion

In this study, we aimed to understand the nature of viral particle stiffness and its regulation. First, we showed that Gag integrity from MA to NC is important to suppress immature viral entry, and likely viral particle stiffness. This result agrees with our expectation that viral particle stiffness originates from the organization of the Gag shell, and the stiffness switch is due to the dramatic reorganization of the Gag shell during maturation. The immature Gag lattice and mature capsid have been intensively studied using various structural methods (*16, 17, 19*). These studies showed that the Gag lattice or mature capsid is mainly composed of hexamer rings formed by CA, while MA and NC do not display a hexagonal arrangement. Recent studies of membrane-bound CA symmetry posed an interesting point on Gag assembly. Individual CA protein can form two forms of hexamer: one is more tightly packed like immature Gag lattice, and another is more loosely packed, similar to mature capsid core (*45*). More intact Gag including all structural proteins (MA, CA, p2 and NC) constrains the hexagonal arrangement to the tightly packing form (*18*), suggesting that the tight-to-loose packing might represent the reorganization of the Gag shell and the changes of viral structure and physical properties.

Gag shell reorganization is not solely limited to the CA layer. MA contains an N-terminal myristyol group that is important for membrane binding of Gag (*7, 46*). Individual MA proteins bind membrane much less efficiently than intact Gag, and deletion of the C-terminal domain of MA enhances membrane binding (*47, 48*). Therefore, a “myristyol switch” model has been proposed in which the myristyol group is

fully exposed in the immature state to enhance membrane binding, but is partially hidden in the mature state. A structural study has revealed the detailed repositioning of several residues within the myristyol group to enhance MA's membrane binding, further supporting this model (*49*). A thermal stability study shows that myristoylated MA polymerizes more stably than unmyristyolated MA (*50*). These results suggest that the maturation process, which induces the partial sequestration of MA's myristyol group, may destabilize the matrix layer. Combining our result that Gag's structural integrity is important for regulation of viral entry (and therefore likely particle stiffness), all the above data suggest that in immature virions, Gag molecules pack more tightly to form a rigid and stiff protein shell, and PR cleavage loosens up the packing of MA and CA layers to generate much softer virions that may lower the energy barrier for membrane fusion and uncoating.

Why is Env CT important? Our study shows that the N-terminal CT is important for regulating viral entry activity, which disagrees with a previous report from the Aiken group. This disparity may be attributed to different measurements of viral entry. The Aiken report focused on the entry activity per virion, while we measure viral entry activity per Env. Moreover, we show that the CT-Gag interaction may be important for particle stiffness, and CT may not be required for stiff particles after budding, although it is currently a preliminary result waiting for AFM confirmation. These results suggest that the CT-MA interaction helps Gag overcome the energy barrier to initiate the formation of a tightly packed Gag shell. However, due to the overwhelming number of MA or Gag to CT, CT cannot maintain the organization of Gag shell during PR cleavage. An alternative explanation for cleavable CT data is that cleaved CT still associates with Gag to stiffen

the immature particles. Env constructs with additional cleavage sites within CT may help us rule out this possibility.

Intracellular organelle or plasma membranes are not homogeneous but rather contain various lipid microdomains. As mentioned above, Gag preferably assembles at one type of microdomain, lipid raft(s), which is highly enriched in sphingolipids and cholesterol. Therefore, HIV-1's membrane also contains relatively high amounts of sphingolipids and cholesterol. The Freed group has reported that a cholesterol-binding compound, AME (amphotericin B methyl ester), specifically inhibits viral entry, and this inhibition is abolished if Env CT is truncated. This result suggests that AME may stiffen viral particles through its binding to viral membrane to inhibit viral entry, while softening by CT truncation reverses the phenotype. AFM measurement of AME-bound viral particles may reveal whether viral membrane also plays a role in particle stiffness.

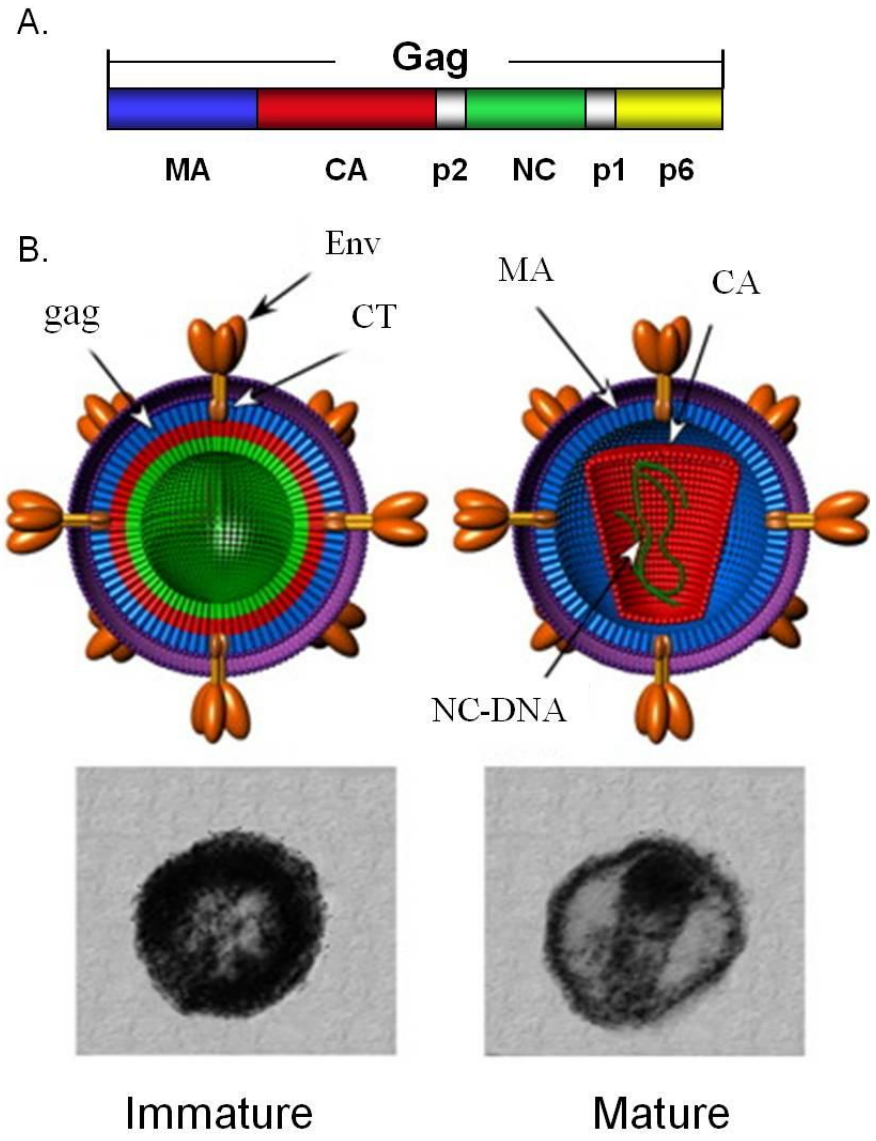

Fig 4-1. HIV-1 Gag and viral structure change during maturation.
(A). Schematic representation of HIV-1 Gag domains.
(B). Schematic models (top) and EM images (bottom) of HIV-1 immature and mature virions. Viral lipid membrane is labeled in purple and HIV Env trimer spikes are in brown. HIV-1 Env does not undergo proteolytic processing during maturation. For simplicity, the unstructrual Gag proteins (p1, p2 and p6) are not included in the virion model. The models are reprinted with permission from (*2*) and the EM images are courtesy of W. Sundquist.

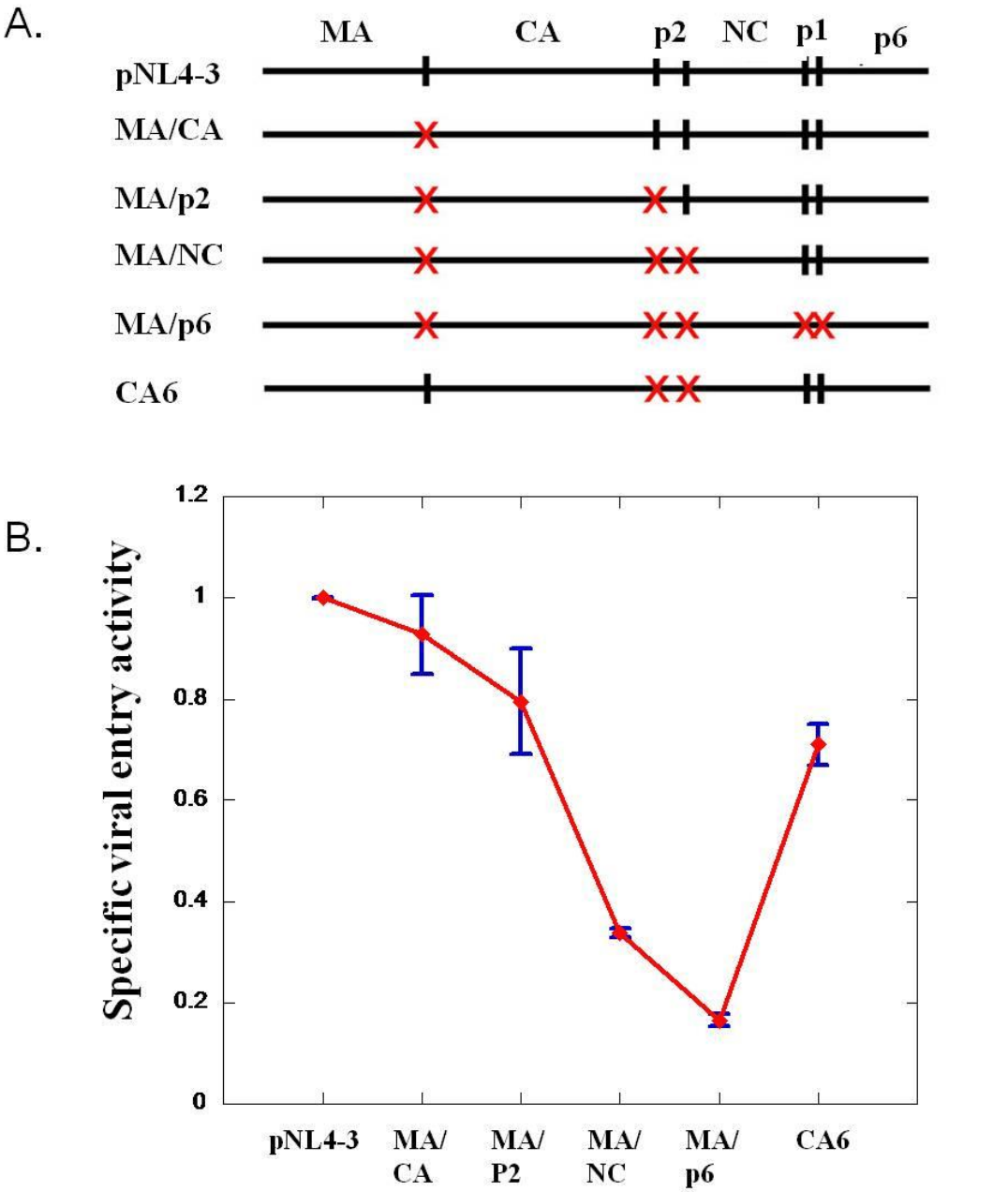

Fig 4-2. Mapping Gag domains important for regulating immature viral entry.

(A). Schematic representation of partial maturation Gag mutants. The red crossing means that the PR cleavage site at that location is mutated. The figure is reprinted with permission from (*1*). (B). The effect of different Gag processing on viral entry. X-axis shows different Gag mutants and Y-axis values represent their viral entry activities normalized to incorporated Env amount and that of pNL4-3.

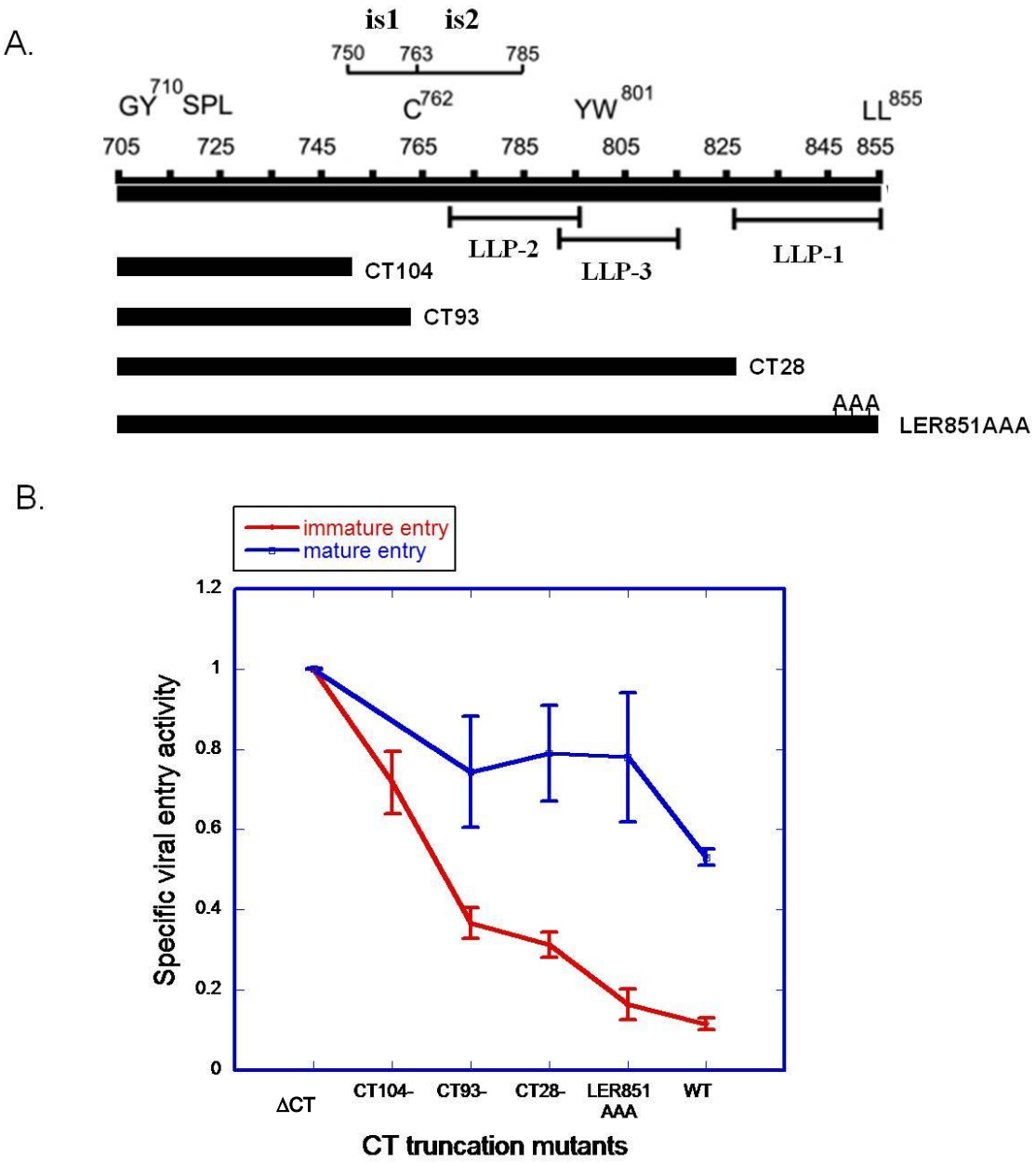

Fig 4-3. Mapping CT sub-domains important for regulating viral entry. (A). Schematic representation of putative CT sub-domains, and CT truncation or point mutation mutants. The figure is reprinted with permission from (*3*). (B). The effect of CT truncation on immature viral entry activity. X-axis shows the CT mutants and Y-axis values represent their viral entry activities normalized to incorporated Env amount and that of ΔCT.

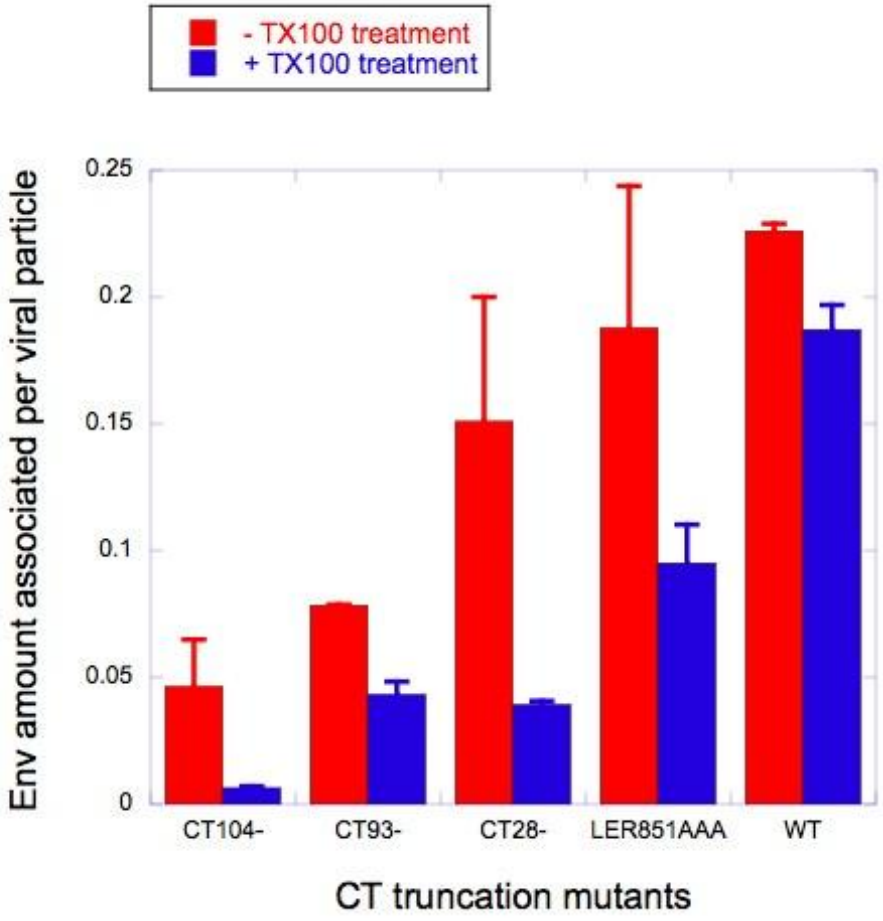

Fig 4-4. Isolation of CT region important for CT-Gag interaction.
The CT mutants listed on the X-axis were expressed on immature HIV particles, which were treated with (blue bar) or without (red bar) 0.5% TX100. Y-axis values were calculated as the ratio of Env:Gag.

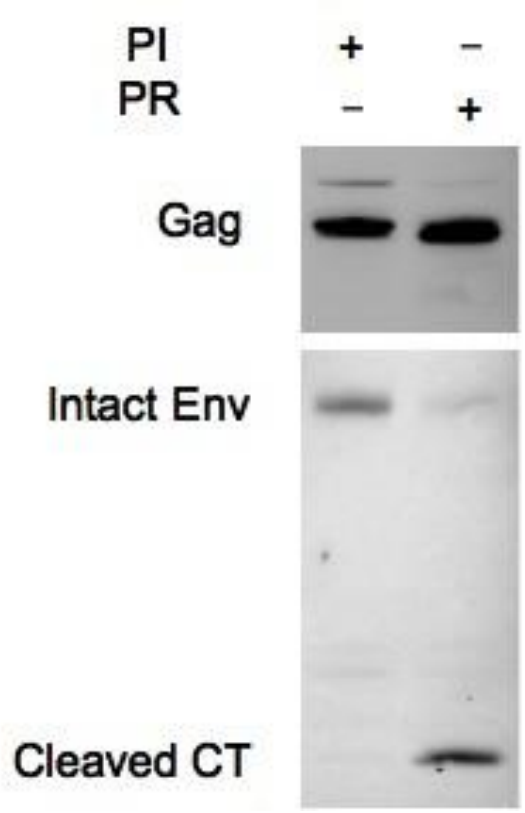

Fig 4-5. CT cleavage by reactivated PR.
Env mutant P203L was coexpressed with MA/NC Gag mutant. Gag and CT were detected by anti-CA (top panel) and anti-CT (bottom panel) antibodies, respectively. In the presence of PI (1 μM indinavir), CT is associated with the rest of Env (higher MW band). After removal of PI and reactivation of PR, CT is cleaved from Env, yielding a low MW band.

References

1. Wyma, D. J., Jiang, J., Shi, J., Zhou, J., Lineberger, J. E., Miller, M. D., and Aiken, C. (2004) Coupling of human immunodeficiency virus type 1 fusion to virion maturation: a novel role of the gp41 cytoplasmic tail, *J Virol 78*, 3429-3435.

2. Kol, N., Shi, Y., Tsvitov, M., Barlam, D., Shneck, R. Z., Kay, M. S., and Rousso, I. (2007) A stiffness switch in human immunodeficiency virus, *Biophysical journal 92*, 1777-1783.

3. Jiang, J., and Aiken, C. (2007) Maturation-dependent human immunodeficiency virus type 1 particle fusion requires a carboxyl-terminal region of the gp41 cytoplasmic tail, *J Virol 81*, 9999-10008.

4. Kol, N., Gladnikoff, M., Barlam, D., Shneck, R. Z., Rein, A., and Rousso, I. (2006) Mechanical properties of murine leukemia virus particles: effect of maturation, *Biophys J 91*, 767-774.

5. Carrasco, C., Carreira, A., Schaap, I. A., Serena, P. A., Gomez-Herrero, J., Mateu, M. G., and de Pablo, P. J. (2006) DNA-mediated anisotropic mechanical reinforcement of a virus, *Proc Natl Acad Sci U S A 103*, 13706-13711.

6. Coffin, J. M., S.H. Hughes, and H.E. Varmus. (1997) Retroviruses, *Cold Spring Harbor Laboratory Press, Plainview, NY*.

7. Gottlinger, H. G., Sodroski, J. G., and Haseltine, W. A. (1989) Role of capsid precursor processing and myristoylation in morphogenesis and infectivity of human immunodeficiency virus type 1, *Proc Natl Acad Sci U S A 86*, 5781-5785.

8. Briggs, J. A., Simon, M. N., Gross, I., Krausslich, H. G., Fuller, S. D., Vogt, V. M., and Johnson, M. C. (2004) The stoichiometry of Gag protein in HIV-1, *Nat Struct Mol Biol 11*, 672-675.

9. Murakami, T. (2008) Roles of the interactions between Env and Gag proteins in the HIV-1 replication cycle, *Microbiol Immunol 52*, 287-295.

10. Gheysen, D., Jacobs, E., de Foresta, F., Thiriart, C., Francotte, M., Thines, D., and De Wilde, M. (1989) Assembly and release of HIV-1 precursor Pr55gag virus-like particles from recombinant baculovirus-infected insect cells, *Cell 59*, 103-112.

11. Campbell, S., and Rein, A. (1999) In vitro assembly properties of human immunodeficiency virus type 1 Gag protein lacking the p6 domain, *J Virol 73*, 2270-2279.

12. Gross, I., Hohenberg, H., Wilk, T., Wiegers, K., Grattinger, M., Muller, B., Fuller, S., and Krausslich, H. G. (2000) A conformational switch controlling HIV-1 morphogenesis, *EMBO J 19*, 103-113.

13. Ganser-Pornillos, B. K., Yeager, M., and Sundquist, W. I. (2008) The structural biology of HIV assembly, *Curr Opin Struct Biol 18*, 203-217.

14. Freed, E. O. (1998) HIV-1 gag proteins: diverse functions in the virus life cycle, *Virology 251*, 1-15.

15. Reil, H., Bukovsky, A. A., Gelderblom, H. R., and Gottlinger, H. G. (1998) Efficient HIV-1 replication can occur in the absence of the viral matrix protein, *EMBO J 17*, 2699-2708.

16. Wright, E. R., Schooler, J. B., Ding, H. J., Kieffer, C., Fillmore, C., Sundquist, W. I., and Jensen, G. J. (2007) Electron cryotomography of immature HIV-1 virions reveals the structure of the CA and SP1 Gag shells, *EMBO J 26*, 2218-2226.

17. de Marco, A., Muller, B., Glass, B., Riches, J. D., Krausslich, H. G., and Briggs, J. A. (2010) Structural analysis of HIV-1 maturation using cryo-electron tomography, *PLoS Pathog 6*, e1001215.

18. Huseby, D., Barklis, R. L., Alfadhli, A., and Barklis, E. (2005) Assembly of human immunodeficiency virus precursor gag proteins, *J Biol Chem 280*, 17664-17670.

19. Li, S., Hill, C. P., Sundquist, W. I., and Finch, J. T. (2000) Image reconstructions of helical assemblies of the HIV-1 CA protein, *Nature 407*, 409-413.

20. Briggs, J. A., Wilk, T., Welker, R., Krausslich, H. G., and Fuller, S. D. (2003) Structural organization of authentic, mature HIV-1 virions and cores, *EMBO J 22*, 1707-1715.

21. Cimarelli, A., Sandin, S., Hoglund, S., and Luban, J. (2000) Basic residues in human immunodeficiency virus type 1 nucleocapsid promote virion assembly via interaction with RNA, *J Virol 74*, 3046-3057.

22. Li, H., Dou, J., Ding, L., and Spearman, P. (2007) Myristoylation is required for human immunodeficiency virus type 1 Gag-Gag multimerization in mammalian cells, *J Virol 81*, 12899-12910.

23. Gottlinger, H. G., Dorfman, T., Sodroski, J. G., and Haseltine, W. A. (1991) Effect of mutations affecting the p6 gag protein on human immunodeficiency virus particle release, *Proc Natl Acad Sci U S A 88*, 3195-3199.

24. Strack, B., Calistri, A., Craig, S., Popova, E., and Gottlinger, H. G. (2003) AIP1/ALIX is a binding partner for HIV-1 p6 and EIAV p9 functioning in virus budding, *Cell 114*, 689-699.

25. von Schwedler, U. K., Stuchell, M., Muller, B., Ward, D. M., Chung, H. Y., Morita, E., Wang, H. E., Davis, T., He, G. P., Cimbora, D. M., Scott, A.,

Krausslich, H. G., Kaplan, J., Morham, S. G., and Sundquist, W. I. (2003) The protein network of HIV budding, *Cell 114*, 701-713.

26. Wilk, T., Gross, I., Gowen, B. E., Rutten, T., de Haas, F., Welker, R., Krausslich, H. G., Boulanger, P., and Fuller, S. D. (2001) Organization of immature human immunodeficiency virus type 1, *J Virol 75*, 759-771.

27. Oliva, R., Leone, M., Falcigno, L., D'Auria, G., Dettin, M., Scarinci, C., Di Bello, C., and Paolillo, L. (2002) Structural investigation of the HIV-1 envelope glycoprotein gp160 cleavage site, *Chemistry 8*, 1467-1473.

28. Veronese, F. D., Joseph, B., Copeland, T. D., Oroszlan, S., Gallo, R. C., and Sarngadharan, M. G. (1989) Identification of simian immunodeficiency virus SIVMAC env gene products, *J Virol 63*, 1416-1419.

29. Hunter, E., and Swanstrom, R. (1990) Retrovirus envelope glycoproteins, *Curr Top Microbiol Immunol 157*, 187-253.

30. Murakami, T., and Freed, E. O. (2000) The long cytoplasmic tail of gp41 is required in a cell type-dependent manner for HIV-1 envelope glycoprotein incorporation into virions, *Proc Natl Acad Sci U S A 97*, 343-348.

31. Zhu, P., Liu, J., Bess, J., Jr., Chertova, E., Lifson, J. D., Grise, H., Ofek, G. A., Taylor, K. A., and Roux, K. H. (2006) Distribution and three-dimensional structure of AIDS virus envelope spikes, *Nature 441*, 847-852.

32. Miller, M. A., Cloyd, M. W., Liebmann, J., Rinaldo, C. R., Jr., Islam, K. R., Wang, S. Z., Mietzner, T. A., and Montelaro, R. C. (1993) Alterations in cell membrane permeability by the lentivirus lytic peptide (LLP-1) of HIV-1 transmembrane protein, *Virology 196*, 89-100.

33. Miller, M. A., Garry, R. F., Jaynes, J. M., and Montelaro, R. C. (1991) A structural correlation between lentivirus transmembrane proteins and natural cytolytic peptides, *AIDS Res Hum Retroviruses 7*, 511-519.

34. West, J. T., Weldon, S. K., Wyss, S., Lin, X., Yu, Q., Thali, M., and Hunter, E. (2002) Mutation of the dominant endocytosis motif in human immunodeficiency virus type 1 gp41 can complement matrix mutations without increasing Env incorporation, *J Virol 76*, 3338-3349.

35. Byland, R., Vance, P. J., Hoxie, J. A., and Marsh, M. (2007) A conserved dileucine motif mediates clathrin and AP-2-dependent endocytosis of the HIV-1 envelope protein, *Mol Biol Cell 18*, 414-425.

36. Wyss, S., Berlioz-Torrent, C., Boge, M., Blot, G., Honing, S., Benarous, R., and Thali, M. (2001) The highly conserved C-terminal dileucine motif in the cytosolic domain of the human immunodeficiency virus type 1 envelope glycoprotein is

critical for its association with the AP-1 clathrin adaptor [correction of adapter], *J Virol 75*, 2982-2992.

37. Yang, C., Spies, C. P., and Compans, R. W. (1995) The human and simian immunodeficiency virus envelope glycoprotein transmembrane subunits are palmitoylated, *Proc Natl Acad Sci U S A 92*, 9871-9875.

38. Bhattacharya, J., Peters, P. J., and Clapham, P. R. (2004) Human immunodeficiency virus type 1 envelope glycoproteins that lack cytoplasmic domain cysteines: impact on association with membrane lipid rafts and incorporation onto budding virus particles, *J Virol 78*, 5500-5506.

39. Murakami, T., Ablan, S., Freed, E. O., and Tanaka, Y. (2004) Regulation of human immunodeficiency virus type 1 Env-mediated membrane fusion by viral protease activity, *J Virol 78*, 1026-1031.

40. Dehart, J. L., Andersen, J. L., Zimmerman, E. S., Ardon, O., An, D. S., Blackett, J., Kim, B., and Planelles, V. (2005) The ataxia telangiectasia-mutated and Rad3-related protein is dispensable for retroviral integration, *J Virol 79*, 1389-1396.

41. Chen, B. K., Saksela, K., Andino, R., and Baltimore, D. (1994) Distinct modes of human immunodeficiency virus type 1 proviral latency revealed by superinfection of nonproductively infected cell lines with recombinant luciferase-encoding viruses, *J Virol 68*, 654-660.

42. Dubay, J. W., Roberts, S. J., Hahn, B. H., and Hunter, E. (1992) Truncation of the human immunodeficiency virus type 1 transmembrane glycoprotein cytoplasmic domain blocks virus infectivity, *J Virol 66*, 6616-6625.

43. Waheed, A. A., Ablan, S. D., Roser, J. D., Sowder, R. C., Schaffner, C. P., Chertova, E., and Freed, E. O. (2007) HIV-1 escape from the entry-inhibiting effects of a cholesterol-binding compound via cleavage of gp41 by the viral protease, *Proc Natl Acad Sci U S A 104*, 8467-8471.

44. Davis, D. A., Yusa, K., Gillim, L. A., Newcomb, F. M., Mitsuya, H., and Yarchoan, R. (1999) Conserved cysteines of the human immunodeficiency virus type 1 protease are involved in regulation of polyprotein processing and viral maturation of immature virions, *J Virol 73*, 1156-1164.

45. Mayo, K., Huseby, D., McDermott, J., Arvidson, B., Finlay, L., and Barklis, E. (2003) Retrovirus capsid protein assembly arrangements, *J Mol Biol 325*, 225-237.

46. Bryant, M., and Ratner, L. (1990) Myristoylation-dependent replication and assembly of human immunodeficiency virus 1, *Proc Natl Acad Sci U S A 87*, 523-527.

47. Zhou, W., and Resh, M. D. (1996) Differential membrane binding of the human immunodeficiency virus type 1 matrix protein, *J Virol 70*, 8540-8548.

48. Spearman, P., Horton, R., Ratner, L., and Kuli-Zade, I. (1997) Membrane binding of human immunodeficiency virus type 1 matrix protein in vivo supports a conformational myristyl switch mechanism, *J Virol 71*, 6582-6592.

49. Saad, J. S., Miller, J., Tai, J., Kim, A., Ghanam, R. H., and Summers, M. F. (2006) Structural basis for targeting HIV-1 Gag proteins to the plasma membrane for virus assembly, *Proc Natl Acad Sci U S A 103*, 11364-11369.

50. Wu, Z., Alexandratos, J., Ericksen, B., Lubkowski, J., Gallo, R. C., and Lu, W. (2004) Total chemical synthesis of N-myristoylated HIV-1 matrix protein p17: structural and mechanistic implications of p17 myristoylation, *Proc Natl Acad Sci U S A 101*, 11587-11592.

APPENDIX A

PEPTIDE MIMIC OF THE HIV ENVELOPE GP120-GP41 INTERFACE

Sunghwan Kim, Hong-Bo Pang and Michael S. Kay

Reproduced with permission from:

Kim S, Pang HB and Kay MS. The Journal of Molecular Biology

Volume 376, Issue 3, Feb 2008, Pages 786-797

doi:10.1016/j.jmb.2007.12.001 *J. Mol. Biol.* (2008) **376**, 786–797

JMB

Available online at www.sciencedirect.com

ScienceDirect

ELSEVIER

Peptide Mimic of the HIV Envelope gp120–gp41 Interface

Sunghwan Kim, Hong-Bo Pang and Michael S. Kay*

Department of Biochemistry, University of Utah School of Medicine, 15 North Medical Drive East, Room 4100, Salt Lake City, UT 84112-5650, USA

Received 19 June 2007; received in revised form 29 September 2007; accepted 3 December 2007

The human immunodeficiency virus envelope glycoprotein (Env) is composed of surface (gp120) and transmembrane (gp41) subunits, which are noncovalently associated on the viral surface. Human immunodeficiency virus Env mediates viral entry after undergoing a complex series of conformational changes induced by interaction with cellular CD4 and a chemokine coreceptor. These changes propagate from gp120 to gp41 via the gp120–gp41 interface, ultimately exposing gp41 and allowing it to form the trimer-of-hairpins structure that provides the driving force for membrane fusion. Key unresolved questions about the gp120–gp41 interface include the specific regions of gp41 and gp120 involved, the mechanism by which receptor and coreceptor-binding-induced conformational changes in gp120 are communicated to gp41, how trimer-of-hairpins formation is prevented in the prefusogenic gp120–gp41 complex, and, ultimately, the structure of the prefusion gp120–gp41 complex. Here, we develop a biochemical model system that mimics a key portion of the gp120–gp41 interface in the prefusogenic state. We find that a gp41 fragment containing the disulfide bond loop and C-peptide region binds primarily to the gp120 C5 region and that this interaction is incompatible with trimer-of-hairpins formation. Based on these data, we propose that in prefusogenic Env, gp120 sequesters the gp41 C-peptide region away from the N-trimer region, preventing trimer-of-hairpins formation until coreceptor binding disrupts this interface. This model system is a valuable tool for studying the gp120–gp41 complex, conformational changes induced by CD4 and coreceptor binding, and the mechanism of membrane fusion.

Edited by M. F. Summers

Keywords: HIV; gp120; gp41; viral entry

Introduction

Human immunodeficiency virus (HIV) enters target cells by fusion of the virus and cell membranes, mediated by the viral envelope glycoprotein (Env). HIV Env is initially synthesized as gp160, which is cleaved by cellular proteases into transmembrane (gp41) and surface (gp120) subunits. After cleavage, gp41 and gp120 remain noncovalently associated and form trimeric spikes on the surface of virions (reviewed by Wyatt and Sodroski[1] and Eckert and Kim[2]) (Fig. 1a). gp120 recognizes appropriate target cells by interacting with CD4 and a coreceptor (typically CXCR4 or CCR5). The initial binding of CD4 induces a major conformational change in gp120 that creates and exposes the coreceptor-binding site.[1,3–5] Subsequent coreceptor binding induces additional poorly characterized conformational changes in the gp120–gp41 complex that are required for membrane fusion and viral entry.

Membrane fusion is directly mediated by gp41, which contains an ectodomain (ED), a transmembrane domain (TM), and a long cytoplasmic tail domain (CT) (Fig. 1b). The ED can be further divided into several regions, listed from N- to C-terminus: hydrophobic fusion peptide (FP), N-peptide region, disulfide bond loop (DSL), C-peptide region, and membrane proximal domain. Currently, only the postfusion structure of gp41 is

*Corresponding author. E-mail address: kay@biochem.utah.edu.

Abbreviations used: HIV, human immunodeficiency virus; ED, ectodomain; TM, transmembrane domain; CT, cytoplasmic tail domain; FP, fusion peptide; DSL, disulfide bond loop; wt, wild type; NEM, *N*-ethylmaleimide; Ac, iodoacetate; RP-HPLC, reverse-phase HPLC; PBS, phosphate-buffered saline; RT, room temperature.

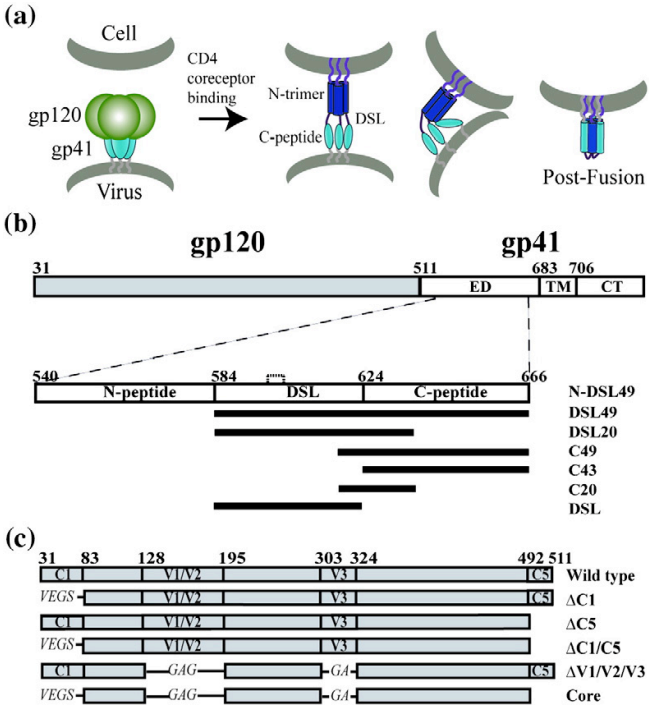

Fig. 1. HIV entry model and schematic of gp41 and gp120 fragments. (a) Working model of HIV entry. (b) Schematic of gp41 fragments. gp41 consists of the ED, TM, and CT. Constructs N-DSL49 (residues 540–666), DSL49 (residues 584–666), DSL20 (residues 584–637), C49 (residues 618–666), C43 (residues 624–666), C20 (residues 618–637), and DSL (residues 584–622) are shown. DSL has one intramolecular disulfide bond, indicated by the dashed line between Cys598 and Cys604. All gp41 fragments contain a C-terminal His tag. (c) JRFL-gp120 deletion constructs. ΔC1 (residues 33–82), ΔC5 (residues 493–511), ΔV1/V2 (residues 128–194), and ΔV3 (residues 303–323) are indicated. For ΔC1, ΔV1/V2, and ΔV3, the deleted loops are substituted with GS, GAG, and GA, respectively. Core gp120 contains all of the deletions (ΔV1/V2/V3 and ΔC1/C5). Amino acid numbering is based on the prototypic HXB2 gp160 sequence.

known. In this structure, three N-peptides form a central parallel trimeric coiled coil that is surrounded by three antiparallel C-peptides, forming a very stable six-helix bundle structure (also known as trimer-of-hairpins).[6–9] Before the formation of this six-helix bundle, gp41 transiently adopts an extended conformation (prehairpin intermediate), in which the N-peptide trimer (N-trimer) has formed but the C-peptide regions have not yet associated with it. This intermediate state of fusion is vulnerable to inhibition by peptides that bind to the N- or C-peptide regions (including the HIV entry inhibitor, T20/Fuzeon).[10–14]

Formation of the six-helix bundle provides the driving force for membrane fusion by bringing the viral and cellular membranes (attached by the TM and FP, respectively) into close apposition (reviewed by Chan and Kim[15]) (Fig. 1a). gp41 stores energy for fusion by initially separating the N- and C-peptide regions and by preventing them from forming the stable six-helix bundle until after CD4 and coreceptor engagement of gp120 triggers fusion at the appropriate time and place. The least understood component of the pathway is the prefusogenic gp120–gp41 complex, which has resisted high-resolution structural analysis. A key unanswered question is how the gp120–gp41 interface maintains gp41 in its metastable prefusogenic conformation (i.e., preventing formation of the very stable trimer-of-hairpins structure).

gp120 contains five conserved constant regions, C1–C5, and five variable loop regions, V1–V5.[16] The most direct evidence implicating specific regions of Env in the gp120–gp41 interface comes from SOS Env, which contains an engineered disulfide bond between the gp41 DSL and gp120 C5 regions. These regions are spatially close enough to form an intermolecular disulfide bond in the native prefusogenic state of Env.[17] The C1 region of gp120 is also thought to be a contributor to the gp120–gp41 interface because mutations that cause gp120 "shedding" from gp41 on the viral surface are predominantly localized to this region, as well as C5 of gp120 and the DSL region of gp41.[18–23] However, many of these Env mutants are also associated with poor proteolytic processing, expression, or trafficking, suggesting global Env misfolding in a substantial fraction of Env rather than direct disruption of the gp120–gp41 interface. In addition, since even a significant fraction of wild-type (wt) Env on the viral surface is misfolded or unprocessed,[24] cell/virus-based studies do not provide clear data on the nature of the gp120–gp41 interface in properly folded Env.

The main obstacle to a detailed understanding of the gp120–gp41 interface has been the lack of high-resolution structural information. Existing HIV Env structures have been extremely informative, but only reveal the gp41 postfusion state (six-helix bundle)[6–9] or the "core" structure of gp120 (excluding most of the variable loops and the C1/C5 regions).[5,25,26] Unfortunately, all currently available gp120 structures lack the N- and C-terminal regions that are most likely to participate in the gp120–gp41 interface. An NMR structure of the isolated C5 region peptide has been determined using trifluoroethanol to induce secondary structure in the other-

wise disordered C5 peptide,[27] but the relevance of this structure under native conditions is not known.

Initial studies on the gp120–gp41 interaction implicated CD4 binding as the trigger for gp120–gp41 dissociation, since exposure to soluble CD4 (sCD4) caused "shedding" of gp120 (e.g., Sattentau and Moore[3] and Moore *et al.*[28]). However, this conclusion has been supplanted by more recent work showing that sCD4-induced shedding is not physiologically relevant to the fusion pathway of primary isolates and may be an artifact due to the significant population of misfolded Env present on virus and cell surfaces.[2,24,29,30]

In order to better define the gp120–gp41 complex and to study its conformational changes during the entry process, we have developed a stable biochemical model system of this interface. First, we have identified gp41 fragments that bind to gp120 and mimic a major portion of the prefusogenic gp120–gp41 interface. Second, using these fragments, we have characterized the regions of gp41 and gp120 contributing to this interface. Finally, we used these fragments to study conformational changes in gp41 affecting the gp120–gp41 interface and changes in the complex by CD4 binding. Most interestingly, this study suggests a mechanism for the separation of the gp41 N- and C-peptide regions in the prefusogenic conformation of the gp120–gp41 complex. This biochemical model system will also likely find broad utility in future mechanistic and structural studies of the gp120–gp41 interface.

Results

Identification of gp41 fragments that bind to gp120

In this study, we employ gp120 from JRFL (a standard primary HIV-1 isolate) for two main reasons. First, primary isolates of HIV-1 do not suffer from the gp120 shedding artifact seen in many laboratory-adapted isolates in the presence of sCD4.[31] As a typical primary R5 strain, JRFL is more likely to reflect the gp120–gp41 interaction of clinical isolates. Second, a previously studied C-peptide, T20, has been reported to bind in a non-specific manner to the V3 loop of X4 strain gp120 in the presence of sCD4, but not to R5 strain gp120.[32,33]

We constructed a variety of HIV-1 gp41 fragments (named as shown in Fig. 1b) to find those that bind to JRFL gp120 and potentially mimic the gp120–gp41 binding interface. Importantly, to prevent gp41 trimer-of-hairpins formation, we avoided including both N- and C-peptide regions in the same fragment. We excluded the N-peptide region from further studies based on preliminary screening showing that gp41 fragments containing both the N-peptide and DSL regions did not interact with gp120 (data not shown). Therefore, our main series of fragments focused on the DSL and C-peptide regions.

DSL49, DSL20, and C49 show weak binding to gp120, which is significantly enhanced in the presence of sCD4 (Fig. 2a and b). Both with and without sCD4, DSL49 shows the strongest binding, followed by DSL20 and C49, while DSL, C20, and C43 do not show detectable binding to gp120. Thus, the N-terminal part of the C-peptide region has a significant role in this interaction, as shown by the increased binding of DSL20 *versus* DSL and C49 *versus* C43. The increased binding of DSL49 compared to DSL20 also suggests a contributing role of the C-terminal part of the C-peptide region.

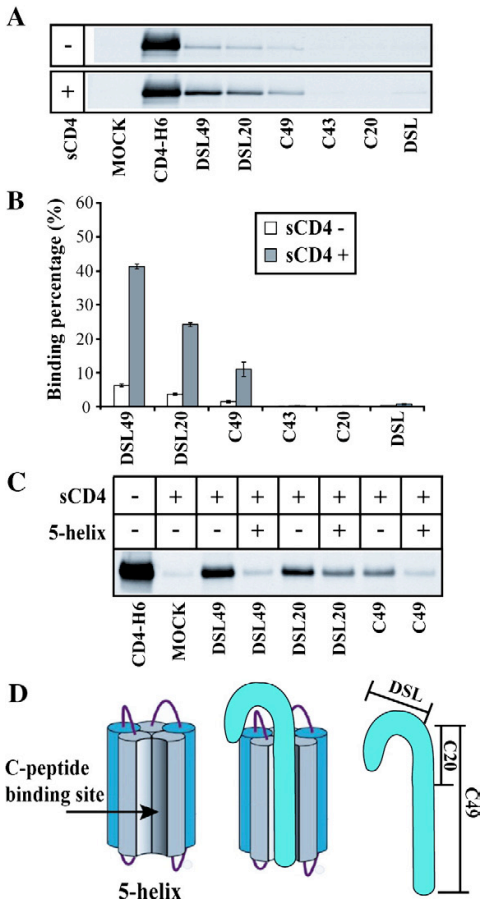

Fig. 2. Binding of gp41 fragments to gp120. (a) gp41 fragments were incubated with gp120 in the presence or in the absence of untagged sCD4 and precipitated with Ni^+ beads. Eluents were deglycosylated and analyzed by nonreducing SDS-PAGE Western blot analysis with anti-gp120 antibody. Mock lane contains gp120 without any gp41 fragment. (b) Quantification of monomeric gp120 binding from (a). Binding percentage was normalized to the amount of gp120 precipitated by CD4-H6 in the absence of untagged sCD4. (c) DSL49, DSL20, and C49 incubated with gp120 in the presence or in the absence of sCD4 and 5-helix as indicated. (d) Schematic diagram of 5-helix binding to gp41 fragments.

Maintaining the metastable prefusogenic gp41 conformation

For trimer-of-hairpins formation and membrane fusion to occur at the appropriate time and place, the N- and C-peptide regions must be prevented from associating until after both CD4 and coreceptor have bound to gp120. The interaction we observed between C-peptide-containing fragments (DSL49, DSL20, and C49) and gp120 suggests a possible mechanism for the sequestration of the C-peptide region from the N-peptide region. To test this idea, we measured the interaction of our gp41 fragments with gp120 in the presence of 5-helix. 5-Helix is an engineered protein that binds to C-peptides with high (subpicomolar) affinity to reconstitute the six-helix bundle (Fig. 2d).[10] The addition of 5-helix to DSL49 or C49 dramatically decreased their interaction with gp120 (Fig. 2c). In order to show that this effect was not induced by competitive binding of 5-helix to gp120, we used glutaraldehyde cross-linking to monitor the interaction of 5-helix and gp120. While DSL49 made a crosslinked complex with gp120 and sCD4, 5-helix could not (data not shown). DSL20's interaction with gp120 was also decreased by 5-helix, but less dramatically than for DSL49 and C49 (Fig. 2c). This smaller decrease likely results from DSL20's partial C-peptide sequence, which reduces its binding affinity for 5-helix. These results show that the six-helix bundle conformation of gp41 is not compatible with the stable formation of the interface between our gp41 fragments and gp120, supporting the idea that this interface sequesters the C-peptide region and prevents six-helix bundle formation.

The gp120 C5 region forms the main interaction interface with gp41 fragments

To define the binding site for our gp41 fragments in gp120, we examined a series of gp120 deletion constructs (Fig. 1c). Each deletion mutant was incubated with DSL49 and DSL20, which show the strongest interaction with wt gp120 (Fig. 2a and b). First, ΔC1-gp120, ΔC5-gp120, and ΔC1/C5-gp120 were examined, since the C1 and C5 regions have been previously suggested to participate in the gp120–gp41 interface. In the presence of sCD4, ΔC5 and ΔC1/C5 show significantly weakened interactions, while ΔC1 is only slightly weakened compared to wt gp120 (Fig. 3a and b). These results indicate that the gp120's C5 region is critical for DSL49 or DSL20 binding, while the C1 region is of lesser importance.

Next, the contribution of gp120's variable loops was examined using ΔV1/V2/V3-gp120 and core-gp120 (ΔV1/V2/V3/C1/C5) (Fig. 3). In the absence of sCD4, ΔV1/V2/V3-gp120 showed stronger binding than wt gp120 to DSL49 and DSL20, but core-gp120 only showed a very weak residual interaction, similar to ΔC1/C5-gp120. In the presence of sCD4, ΔV1/V2/V3-gp120 and wt gp120 showed similar binding to DSL20 and DSL49, while core-gp120 only bound weakly. These results indicate that the main variable loops of gp120 (V1/V2/V3) are not required for the interaction with our gp41

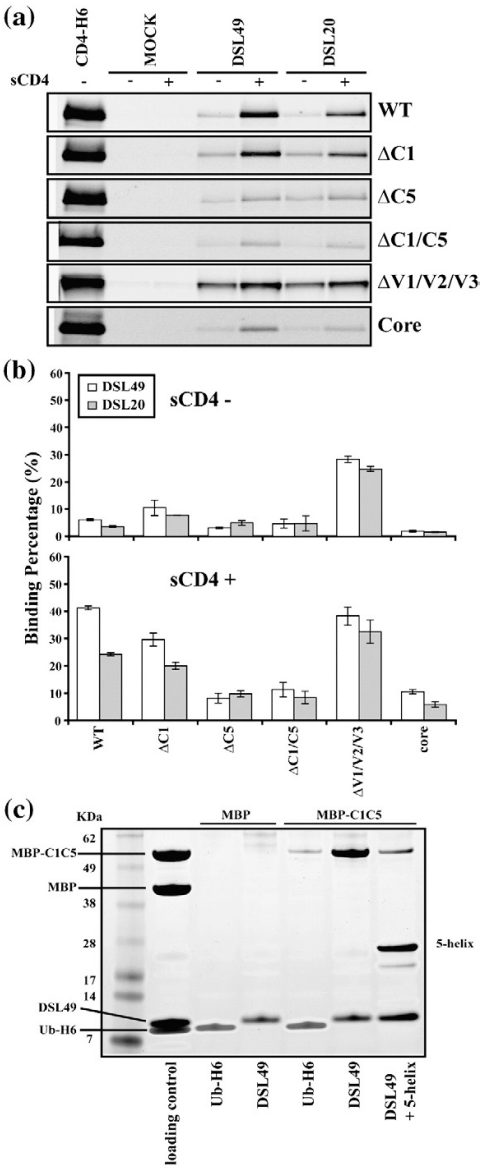

Fig. 3. Interaction between gp41 fragments and gp120 deletion mutants or MBP-C1/C5. (a) gp120 deletion constructs were coprecipitated with DSL49 and DSL20± sCD4 as described in Fig. 2a. (b) Quantification of monomeric gp120 binding from (a), normalized as in Fig. 2b. (c) Coprecipitation of 10 μM MBP or MBP-C1/C5 with 2 μM DSL49. As a negative control, His-tagged Ub (Ub-H6) was used. Loading control contains 1 μM MBP and MBP-C1/C5 (corresponding to 50% of maximal binding to 2 μM DSL49) and 2 μM DSL49 and Ub-H6 (100% of maximal binding). Proteins precipitated by Ni^{+} beads were analyzed by SDS-PAGE.

fragments, in contrast to the previously reported nonspecific T20 binding to X4 strain gp120.[32,33]

To confirm that the gp120 regions identified by screening with deletion mutants bind to DSL49 specifically, we produced C5 and C1/C5 fragments of gp120 fused to the C-terminus of maltose-binding protein (MBP; MBP-C5 and MBP-C1/C5, respectively). MBP is commonly used as a fusion partner and aids the production, detection, and solubility of these small peptide fragments. DSL49 showed strong binding to MBP-C1/C5 (Fig. 3c), but did not bind to MBP-C5 (data not shown). This interaction was reduced by the addition of 5-helix, as observed with binding to gp120 (Fig. 2c). As an additional control, we observed that sCD4 had no effect on this interaction, as expected, since MBP-C1/C5 lacks the CD4-binding site of gp120 (data not shown). Although C1 did not show a major role in the interaction with DSL49 in the context of gp120, C1 may help stabilize or solubilize the isolated C5 fragment in the context of our MBP construct.

Mapping the minimal determinants of gp41 fragment binding to gp120

We further dissected DSL20 to determine the minimal fragment capable of interacting with gp120. First, we investigated the role of the DSL N-terminal region in gp120 binding by truncating the N-terminus of DSL20 (Fig. 4a). Both 13- and 20-residue deletion mutants (Δ13-DSL20 and L20, respectively) dramatically decreased interaction with both wt and ΔV1/V2/V3-gp120 (Fig. 4b) compared to DSL20, indicating that the N-terminal 13 residues of DSL20 are required for this interaction. Next, we tested the role of the disulfide bond in DSL20 by mutating both Cys residues to Ser to produce DSL20ss (Fig. 4a). DSL20 and DSL20ss showed similar binding affinities for both wt and ΔV1/V2/V3-gp120 (Fig. 4b), indicating that the DSL disulfide does not play a significant role in binding gp120.

Since the DSL disulfide is highly conserved in all known HIV and SIV strains,[8,34] it likely plays a critical role in Env function. Previous studies have reported that peptides from the DSL region may bind directly to membranes.[35,36] To address the specific role of the disulfide bond in DSL, we measured the binding of DSL20 and DSL49 to cellular membranes. DSL49 and DSL20 both showed significant cell surface binding by Western blot analysis (Fig. 4c). This result was confirmed by cell surface immunostaining, which also revealed a punctate-binding pattern (Fig. 5). In contrast, C49 shows minimal cell surface binding (data not shown).

To further examine the role of the DSL disulfide bond in mediating membrane binding, we disrupted the disulfide bonds using: mutagenesis (DSL49ss and DSL20ss), reduction (DSL49-red), and reduction with blocking by the hydrophobic *N*-ethylmaleimide (NEM) and hydrophilic iodoacetate (Ac) to produce DSL49-NEM and DSL49-Ac, respectively. DSL20ss, DSL49ss, and DSL49-red bound to the cell surface much less efficiently (Figs. 4c and 5). DSL49-Ac also bound to the cell surface very weakly (Fig. 4d). In contrast, DSL49-NEM displayed more cell surface binding than DSL49ss, DSL49-Ac, and DSL49-red. These results indicate that the DSL disulfide's hydrophobic character is likely the most important determinant for membrane binding, since the introduction of more polar groups (e.g., reduced Cys, Ser, or Ac) is more disruptive than hydrophobic substitutions (e.g., oxidized Cys or NEM). In addition, the cell surface binding of DSL49 and DSL20 is distinct from their binding to gp120, which is not affected by the mutagenesis of the DSL disulfide bond (Fig. 4b). This conclusion is further supported by the cell surface binding of DSL49 in the presence of 5-helix (Fig. 4c), which actually enhances cell surface binding, possibly due to induced helical structure

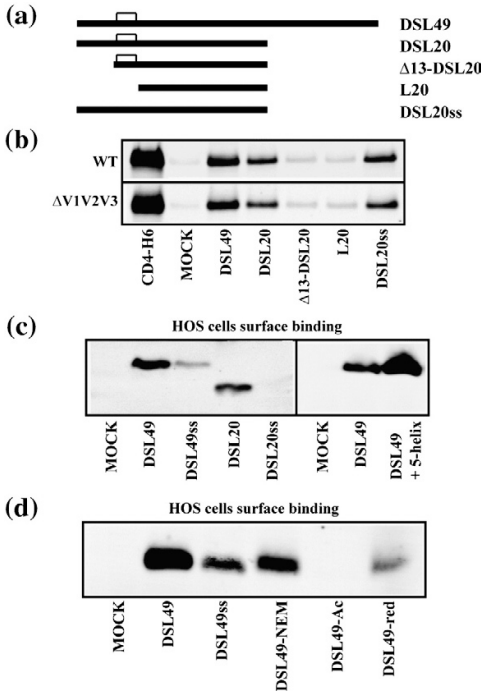

Fig. 4. Binding of DSL20 mutants to gp120 and cell surface. (a) DSL20 mutant constructs: Δ13-DSL20 (residues 597–637), L20 (residues 605–637), and DSL20ss (C598S and C604S). (b) DSL49, DSL20, and DSL20 mutants were incubated with gp120 in the presence of sCD4. Mock lane contains only gp120 and sCD4. (c) Binding of DSL49, DSL49ss, DSL20, and DSL20ss to HOS cells. Right panel shows the effect of 5-helix addition on cell surface binding. Bound proteins on the cell surface were analyzed by Western blot analysis with anti-His tag antibody. Mock lanes were prepared without addition of gp41 fragment. (d) Binding of DSL49, DSL49ss, DSL49-NEM, DSL49-Ac, and DSL49-red to HOS cells.

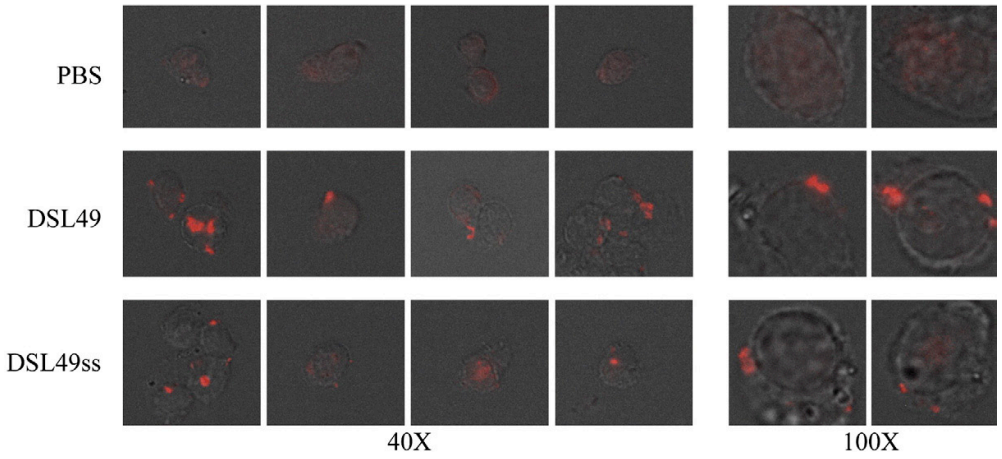

Fig. 5. Immunostaining of DSL49 and its DSL49ss on cellular membrane. DSL49 or DSL49ss was incubated with HOS-pBABE cells and stained with rabbit anti-His_6 antibody and Alexa Fluor 568 goat anti-rabbit antibody. Cells were placed on the slide and photographed at magnifications of 40× and 100×.

or enhanced solubility (a similar enhancement is seen with DSL49ss; data not shown).

Discussion

The gp120–gp41 interface has resisted detailed biochemical and structural characterization for several reasons, including: (1) the fragility of the native gp41 conformation (due to its metastability and strong tendency to adopt the postfusion six-helix bundle structure); (2) the flexible nature of gp120 regions participating in this interface (requiring their removal for crystallography[5,25,26]); and (3) lack of a detailed understanding of the residues in gp120 and gp41 participating in this interface (due to challenges in interpreting Env mutants *in vivo*). The structural and mechanistic details of how the gp120–gp41 interface is affected by receptor and coreceptor binding during HIV entry are also poorly understood. In this work, we make significant progress towards overcoming these barriers by developing a stable biochemical system that partially mimics the gp120–gp41 interface. Using this system, we strengthen previous findings that the gp120 C5 and gp41 DSL regions contribute to the gp120–gp41 interface. The value of this biochemical system is demonstrated by our new findings that the C-peptide region makes key contact with the gp120 C5 region and that this interaction may be responsible for sequestering the C-peptide region and for preventing six-helix bundle formation in the prefusogenic state.

Role of the V1/V2 loops in the gp120–gp41 interface

Most interactions between our gp41 fragments and gp120 are strengthened by sCD4 binding. This result may seem surprising in the context of earlier studies showing sCD4-induced shedding of gp120 in laboratory-adapted strains.[3,28] However, the impact of CD4 binding on the gp120–gp41 interaction in properly folded Env from primary strains is currently unknown. There is strong evidence that sCD4 binding alone is insufficient to release gp120 from gp41, including the ability of HIV to enter CD4(−) cells when sCD4 is provided in *trans* (sCD4-activated fusion)[40] and the existence of CD4-independent HIV strains.[41] The sCD4-induced enhancement of binding may be explained by two possibilities. First, unliganded monomeric gp120 is known to have a flexible structure that is significantly rigidified upon CD4 or antibody binding,[42] which may stabilize the monomeric gp120–gp41 interface. Second, sCD4 binding also triggers specific conformational changes in monomeric gp120 that may facilitate the gp120–gp41 interaction in this biochemical system.

To help explain the effect of sCD4 binding on the monomeric gp120–gp41 interaction, we compared the crystal structures of unliganded and sCD4-bound core gp120 (ΔC1/C5/V1/V2/V3) (Fig. 6). In the unliganded gp120 structure, the V1/V2 stem is located near the N- and C-termini (C1 and C5 stumps), which may allow the V1/V2 loop to occlude the C1/C5 region when the ~80 deleted residues of V1/V2 are present. In the sCD4-bound gp120 structure, the V1/V2 stem undergoes a dramatic movement away from the N- and C-terminal regions and is now located near the V3 loop and coreceptor-binding site.[43] If the V1/V2 loop obstructs gp41 fragment binding in unliganded gp120, we would expect either sCD4 binding or V1/V2 loop deletion to enhance gp41 fragment binding, consistent with our data (see Fig. 3). In support of this idea, deletion of the V1/V2 loop has been shown to functionally substitute for CD4 binding in exposing the coreceptor-binding site of the monoclonal antibody 17b.[44]

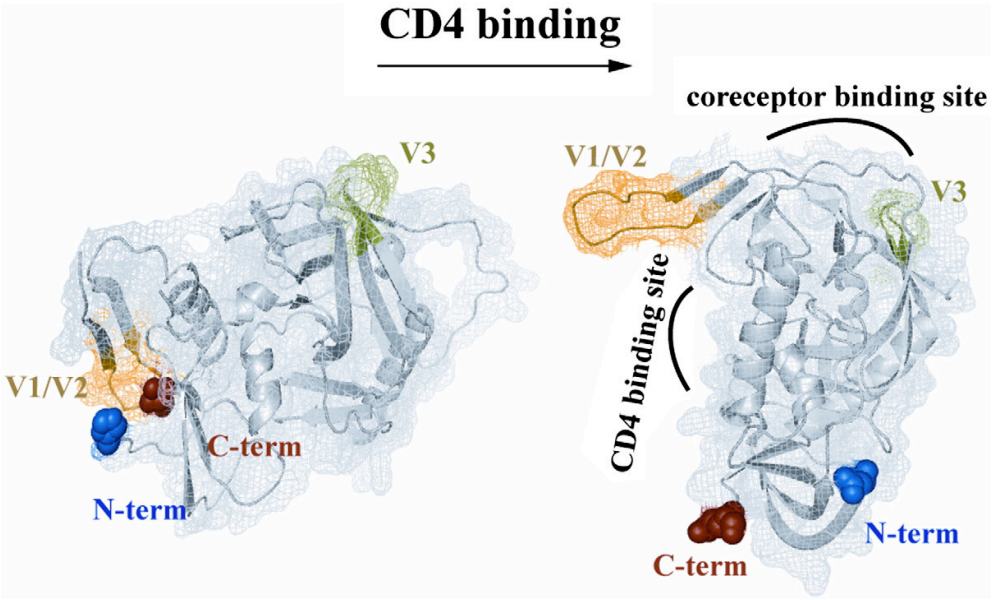

Fig. 6. CD4-induced conformational changes in gp120. Structural comparison between unliganded (left) and CD4-bound (right) gp120. Structures are rendered from Protein Data Bank accession numbers 2BF1 and 1RZJ, respectively,[5,26] using PyMol. Blue and red spheres indicate the N-terminus and the C-terminus, respectively. Yellow and green indicate the V1/V2 stem and the V3 stem, respectively.

In the context of trimeric gp41 interacting with three gp120 proteins, it is very likely that gp120 also makes important intersubunit contacts to stabilize the trimeric spike. Models of trimeric gp120 have been proposed based on electron microscopy and crystallographic data, in which the V1/V2 loop contacts the V3 loop of a neighboring gp120 within the trimer.[5,45] If the V1/V2 loop is involved in such an intermolecular interaction, this alternate conformation would explain why the monomeric gp120–gp41 interaction appears relatively weak in the absence of sCD4 (in our system), but is more robust on the virion surface. In the monomer, the V1/V2 loop appears to obscure the gp41 interface region, but in the context of a trimer, the V1/V2 loop would be removed from this interface by lateral contacts with neighboring gp120s.

Conformational changes during fusion

HIV Env undergoes complex and extensive conformational changes upon interaction with CD4 and a coreceptor. How and when conformational changes in gp120 are transmitted to gp41 via their interface are important unanswered questions. For completion of membrane fusion, the interaction between gp41 and gp120 must be weakened to allow formation of the six-helix bundle. Strong evidence for this requirement is provided by SOS Env, which can only mediate membrane fusion when its engineered gp120–gp41 disulfide bond is broken with a weak reducing agent.[37,38] Coreceptor binding is likely the most critical step in the fusion pathway, since several CD4-independent Envs can fuse, but no coreceptor-independent strains have yet been identified.

Our biochemical results show that the C-peptide region of gp41 maintains binding to gp120 after sCD4 binding, but this interaction must ultimately be dissociated to allow the formation of the trimer-of-hairpins structure that mediates membrane fusion. Coreceptor binding to gp120 is the most likely remaining stimulus that can induce this conformational change. Using the data obtained here and in previous studies, we propose a modified model for the gp120–gp41 interface and how this interface responds to CD4 and coreceptor binding. In the native (prefusogenic) state, the DSL and C-peptide regions interact with gp120 primarily via the C5 region. Interaction of the C-peptide region with gp120 can sequester it and prevent the formation of the six-helix bundle until coreceptor engagement disrupts this interface and liberates the C-peptide region (Fig. 7).

In support of this idea, a recent report by Steger and Root shows that the C-peptide region is accessible to inhibitors for a much shorter period of time (in seconds) than the N-peptide region (in minutes) during fusion.[39] This observation is consistent with the sequestration of the C-peptide region by gp120 observed here. If coreceptor binding triggers the dissociation of the C-peptide from gp120, the short kinetic window of C-peptide accessibility to 5-helix may reflect the time needed to form the six-helix bundle after the C-peptide is liberated from its interaction with gp120.

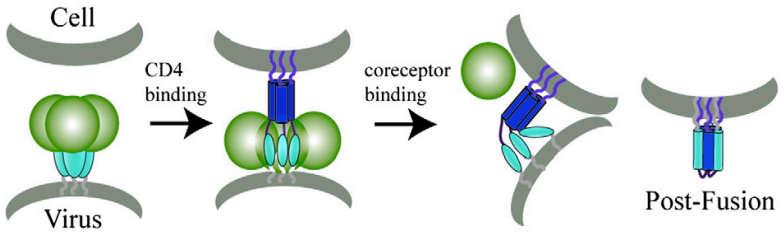

Fig. 7. Revised model of HIV entry. Based on the results of this study, we propose this altered model of HIV entry. CD4 binding induces formation of the prehairpin intermediate, in which the N-trimer region is exposed and the FP is embedded in the target cell membrane. In this intermediate, the DSL and C-peptide regions of gp41 interact with gp120, preventing association with the N-trimer region. Coreceptor binding to gp120 triggers conformational changes that weaken the gp120–gp41 interface. The liberated C-peptide region can then interact with the N-trimer region to form the trimer-of-hairpins structure, leading to membrane fusion and viral entry.

Roles of the DSL region disulfide bond

The intramolecular disulfide bond in the DSL region is highly conserved and thought to be important for the structure and function of HIV Env.[8,34,46] Although gp41 can adopt a postfusion six-helix bundle structure without this disulfide,[8] it is currently thought to exist in the prefusogenic gp41 structure.[47] The functional role of this disulfide bond in HIV entry has been difficult to assess because mutations of these cysteines or intermolecular disulfide bond formation has been shown to disrupt Env proteolytic processing and trafficking.[46,48–50] Several studies have reported that the DSL region exhibits membrane-binding properties.[35,36] Membrane binding of the DSL region could provide additional force right before membrane fusion by bringing viral and target cell membranes more closely together.[35,51] Here, we show that the DSL disulfide is not required for gp120 binding, but does play a role in cell surface binding. Interestingly, the cell surface interaction is affected by the hydrophobicity of the disulfide region rather than by formation of the disulfide itself. The cell-surface-binding properties of DSL49 are not disrupted by six-helix bundle formation, providing additional evidence that DSL49's cell surface and gp120 binding interactions are distinct. This result also implies that the cell-surface-binding interaction can be maintained late in the fusion reaction after six-helix bundle formation. Our gp41 fragment model system will be useful for dissecting the distinct properties of gp120 and cell binding to study how they relate to Env trafficking, processing, and fusion activity.

Overcoming barriers to obtaining a high-resolution gp120–gp41 interface structure

In contrast to the intrinsically flexible variable loops of gp120, the flexibility of the gp120 C1 and C5 regions in monomeric gp120 is likely due to the absence of their natural binding partner, gp41. Binding of these regions to an appropriate gp41 fragment may stabilize these regions and allow structural characterization of the gp120–gp41 interface. Further work will be required to achieve this goal, including optimization of fragment solubility and complex stability, possibly via covalent linkage (e.g., crosslinking or flexible linker).

Limitations of our biochemical system

An important caveat for interpreting these studies is that DSL49 likely does not mimic the entire gp120–gp41 interaction interface due to the absence of the gp41 FP and N-peptide regions. Biochemical studies of the FP's role in the gp120–gp41 interface are hampered by its poor solubility (leading to its absence in these studies). The FP ultimately inserts into the target cell membrane, but its status during each step of the entry pathway is poorly understood. In preliminary studies, the N-peptide region did not interact with gp120. However, it remains possible that portions of the N-peptide region, when combined with the DSL and C-peptide regions, may contribute to the stability of the gp120–gp41 interface. Finally, while we find a limited role for the gp120 C1 region in this study, it may stabilize the gp120–gp41 interaction on virions via contacts with the gp41 FP or N-peptide regions.

The trimeric Env complex is thought to be stabilized primarily by gp41–gp41 interactions, since gp120 is monomeric in solution. Ultimately, trimeric gp120–gp41 must be studied for a full understanding of HIV's entry mechanism. The nature of gp41's trimerization in the prefusogenic state is currently unknown, although experiments with engineered disulfide bonds show that the N-peptide region is in a conformation different from that in the six-helix bundle.[52] Recently, Pancera *et al.* described a trimeric gp120 construct stabilized by an appended C-terminal coiled-coil domain.[53] Constructs of this type, combined with trimeric versions of gp41 fragments such as DSL49, may prove useful for structural characterization of the trimeric gp120–gp41 interface. The relatively modest (low micromolar) affinities observed here in the monomeric gp120–gp41 interface are also likely to be much stronger in the context of the trimeric Env complex due to avidity effects.

The biochemical system we describe here for mimicking the gp120–gp41 interaction will likely find wide utility in future structural and mechanistic studies of the gp120–gp41 interface. Future studies will focus on using this system to learn how conformational changes of the gp120–gp41 interface caused by CD4/coreceptor binding enable gp41 to convert from its inactive prefusogenic conformation to the postfusogenic six-helix bundle. This system will also allow more detailed studies of the contributions of specific residues in gp120 and gp41 to formation of the interface, free of confounding *in vivo* issues such as folding, trafficking, and processing. A better understanding of this interface is likely to aid efforts to discover neutralizing antibodies and novel entry inhibitors that inactivate HIV's fusion machinery by promoting premature dissociation of the gp120–gp41 interface or, conversely, by stabilizing this interface to prevent gp120 dissociation.

Materials and Methods

Protein expression and purification

gp41 sequences were obtained from pEBB-JRFL. All gp41-derived sequences contain a C-terminal His_6 tag. C43 was produced from N-C43, constructed as previously described.[10] Briefly, N-C43 was constructed by linking C43 with its corresponding N-peptide sequences (N38, residues 540–577) via a GGRGGS linker to form a stable six-helix bundle (trimer of N-linker-C). N-C43 was digested by trypsin, followed by reverse-phase HPLC (RP-HPLC) (C18; Vydac) purification. DSL49, DSL20, C49, DSL49ss, DSL20ss, Δ13-DSL20, L20, C20, and DSL were expressed as C-terminal fusions to MBP linked by the TEV protease recognition sequence, ENLYFQG. All constructs were cloned into pET-17b (Novagen). Proteins were overexpressed in BL21-Gold(DE3) or BL21-Gold(DE3)-pLysS (Stratagene) and purified by Ni^+-affinity column (His-Select HC nickel affinity gel; Sigma). Purified MBP-fused proteins were digested by TEV protease (kindly provided by C. Hill, University of Utah) in 50 mM Tris (pH 8.0), 0.5 mM ethylenediaminetetraacetic acid, and 0.5 mM DTT overnight at 4 °C. RP-HPLC was performed using a C18 column (Vydac) for further purification of gp41 fragments.

The DSL region has an intramolecular disulfide bond. Although the two Cys residues in the DSL region are close enough to potentially form intermolecular disulfide bonds in the gp41 trimer,[8,54,55] we exclusively produced the intramolecular disulfide bond. This configuration is currently thought to exist in the native gp41 structure because it is immunologically active,[47] and intermolecular disulfide bonds have been shown to disrupt Env proteolytic processing.[48]

For DSL-containing fragments, disulfide bond formation was carried out in 50 mM Tris (pH 8), 2% Dimethyl Sulfoxide, and 3–6 M guanidine hydrochloride. DSL-containing fragments with an intramolecular disulfide bond were separated and purified by RP-HPLC (Supplementary Data). All gp41 fragments were lyophilized after HPLC purification and reconstituted in 0.1% Trifluoroacetic acid to obtain high-concentration stock solutions. 5-Helix was expressed, purified, and prepared as described previously.[10] All purified gp41 fragments were confirmed by SDS-PAGE and mass spectrometry University of Utah Mass Spectrometry Core Facility) and were soluble at 2 μM in phosphate-buffered saline (PBS).

V1jns expression plasmids containing JRFL codon-optimized gp120, ΔV3-gp120, and ΔV1/V2/V3-gp120 were gifts from X. Liang (Merck Research Laboratories). For ΔC1 and ΔC5, nucleotides corresponding to residues K33-Q82 were replaced with a BamHI restriction site encoding Gly-Ser, and a stop codon was added prior to P493 using the XbaI site in V1jns-JRFL-gp120 plasmid, respectively. In each deletion construct, the following regions were removed from JRFL gp120: ΔC1, K33 to Q82; ΔC5, P493 to C-terminus; ΔV1/V2, T128 to I194; ΔV3, T303 to I323 (Fig. 1c). All gp120 proteins were expressed in 293T-EBNA cells (Invitrogen) by transient transfection with FuGENE 6 (Roche). Starting 24 h posttransfection, supernatant was harvested each day for 3 days, clarified through a 0.22-μm filter, and concentrated with a 10-kDa cutoff Centricon (Millipore), if necessary. wt JRFL-gp120 was purified using a Lentil Lectin column (Amersham Biosciences) as described in the manufacturer's instructions and concentrated with a 10-kDa cutoff Centricon. Approximate gp120 concentration was measured by Western blot analysis using commercial YU2-gp120 (ImmunoDiagnostics, Inc.) as standard.

MBP and MBP-C1/C5 were constructed into pET-17b. C1 (residues 31–94) and C5 (residues 482–511) sequences derived from pEBB-JRFL were linked by SGGGSGGGS. The N-terminus of C1 was fused to MBP linked by a TEV cleavage site (ENLYFQGS) and C9 tag (TETSQVAPA). For the MBP control protein, a TEV cleavage sequence was added at the C-terminus. MBP and MBP-C1/C5 were expressed in BL21-Gold(DE3)-pLysS and purified by amylose column (New England BioLaboratories).

The two-domain sCD4 expression plasmid, pET-9a CD4-D1D2, was kindly provided by Raghavan Vardarajan (Indian Institute of Science). CD4-D1D2-H6 (sCD4-H6) was expressed in BL21-DE3-pLysS and purified by Ni^+-affinity column in 6 M guanidine hydrochloride. Purified sCD4-H6 was refolded by dialysis into PBS (pH 7.4).

Binding assay

gp120 (~100 nM) and gp41 (2 μM) fragments were mixed for 2 h at 23 °C in DMEM (Gibco) supplemented with 10% fetal calf serum (Gibco). sCD4 [400 nM; National Institutes of Health (NIH) AIDS Research and Reference Program, contributed by Pharmacia] was added to the mixture, as indicated. As a positive control, 2 μM sCD4-H6 was used to measure the total amount of active gp120 in this assay. Next, 15 μl of Talon Dynabeads (binding to the C-terminal His_6 tag present in all gp41 fragments and sCD4-H6; Dynal) was added and incubated for 15 min at room temperature (RT). Beads were then magnetically precipitated and washed twice with 500 μl of PBS containing 0.01% Tween-20 and 10 mM imidazole. Bound proteins were eluted with 400 mM imidazole and analyzed by nonreducing SDS-PAGE (NuPAGE; Invitrogen) and Western blot analysis with sheep anti-gp120 serum (NIH AIDS Research and Reference Program, contributed by Michael Phelan). JRFL-gp120 showed broad smearing in Western blot analysis due to variable glycosylation. To sharpen these bands for quantification, eluted gp120 was deglycosylated by PNGaseF (NEB) following the manufacturer's instructions. Western blot analysis of expressed gp120 showed the expected

monomer, but also dimers and trimers linked by intermolecular disulfide bonds that can be broken under mild reducing conditions, as previously reported.[56] These oligomers are easily detected by Western blot analysis, but are barely detectable using direct protein staining. Since these dimers and trimers do not have completely native conformations (due to shuffled disulfide bonds), only the binding of monomeric gp120 was measured in this study using nonreducing SDS-PAGE. Bands were quantified using the Odyssey Western Blot Imaging System (LI-COR) with the included software. MBP (10 μM) and MBP-C1/C5 were mixed with 2 μM DSL49 or ubiquitin H6 (Ub-H6) in PBS containing 10% fetal bovine serum. Ub-H6 used as a negative control was prepared as previously described.[57] To see the effect of the formation of the trimer-of-hairpins, 3 μM 5-helix was preincubated with DSL49 as indicated (Fig. 3a). The mixture was precipitated and washed as described above. Bound proteins were analyzed by nonreducing SDS-PAGE and Coomassie blue staining.

Crosslinking

gp120 purified by Lectin Lentil column (GE Healthcare) was dialyzed into PBS (Gibco). gp120 (0.9 μg) was mixed with 0.25 μg of sCD4, 0.28 μg of DSL49, and/or 0.5 μg of 5-helix in 10 μl of PBS at RT. Glutaraldehyde (10 mM; Fisher) was added and incubated for 5 min at RT, followed by quenching with Tris. Crosslinked mixtures were analyzed by SDS-PAGE and Krypton infrared protein staining (Pierce).

Modification of cysteines in DSL49

DSL49 was completely reduced by boiling in 100 mM DTT and PBS (pH 7.4). Reduced cysteines were blocked by reaction with 50 mM NEM (Sigma) or 50 mM Ac (Sigma) in PBS or Tris-buffered saline (pH 7.4), respectively, for 1 h at RT. Unreacted NEM or Ac was removed by ultrafiltration (Centricon; Millipore).

Cell-binding assay

HOS-pBABE-puro cells were obtained from the NIH AIDS Reagent Program (N. Landau) and propagated in DMEM supplemented with 10% fetal calf serum and 1 μg/ml puromycin. Cells were dissociated using cell dissociation buffer (Invitrogen), washed and resuspended with PBS containing 0.1% sodium azide, and incubated for 30 min at RT to prevent endocytosis.[58] Cells (2.5×10^5) were incubated with 2 μM gp41 fragments for 1 h at RT and washed three times with 500 μl of PBS containing 0.01% Tween. Cells were resuspended with SDS loading buffer and completely lysed by sonication and boiling. Bound gp41 fragments were analyzed by SDS-PAGE and Western blot analysis using anti-His tag polyclonal antibody (Abcam).

Immunostaining

DSL49 (2 μM) or DSL49ss (2 μM) was incubated with 5×10^6 HOS-pBABE-puro cells in the presence of 0.1% sodium azide to block endocytosis and 5% fetal bovine serum as blocking solution for 2 h at RT. Cells were washed three times with 500 μl of PBS containing 0.01% Tween (PBS-T). Cells were fixed by 4% PFA (Electron Microscopy Sciences) in PBS for 15 min at RT, followed by three washes with 500 μl of PBS. After blocking with 5% goat serum (Invitrogen) in PBS for 1 h at RT, cells were incubated with 250 μl of rabbit anti-His_6 antibody (Abcam) at 1:200 dilution in blocking solution containing 0.01% Tween overnight at 4 °C. Unbound antibody was removed by three washes with PBS-T (10 min each at RT). Cells were incubated with Alexa Fluor 568 goat anti-rabbit antibody (Molecular Probes) at 1:500 dilution in blocking solution containing 0.01% Tween for 1 h at RT, followed by three washes with PBS-T (20 min each at RT). Cells were placed on the slide with VectaShield (Vector Laboratories) and photographed at magnifications of 40× and 100×.

Acknowledgements

This work was supported, in part, by NIH grants P01GM066521 and P50GM082545.

Special thanks to Debra Eckert, Brett Welch, and Michael Root for helpful discussions and critical review of the manuscript.

Supplementary Data

Supplementary data associated with this article can be found, in the online version, at doi:10.1016/j.jmb.2007.12.001

References

1. Wyatt, R. & Sodroski, J. (1998). The HIV-1 envelope glycoproteins: fusogens, antigens, and immunogens. *Science*, **280**, 1884–1888.
2. Eckert, D. M. & Kim, P. S. (2001). Mechanisms of viral membrane fusion and its inhibition. *Annu. Rev. Biochem.* **70**, 777–810.
3. Sattentau, Q. J. & Moore, J. P. (1991). Conformational changes induced in the human immunodeficiency virus envelope glycoprotein by soluble CD4 binding. *J. Exp. Med.* **174**, 407–415.
4. Wu, L., Gerard, N. P., Wyatt, R., Choe, H., Parolin, C., Ruffing, N. *et al.* (1996). CD4-induced interaction of primary HIV-1 gp120 glycoproteins with the chemokine receptor CCR-5. *Nature*, **384**, 179–183.
5. Chen, B., Vogan, E. M., Gong, H., Skehel, J. J., Wiley, D. C. & Harrison, S. C. (2005). Structure of an unliganded simian immunodeficiency virus gp120 core. *Nature*, **433**, 834–841.
6. Tan, K., Liu, J., Wang, J., Shen, S. & Lu, M. (1997). Atomic structure of a thermostable subdomain of HIV-1 gp41. *Proc. Natl Acad. Sci. USA*, **94**, 12303–12308.
7. Chan, D. C., Fass, D., Berger, J. M. & Kim, P. S. (1997). Core structure of gp41 from the HIV envelope glycoprotein. *Cell*, **89**, 263–273.
8. Caffrey, M., Cai, M., Kaufman, J., Stahl, S. J., Wingfield, P. T., Covell, D. G. *et al.* (1998). Three-dimensional solution structure of the 44 kDa ectodomain of SIV gp41. *EMBO J.* **17**, 4572–4584.
9. Weissenhorn, W., Dessen, A., Harrison, S. C., Skehel, J. J. & Wiley, D. C. (1997). Atomic structure of the ectodomain from HIV-1 gp41. *Nature*, **387**, 426–430.

10. Root, M. J., Kay, M. S. & Kim, P. S. (2001). Protein design of an HIV-1 entry inhibitor. *Science*, **291**, 884–888.
11. Eckert, D. M. & Kim, P. S. (2001). Design of potent inhibitors of HIV-1 entry from the gp41 N-peptide region. *Proc. Natl Acad. Sci. USA*, **98**, 11187–11192.
12. Eckert, D. M., Malashkevich, V. N., Hong, L. H., Carr, P. A. & Kim, P. S. (1999). Inhibiting HIV-1 entry: discovery of D-peptide inhibitors that target the gp41 coiled-coil pocket. *Cell*, **99**, 103–115.
13. Wild, C., Greenwell, T. & Matthews, T. (1993). A synthetic peptide from HIV-1 gp41 is a potent inhibitor of virus-mediated cell–cell fusion. *AIDS Res. Hum. Retroviruses*, **9**, 1051–1053.
14. Bewley, C. A., Louis, J. M., Ghirlando, R. & Clore, G. M. (2002). Design of a novel peptide inhibitor of HIV fusion that disrupts the internal trimeric coiled-coil of gp41. *J. Biol. Chem.* **277**, 14238–14245.
15. Chan, D. C. & Kim, P. S. (1998). HIV entry and its inhibition. *Cell*, **93**, 681–684.
16. Starcich, B. R., Hahn, B. H., Shaw, G. M., McNeely, P. D., Modrow, S., Wolf, H. *et al.* (1986). Identification and characterization of conserved and variable regions in the envelope gene of HTLV-III/LAV, the retrovirus of AIDS. *Cell*, **45**, 637–648.
17. Binley, J. M., Sanders, R. W., Clas, B., Schuelke, N., Master, A., Guo, Y. *et al.* (2000). A recombinant human immunodeficiency virus type 1 envelope glycoprotein complex stabilized by an intermolecular disulfide bond between the gp120 and gp41 subunits is an antigenic mimic of the trimeric virion-associated structure. *J. Virol.* **74**, 627–643.
18. Helseth, E., Olshevsky, U., Furman, C. & Sodroski, J. (1991). Human immunodeficiency virus type 1 gp120 envelope glycoprotein regions important for association with the gp41 transmembrane glycoprotein. *J. Virol.* **65**, 2119–2123.
19. York, J. & Nunberg, J. H. (2004). Role of hydrophobic residues in the central ectodomain of gp41 in maintaining the association between human immunodeficiency virus type 1 envelope glycoprotein subunits gp120 and gp41. *J. Virol.* **78**, 4921–4926.
20. Jacobs, A., Sen, J., Rong, L. & Caffrey, M. (2005). Alanine scanning mutants of the HIV gp41 loop. *J. Biol. Chem.* **280**, 27284–27288.
21. Poumbourios, P., Maerz, A. L. & Drummer, H. E. (2003). Functional evolution of the HIV-1 envelope glycoprotein 120 association site of glycoprotein 41. *J. Biol. Chem.* **278**, 42149–42160.
22. Wang, S., York, J., Shu, W., Stoller, M. O., Nunberg, J. H. & Lu, M. (2002). Interhelical interactions in the gp41 core: implications for activation of HIV-1 membrane fusion. *Biochemistry*, **41**, 7283–7292.
23. Cao, J., Bergeron, L., Helseth, E., Thali, M., Repke, H. & Sodroski, J. (1993). Effects of amino acid changes in the extracellular domain of the human immunodeficiency virus type 1 gp41 envelope glycoprotein. *J. Virol.* **67**, 2747–2755.
24. Moore, P. L., Crooks, E. T., Porter, L., Zhu, P., Cayanan, C. S., Grise, H. *et al.* (2006). Nature of nonfunctional envelope proteins on the surface of human immunodeficiency virus type 1. *J. Virol.* **80**, 2515–2528.
25. Huang, C. C., Tang, M., Zhang, M. Y., Majeed, S., Montabana, E., Stanfield, R. L. *et al.* (2005). Structure of a V3-containing HIV-1 gp120 core. *Science*, **310**, 1025–1028.
26. Kwong, P. D., Wyatt, R., Robinson, J., Sweet, R. W., Sodroski, J. & Hendrickson, W. A. (1998). Structure of an HIV gp120 envelope glycoprotein in complex with the CD4 receptor and a neutralizing human antibody. *Nature*, **393**, 648–659.
27. Guilhaudis, L., Jacobs, A. & Caffrey, M. (2002). Solution structure of the HIV gp120 C5 domain. *Eur. J. Biochem.* **269**, 4860–4867.
28. Moore, J. P., McKeating, J. A., Weiss, R. A. & Sattentau, Q. J. (1990). Dissociation of gp120 from HIV-1 virions induced by soluble CD4. *Science*, **250**, 1139–1142.
29. Si, Z., Madani, N., Cox, J. M., Chruma, J. J., Klein, J. C., Schon, A. *et al.* (2004). Small-molecule inhibitors of HIV-1 entry block receptor-induced conformational changes in the viral envelope glycoproteins. *Proc. Natl Acad. Sci. USA*, **101**, 5036–5041.
30. Chertova, E., Bess, J. W., Jr, Crise, B. J., Sowder, I. R., Schaden, T. M., Hilburn, J. M. *et al.* (2002). Envelope glycoprotein incorporation, not shedding of surface envelope glycoprotein (gp120/SU), is the primary determinant of SU content of purified human immunodeficiency virus type 1 and simian immunodeficiency virus. *J. Virol.* **76**, 5315–5325.
31. Moore, J. P., McKeating, J. A., Huang, Y. X., Ashkenazi, A. & Ho, D. D. (1992). Virions of primary human immunodeficiency virus type 1 isolates resistant to soluble CD4 (sCD4) neutralization differ in sCD4 binding and glycoprotein gp120 retention from sCD4-sensitive isolates. *J. Virol.* **66**, 235–243.
32. Alam, S. M., Paleos, C. A., Liao, H. X., Scearce, R., Robinson, J. & Haynes, B. F. (2004). An inducible HIV type 1 gp41 HR-2 peptide-binding site on HIV type 1 envelope gp120. *AIDS Res. Hum. Retroviruses*, **20**, 836–845.
33. Yuan, W., Craig, S., Si, Z., Farzan, M. & Sodroski, J. (2004). CD4-induced T-20 binding to human immunodeficiency virus type 1 gp120 blocks interaction with the CXCR4 coreceptor. *J. Virol.* **78**, 5448–5457.
34. Maerz, A. L., Drummer, H. E., Wilson, K. A. & Poumbourios, P. (2001). Functional analysis of the disulfide-bonded loop/chain reversal region of human immunodeficiency virus type 1 gp41 reveals a critical role in gp120–gp41 association. *J. Virol.* **75**, 6635–6644.
35. Pascual, R., Moreno, M. R. & Villalain, J. (2005). A peptide pertaining to the loop segment of human immunodeficiency virus gp41 binds and interacts with model biomembranes: implications for the fusion mechanism. *J. Virol.* **79**, 5142–5152.
36. Moreno, M. R., Pascual, R. & Villalain, J. (2004). Identification of membrane-active regions of the HIV-1 envelope glycoprotein gp41 using a 15-mer gp41-peptide scan. *Biochim. Biophys. Acta*, **1661**, 97–105.
37. Binley, J. M., Cayanan, C. S., Wiley, C., Schulke, N., Olson, W. C. & Burton, D. R. (2003). Redox-triggered infection by disulfide-shackled human immunodeficiency virus type 1 pseudovirions. *J. Virol.* **77**, 5678–5684.
38. Abrahamyan, L. G., Markosyan, R. M., Moore, J. P., Cohen, F. S. & Melikyan, G. B. (2003). Human immunodeficiency virus type 1 Env with an intersubunit disulfide bond engages coreceptors but requires bond reduction after engagement to induce fusion. *J. Virol.* **77**, 5829–5836.
39. Steger, H. K. & Root, M. J. (2006). Kinetic dependence to HIV-1 entry inhibition. *J. Biol. Chem.* **281**, 25813–25821.
40. Salzwedel, K., Smith, E. D., Dey, B. & Berger, E. A. (2000). Sequential CD4-coreceptor interactions in human immunodeficiency virus type 1 Env function: soluble CD4 activates Env for coreceptor-dependent fusion and reveals blocking activities of antibodies

against cryptic conserved epitopes on gp120. *J. Virol.* **74**, 326–333.
41. Kolchinsky, P., Mirzabekov, T., Farzan, M., Kiprilov, E., Cayabyab, M., Mooney, L. J. *et al.* (1999). Adaptation of a CCR5-using, primary human immunodeficiency virus type 1 isolate for CD4-independent replication. *J. Virol.* **73**, 8120–8126.
42. Myszka, D. G., Sweet, R. W., Hensley, P., Brigham-Burke, M., Kwong, P. D., Hendrickson, W. A. *et al.* (2000). Energetics of the HIV gp120–CD4 binding reaction. *Proc. Natl Acad. Sci. USA*, **97**, 9026–9031.
43. Rizzuto, C. D., Wyatt, R., Hernandez-Ramos, N., Sun, Y., Kwong, P. D., Hendrickson, W. A. & Sodroski, J. (1998). A conserved HIV gp120 glycoprotein structure involved in chemokine receptor binding. *Science*, **280**, 1949–1953.
44. Wyatt, R., Moore, J., Accola, M., Desjardin, E., Robinson, J. & Sodroski, J. (1995). Involvement of the V1/V2 variable loop structure in the exposure of human immunodeficiency virus type 1 gp120 epitopes induced by receptor binding. *J. Virol.* **69**, 5723–5733.
45. Kwong, P. D., Wyatt, R., Sattentau, Q. J., Sodroski, J. & Hendrickson, W. A. (2000). Oligomeric modeling and electrostatic analysis of the gp120 envelope glycoprotein of human immunodeficiency virus. *J. Virol.* **74**, 1961–1972.
46. Sen, J., Jacobs, A., Jiang, H., Rong, L. & Caffrey, M. (2007). The disulfide loop of gp41 is critical to the furin recognition site of HIV gp160. *Protein Sci.* **16**, 1236–1241.
47. Oldstone, M. B., Tishon, A., Lewicki, H., Dyson, H. J., Feher, V. A., Assa-Munt, N. *et al.* (1991). Mapping the anatomy of the immunodominant domain of the human immunodeficiency virus gp41 transmembrane protein: peptide conformation analysis using monoclonal antibodies and proton nuclear magnetic resonance spectroscopy. *J. Virol.* **65**, 1727–1734.
48. Owens, R. J. & Compans, R. W. (1990). The human immunodeficiency virus type 1 envelope glycoprotein precursor acquires aberrant intermolecular disulfide bonds that may prevent normal proteolytic processing. *Virology*, **179**, 827–833.
49. Syu, W. J., Lee, W. R., Du, B., Yu, Q. C., Essex, M. & Lee, T. H. (1991). Role of conserved gp41 cysteine residues in the processing of human immunodeficiency virus envelope precursor and viral infectivity. *J. Virol.* **65**, 6349–6352.
50. Dedera, D., Gu, R. L. & Ratner, L. (1992). Conserved cysteine residues in the human immunodeficiency virus type 1 transmembrane envelope protein are essential for precursor envelope cleavage. *J. Virol.* **66**, 1207–1209.
51. Shu, W., Ji, H. & Lu, M. (2000). Interactions between HIV-1 gp41 core and detergents and their implications for membrane fusion. *J. Biol. Chem.* **275**, 1839–1845.
52. Mische, C. C., Yuan, W., Strack, B., Craig, S., Farzan, M. & Sodroski, J. (2005). An alternative conformation of the gp41 heptad repeat 1 region coiled coil exists in the human immunodeficiency virus (HIV-1) envelope glycoprotein precursor. *Virology*, **338**, 133–143.
53. Pancera, M., Lebowitz, J., Schon, A., Zhu, P., Freire, E., Kwong, P. D. *et al.* (2005). Soluble mimetics of human immunodeficiency virus type 1 viral spikes produced by replacement of the native trimerization domain with a heterologous trimerization motif: characterization and ligand binding analysis. *J. Virol.* **79**, 9954–9969.
54. Weissenhorn, W., Wharton, S. A., Calder, L. J., Earl, P. L., Moss, B., Aliprandis, E. *et al.* (1996). The ectodomain of HIV-1 env subunit gp41 forms a soluble, alpha-helical, rod-like oligomer in the absence of gp120 and the N-terminal fusion peptide. *EMBO J.* **15**, 1507–1514.
55. Wingfield, P. T., Stahl, S. J., Kaufman, J., Zlotnick, A., Hyde, C. C., Gronenborn, A. M. *et al.* (1997). The extracellular domain of immunodeficiency virus gp41 protein: expression in *Escherichia coli*, purification, and crystallization. *Protein Sci.* **6**, 1653–1660.
56. Misse, D., Cerutti, M., Schmidt, I., Jansen, A., Devauchelle, G., Jansen, F. *et al.* (1998). Dissociation of the CD4 and CXCR4 binding properties of human immunodeficiency virus type 1 gp120 by deletion of the first putative alpha-helical conserved structure. *J. Virol.* **72**, 7280–7288.
57. Hamburger, A. E., Kim, S., Welch, B. D. & Kay, M. S. (2005). Steric accessibility of the HIV-1 gp41 N-trimer region. *J. Biol. Chem.* **280**, 12567–12572.
58. Kaljot, K. T., Shaw, R. D., Rubin, D. H. & Greenberg, H. B. (1988). Infectious rotavirus enters cells by direct cell membrane penetration, not by endocytosis. *J. Virol.* **62**, 1136–1144.

APPENDIX B

EXTRACELLULAR STABILITY OF HIV-1 ENTRY

Hong-Bo Pang and Michael S. Kay

Introduction

Human immunodeficiency virus type 1 (HIV-1) assembles as an immature particle and undergoes a maturation process after budding out of infected cells (*2*). In the immature state, Gag, HIV-1's major structural protein, polymerizes underneath the lipid membrane to form a thick protein shell. During maturation, HIV-1 protease (PR) cleaves Gag into several products: MA remains associated with viral membrane to form the matrix layer, which is much thinner than the immature Gag shell; CA condenses to form a conical capsid core housing the NC-viral RNA genome complex; nonstructural spacer peptides, p1 and p2; and a C-terminal p6 peptide thought to interact with host machinery to facilitate viral release. Maturation is required for HIV-1 infectivity.

HIV-1's entry into target cells is mediated by its envelope (Env) protein subunits, gp41 and gp120. gp41 and gp120 form a trimeric complex, in which gp120 interacts with gp41 noncovalently outside the viral membrane. While gp120 mainly functions to recognize target cells and trigger viral entry, gp41 provides the driving force for membrane fusion (*4*). To initiate viral entry, gp120 first recognizes and binds with target cell receptor, CD4. This binding induces conformational change on gp120 and allows its further interaction with cellular coreceptor (CXCR4 or CCR5) (*4*). CD4 binding induces conformational changes not only in gp120, but also in gp41. In the native state, the gp41 N-peptide region is not accessible for exogenous C-peptides. After CD4 binding, the N-peptide region forms a trimeric coiled coil (N-trimer) that is accessible to exogenous C-peptides until the endogenous C-peptide region binds to the N-trimer to form a six-helix bundle, which brings viral and cell membranes together for fusion (*5*). While the Env ectodomain is critical to mediate viral entry, HIV-1 together with all other lentiviruses

has a very long cytoplasmic tail (CT) domain (~150 aa) compared to other retroviruses (~20-30 aa) (*2*). CT interacts with the Gag MA domain, which is important for Env incorporation into virions (*6*). Furthermore, CT has the ability to affect the conformation of the Env ectodomain. CT truncation induces exposure of some conserved epitope regions on gp120, ("inside-out" signaling) (*7-9*). Several groups including ours have reported that the entry activity of mature HIV-1 is ~10-fold higher than that of immature viruses, and deletion of CT restores immature entry activity to the mature level (*1, 10, 11*). All these results suggest that CT functions as a bridge for internal viral components to regulate viral entry.

After budding out of infected cells, virions are transmitted in the extracellular environment until entry into the next target cell. Viral infectivity rapidly decays outside of cells. However, little is known about the determinants of the viral infectivity durability in the extracellular environment. We are especially interested in viral entry, and thus in this study we focused on the extracellular stability of viral entry activity. We discover here that the entry activity of immature HIV-1 is much more stable than that of mature virions, and deletion of CT in immature virions abolishes this difference. Further investigation of CT and Gag reveals that both the C-terminal CT region and Gag integrity are important for preserving viral entry activity. Preliminary mechanistic studies show that neither gp120 shedding nor loss of CD4 binding accounts for this stability difference between immature and mature HIV-1. Little is known about viral activity changes during transmission, and this study may shed some light into this process.

Materials and Methods

Plasmids

Plasmids were obtained or constructed as follows: ΔEnv HIV-1 genome containing an inactivating integrase mutant (DHIV3-GFP-D116G (*12*), provided by V. Planelles), HIV-1 wild type (WT) Env expression vector (pEBB-HXB2 (*13*), provided by B. Chen), vector expressing Vpr-β-lactamase (BlaM-Vpr) fusion protein (pMM310 (*1*)), Env expressing plasmid for JRFL strain (pCAGGS-JRFL-Env WT and ΔCT, provided by Dr. J. Binley), and partial maturation Gag mutants (provided by C. Aiken (*1*)). Immature particles were generated by cloning Gag with all PR cleavage sites mutated (pNL-MA/p6, provided by C. Aiken (*1*)) into the ΔEnv Int− HIV-1 genome, while mature particles were produced using a ΔEnv Int− HIV-1 genome with wild-type (WT) cleavage sites. ΔCT HXB2 Env (Δ147 (*14*)) was provided by E. Hunter and cloned into pEBB-HXB2. CT truncation mutants were obtained from C. Aiken (*3*). Construction of GFP-TM1 was described in Chapter 3.

Viral preparation and analysis

Pseudovirion particles were produced by cotransfection of 293T cells with ΔEnv int- HIV-1 genome, an Env-expressing vector and pMM310. For example, to generate immature or mature WT virus, 2.5 μg of total DNA (1.23 μg genome vector, 0.819 μg WT Env expressing vector and 0.45 μg pMM310) was transfected into ~1 X 10^6 cells using 10 μg polyethylenimine (PEI, Sigma). The amount of Env-expressing plasmid input for immature WT has been defined as 100%. Media was changed at 6 h after transfection to avoid PEI's toxicity. Supernatants containing secreted viral particles were

collected 30 h posttransfection and filtered through 0.2 μm Acrodisc syringe filters (Pall). A series of viruses prepared on the same day is defined as one batch of viruses.

For western blot (WB) analysis of viral concentration and Env incorporation level, virus supernatants were purified by centrifugation through a sucrose cushion (20% sucrose in 1 X TNE buffer: 0.1 M NaCl, 1 mM EDTA, 10 mM Tris, pH 7.6) at 20,000 X g for 90 min at 4℃. The pellet was resuspended in SDS-PAGE reducing sample buffer and resolved by SDS-PAGE. WB was developed using rabbit polyclonal anti-CA (provided by W. Sundquist), mouse monoclonal anti-gp41 Chessie 8 antibody (supernatant from Chessie 8 hybridoma provided by NIH AIDS Research and Reference Reagent Program, ARRRP), sheep polyclonal anti-gp120 (contributed by M. Phelan, ARRRP) and rabbit polyclonal anti-BlaM (Chemicon/Millpore). Blots were quantified using Li-Cor's Odyssey scanner.

Viral entry assay

The viral entry assay was performed as described (*11*). Briefly, HIV-1 particles mixed with DEAE-Dextran (4 μg/ml) were added onto HOS-CD4-CXCR4 cells (provided by B.Chen), followed by centrifugation at 1,800 X g for 30 min at 4℃ and incubation at 37℃ for 2 h. After removal of unbound viruses, 1 μM CCF2-AM solution (β-lactamase substrate, Invitrogen) was incubated with cells at 13℃ for 17 h. Uncleaved and cleaved CCF2-AM have emission peaks of 520 nm (green) and 447 nm (blue), respectively, under 409 nm excitation. Fluorescent signals from both channels were detected using an Olympus MVX10 fluorescent microscope and quantified using ImageJ software (NIH). Viral entry activity is calculated as described in Chapter 3.

Coprecipitation assay

The coprecipitation assay was done as described previously (*15*). Briefly, viruses with or without preheat were incubated at 37 ℃ for 1 h with His_6 tagged CD4 (at a final concentration of 300 ng/μl) in DMEM (Gibco) supplemented with 10% fetal calf serum (Gibco). Then 15 μl of Talon Dynabeads (Ni magnetic beads; Dynal) was added to the solution and incubated for 15 min at room temperature with gentle tapping every 3 min. Beads were then magnetically precipitated and washed twice with 500 μl of PBS containing 0.01% Tween-20 and 10 mM imidazole. Bound viruses were eluted with 400 mM imidazole and dissolved by reducing SDS-PAGE (NuPAGE; Invitrogen).

Results

Immature HIV-1 entry is more stable than that of mature virions

To examine the durability of virions in the extracellular environment, we focused on viral entry activity. At 4 ℃, viral entry activity is well preserved. Therefore, the ratio of the entry activities after incubation at 37 ℃ vs. 4 ℃ is defined as the extracellular stability of viral entry activity. After 24 h incubation at 37 ℃, the entry activity of mature HIV-1 (HXB2 strain, CXCR4-tropic) drops to ~10% of those incubated at 4 ℃ (Fig. B-1 A). In contrast, immature HIV-1 maintains ~50% entry activity. For experimental convenience, we increased incubation temperature to 50 ℃, in order to accelerate the decay process (Fig. B-1 A). After 1 h incubation at 50 ℃, mature HIV-1 retains only ~20% entry activity, while immature virions maintain ~80-90% entry activity. 50 ℃ treatment does not change the relative relationship between immature and mature extracellular stability. Therefore, for all the following experiments, we used 1 h incubation at 50 ℃ vs 4 ℃ as our standard experimental condition.

Determinants for extracellular stability in immature state

Maturation causes a dramatic increase in viral entry activity, which is dependent on CT (*1, 10, 11*). Therefore, we investigated whether CT is important for extracellular stability of viral entry activity. Deletion of CT dramatically decreases the stability of immature viruses to below the mature level (Fig. B-1 A). As a control, mature ΔCT is as unstable as mature WT, suggesting CT only functions to preserve viral entry activity in immature state (Fig. B-1 A). To see whether this is general for HIV-1 strains, we tested JRFL, a primary CCR5-tropic strain, and found a similar result (Fig. B-1 B). Further mapping of CT showed that deletion of 28 or more residues from the C-terminus of CT disrupts stability of immature HIV-1 entry (Fig. B-2).

PR cleavage of Gag induces the dramatic morphological change during HIV-1 maturation. Therefore, we employed a series of Gag mutants with one or more PR cleavage sites mutated, to investigate the importance of Gag integrity for extracellular stability. These Gag mutants were coexpressed with HIV-1 WT Env (HXB2 strain) and their extracellular stability was measured as above. Any PR cleavage between MA and NC greatly reduces the entry activity stability of immature viruses (Fig. B-3). In contrast, PR cleavage only between NC and p6 has a much milder effect, making the viruses ~50% stable as immature WT.

We previously defined particle stiffness as a novel regulatory level for viral entry. During maturation, HIV-1 particles are dramatically softened, contributing to increased viral entry activity. In Chapter 3, we showed that coexpression of a transmembrane anchored CT domain (GFP-TM1) increases particle stiffness of ΔCT immature virions in a dose-dependent manner. However, this coexpression of GFP-TM1 on an immature

virion does not preserve viral entry activity (supplemental Fig. B-1), suggesting that the loss of extracellular stability with CT deletion is not due to lowered particle stiffness.

Neither gp120 shedding nor loss of CD4 binding accounts for the loss of viral entry activity

Although important for viral entry, gp120 is tethered to viral surface by its non-covalent interaction with gp41. Therefore, it is possible that long incubation causes the shedding of gp120. However, the gp120 incorporation level is similar between 4℃ and 50°C treated immature ΔCT viruses, arguing against a role for shedding (Fig. B-4).

Binding with CD4 is an early critical step for viral entry. Therefore, we further looked into whether deletion of CT causes a loss of Env's CD4 binding ability over time. A His-tagged CD4 (CD4-H6) was used to coprecipitate viruses with Env capable of CD4-binding. No significant difference was found between 4℃ and 50℃ treated immature ΔCT or WT (Fig. B-5), suggesting that loss of CD4 binding ability is not the reason that CT truncation destabilizes viral entry activity.

Discussion

Although the detailed time window is yet defined, HIV-1 needs to survive in the extracellular environment to enter the next target cell within the same or from different hosts. Mature HIV-1 loses its infectivity within hours in tissue culture medium, but little is known which biological activity accounts for this loss. An interesting question is whether maturation has an effect on viral durability during transmission. In this study, we focused on viral entry activity and found that immature HIV-1 preserves its entry activity much better than mature virions. Both CT's C-terminus and Gag integrity were shown to

be important for preservation of viral entry activity, but neither gp120 association with virions nor CD4 binding ability is affected by CT deletion.

In Chapter 3, we showed that the low viral entry activity of immature HIV-1 is partly due to the high particle stiffness. Therefore, we speculated that stiff particles in the immature state may function to preserve the viral entry activity in the extracellular environment. However, coexpression of GFP-TM1 with immature ΔCT, which was shown to stiffen the whole particle, failed to preserve the viral entry activity after 50℃ treatment (data not shown). Since GFP-TM1 greatly impairs ΔCT incorporation (Chapter 3), we coexpressed GFP-TM1 with an unrelated viral Env (VSVg). While GFP-TM1 still stiffens the immature virions and does not affect VSVg incorporation, coexpression with GFP-TM1 does not recover the entry activity of immature VSVg from unmeasurable level. This result suggests that stiffening the viral particle cannot preserve the extracellular stability of viral entry. The underlying mechanism that maturation lowers the stability of viral entry activity remains to be characterized.

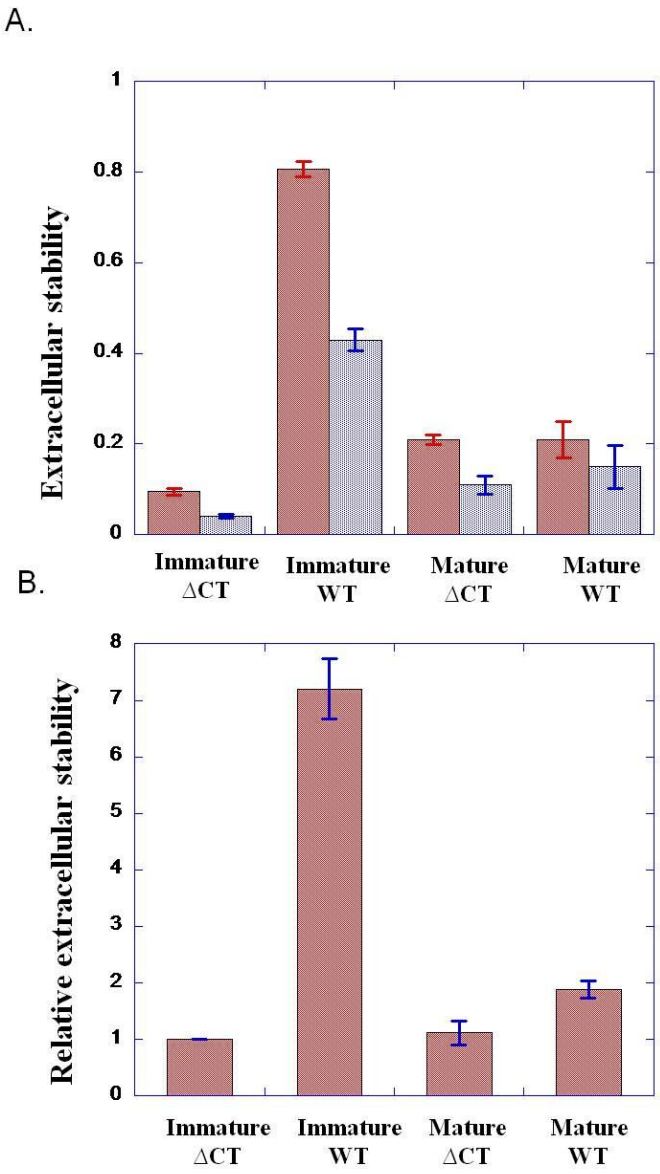

Fig B-1. Extracellular stability of HIV-1 strains.
(A). Extracellular stability of HXB2 strain at 50 ℃ or 37 ℃. Extracellular stability values at y-axis are calculated as relative viral entry activities of viruses after incubation at 50 ℃ for 1 h or at 37 ℃ for 24 h, compared to viral entry activity measured in particles incubated for the same time at 4 ℃.
(B). Extracellular stability of JRFL strain. Relative extracellular stability at y-axis is calculated as relative viral entry activity of viruses after incubation at 50 ℃ for 1 h compared to those incubated at 4 ℃ for 1 h, and then normalized to that of immature ΔCT.
Error bars represent the standard error of the mean (SEM).

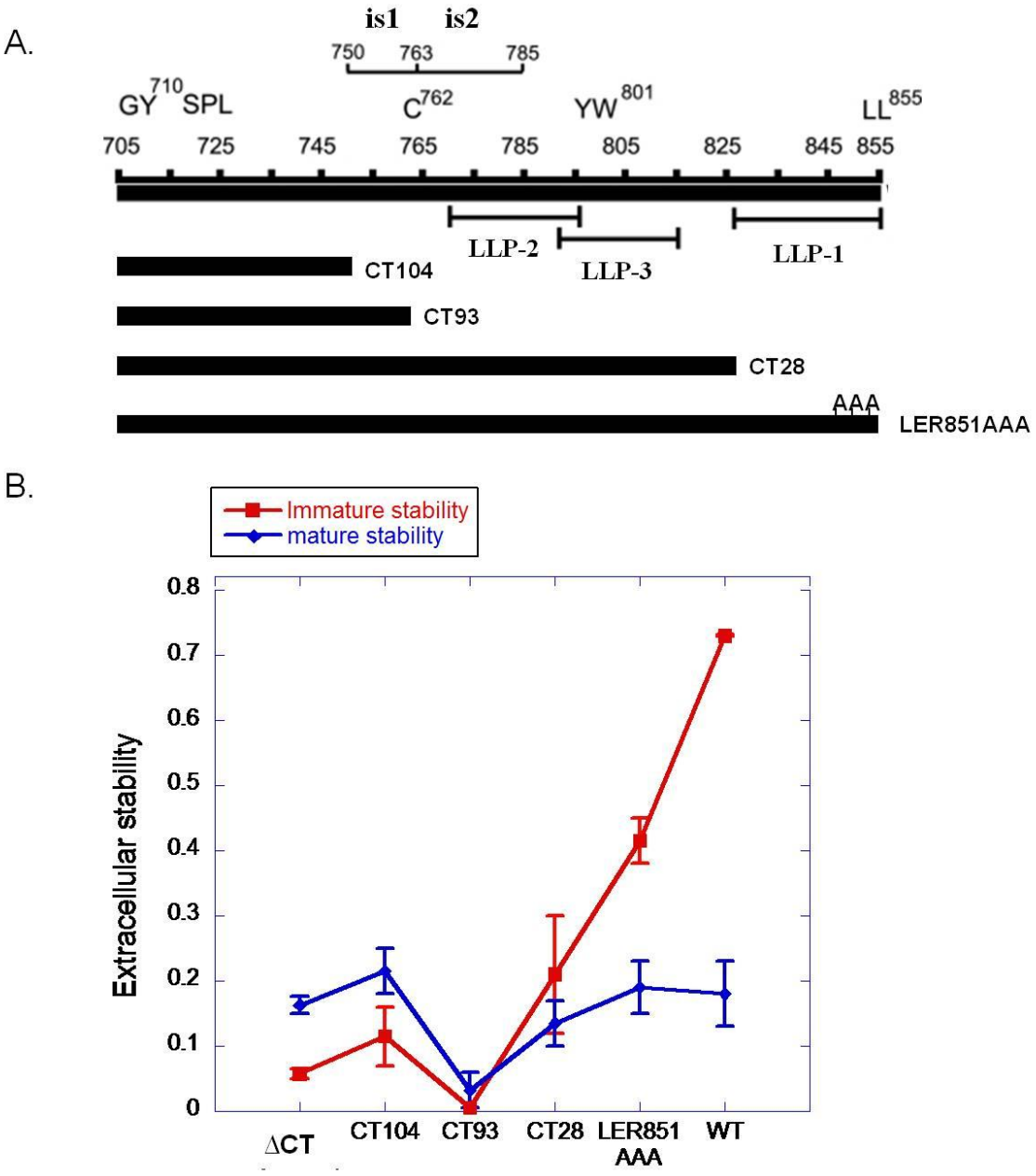

Fig B-2. Important CT regions for extracellular stability.
(A). CT truncation and point mutants. Truncation mutants are named after the number of residues removed from C-terminus of CT. In LER851AAA, three residues ($L_{851}E_{852}R_{853,}$ HXB2 numbering) are replaced by Ala. The figure is reprinted with permission from (*3*).
(B). Extracellular stability of immature HIV-1 bearing these CT mutants. Extracellular stability values at y-axis are calculated as relative viral entry activity of viruses incubated at 50 ℃ for 1 h compared to those at 4 ℃ for 1 h.
Error bars indicate the SEM.

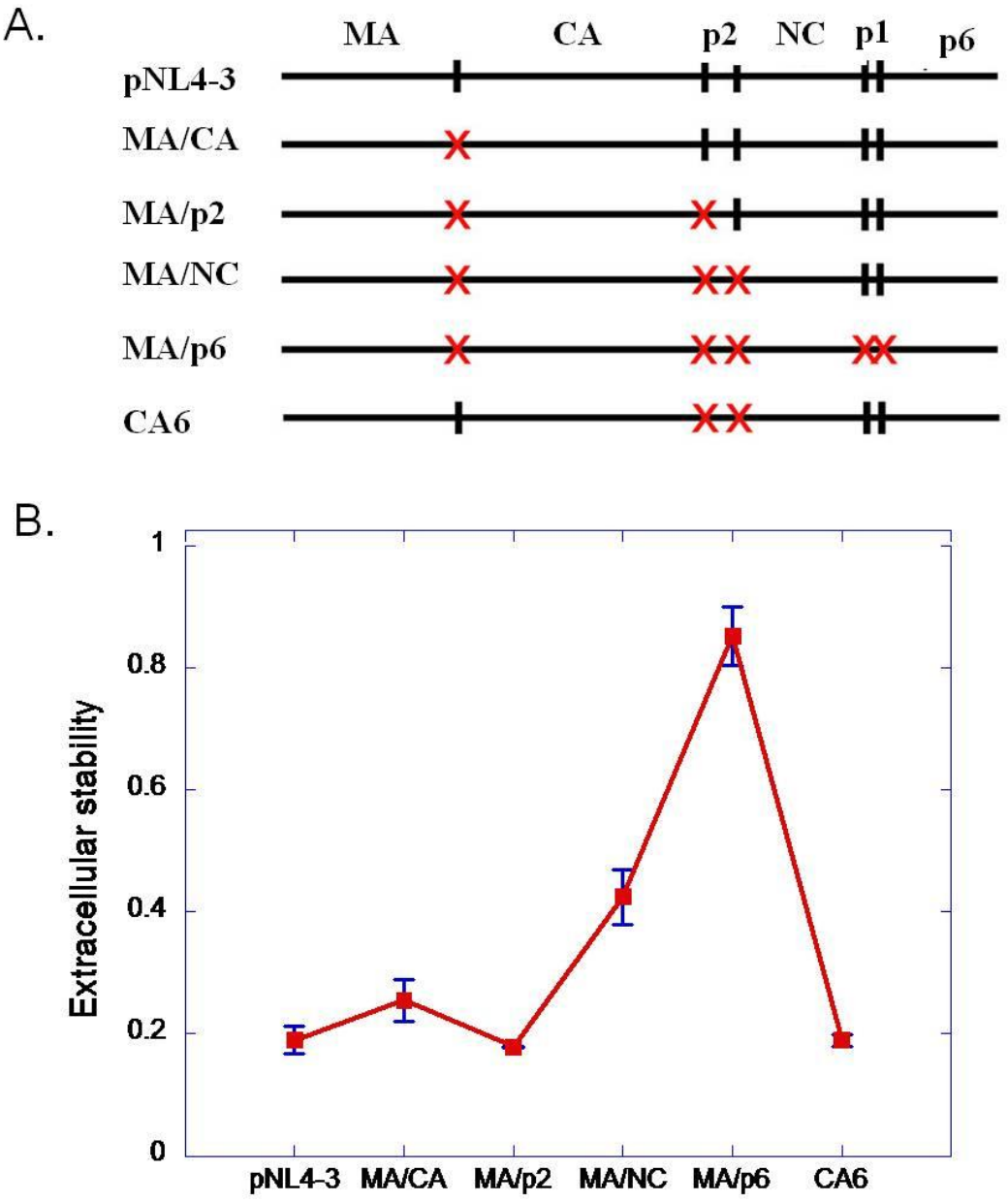

Fig B-3. Gag integrity is important for extracellular stability.
(A). Partial maturation Gag mutants. Red crossing represents that the PR cleavage site at that location has been mutated. The figure is reprinted with permission from (*1*).
(B). Extracellular stability of Gag mutants bearing WT HIV-1 Env. Y-axis values are calculated as relative viral entry activity of viruses incubated at 50 ℃ vs. 4 ℃ (for 1 h).
Error bars indicate the SEM.

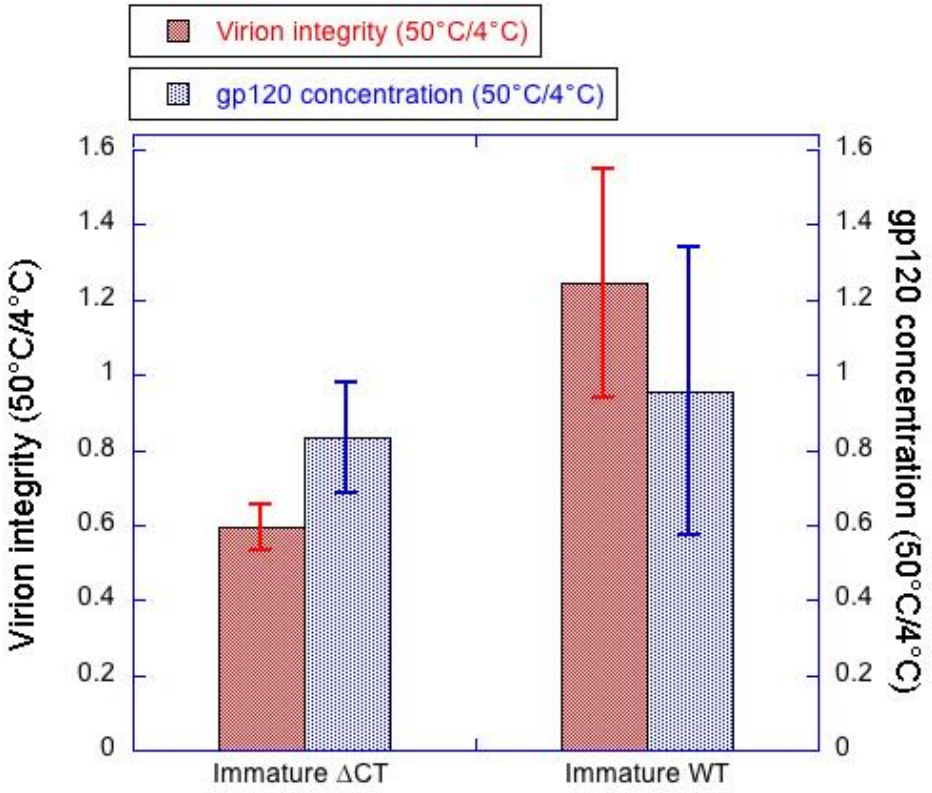

Fig B-4. Loss of stability is not due to disruption of virions or gp120 shedding. Immature ΔCT or WT viruses were incubated at 50°C or 4°C for 1 h, followed by sucrose cushion purification and WB to analyze their Gag and gp120 concentrations. After sucrose purification, only intact viral particles are concentrated (represented by Gag concentration). Therefore, virion integrity at 50 ℃ (y-axis, left) is represented by relative Gag concentration of 50 ℃ treated viruses (purified by sucrose cushion) to those incubated at 4 ℃. Virion integrity of immature ΔCT incubated at 4°C is less than 2 fold higher than that incubated at 50°C, suggesting that the majority of immature ΔCT viruses remain intact after 50 ℃ treatment.

Similarly, if gp120 sheds from viral particles, it will not be concentrated by sucrose cushion together with intact viral particles. The gp120 shedding at 50 ℃ is represented by relative gp120 concentration (y-axis, right) of 50 ℃ treated viruses (purified by sucrose cushion) to those incubated at 4 ℃. The gp120 concentration of intact immature ΔCT incubated at 50°C is similar to that incubated at 4 ℃, suggesting that gp120 does not shed from virions after 50 ℃ treatment.

Error bars indicate the SEM.

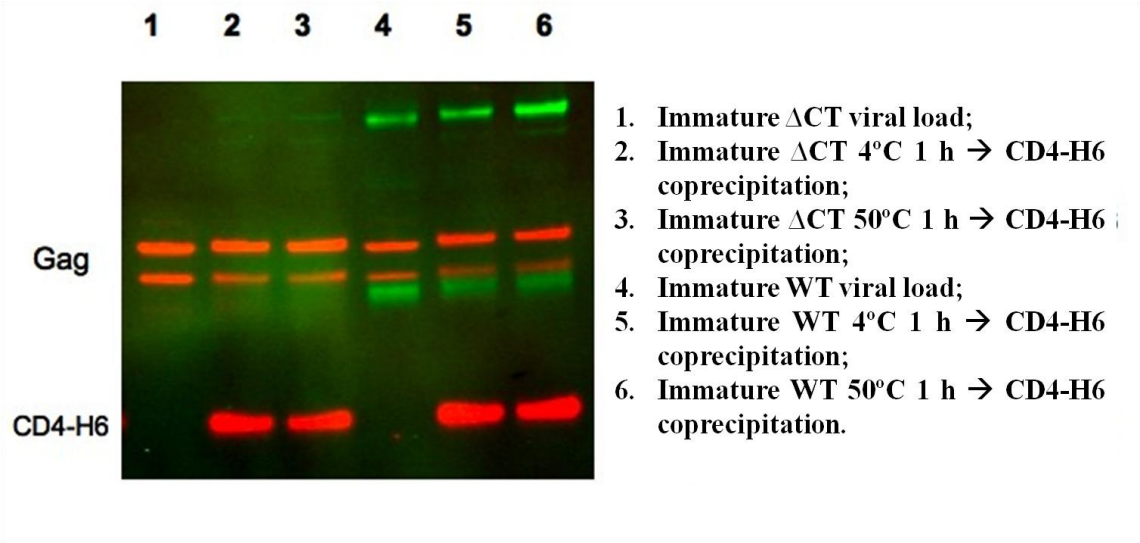

Fig B-5. Disruption of stability is not due to loss of Env's CD4 binding ability. Immature ΔCT or WT viruses were incubated under the condition listed above before going through coprecipitation assay with CD4-H6 (His tagged CD4). WB was developed using anti-CA (red, detect Gag), anti-His (red, detect CD4-H6) and anti-CT (green, detect WT Env) antibodies. The same amount of each virus was added to WB as loading controls (lane 1 and 4). Based on molecular weight, the bottom red bands represent CD4-H6, and the middle red bands represent Gag. Comparison of Gag signal between lane 2 and 3 (or between lane 5 and 6) shows that CD4-H6 can pull down similar amount of ΔCT virions (or WT virions) under either condition, suggesting that ΔCT Env's ability of CD4 binding does not change even after 50℃ incubation. Therefore, loss of extracellular stability for immature ΔCT viruses after 50°C incubation is not due to loss of Env's ability to bind with CD4.

References

1. Wyma, D. J., Jiang, J., Shi, J., Zhou, J., Lineberger, J. E., Miller, M. D., and Aiken, C. (2004) Coupling of human immunodeficiency virus type 1 fusion to virion maturation: a novel role of the gp41 cytoplasmic tail, *J Virol 78*, 3429-3435.

2. Coffin, J. M., S.H. Hughes, and H.E. Varmus. (1997) Retroviruses, *Cold Spring Harbor Laboratory Press, Plainview, NY.*

3. Jiang, J., and Aiken, C. (2007) Maturation-dependent human immunodeficiency virus type 1 particle fusion requires a carboxyl-terminal region of the gp41 cytoplasmic tail, *J Virol 81*, 9999-10008.

4. Chan, D. C., and Kim, P. S. (1998) HIV entry and its inhibition, *Cell 93*, 681-684.

5. Chan, D. C., Fass, D., Berger, J. M., and Kim, P. S. (1997) Core structure of gp41 from the HIV envelope glycoprotein, *Cell 89*, 263-273.

6. Murakami, T. (2008) Roles of the interactions between Env and Gag proteins in the HIV-1 replication cycle, *Microbiol Immunol 52*, 287-295.

7. Edwards, T. G., Wyss, S., Reeves, J. D., Zolla-Pazner, S., Hoxie, J. A., Doms, R. W., and Baribaud, F. (2002) Truncation of the cytoplasmic domain induces exposure of conserved regions in the ectodomain of human immunodeficiency virus type 1 envelope protein, *J Virol 76*, 2683-2691.

8. Wyss, S., Dimitrov, A. S., Baribaud, F., Edwards, T. G., Blumenthal, R., and Hoxie, J. A. (2005) Regulation of human immunodeficiency virus type 1 envelope glycoprotein fusion by a membrane-interactive domain in the gp41 cytoplasmic tail, *J Virol 79*, 12231-12241.

9. Kalia, V., Sarkar, S., Gupta, P., and Montelaro, R. C. (2005) Antibody neutralization escape mediated by point mutations in the intracytoplasmic tail of human immunodeficiency virus type 1 gp41, *J Virol 79*, 2097-2107.

10. Murakami, T., Ablan, S., Freed, E. O., and Tanaka, Y. (2004) Regulation of human immunodeficiency virus type 1 Env-mediated membrane fusion by viral protease activity, *J Virol 78*, 1026-1031.

11. Kol, N., Shi, Y., Tsvitov, M., Barlam, D., Shneck, R. Z., Kay, M. S., and Rousso, I. (2007) A stiffness switch in human immunodeficiency virus, *Biophys J 92*, 1777-1783.

12. Dehart, J. L., Andersen, J. L., Zimmerman, E. S., Ardon, O., An, D. S., Blackett, J., Kim, B., and Planelles, V. (2005) The ataxia telangiectasia-mutated and Rad3-related protein is dispensable for retroviral integration, *J Virol 79*, 1389-1396.

13. Chen, B. K., Saksela, K., Andino, R., and Baltimore, D. (1994) Distinct modes of human immunodeficiency virus type 1 proviral latency revealed by superinfection of nonproductively infected cell lines with recombinant luciferase-encoding viruses, *J Virol 68*, 654-660.

14. Dubay, J. W., Roberts, S. J., Hahn, B. H., and Hunter, E. (1992) Truncation of the human immunodeficiency virus type 1 transmembrane glycoprotein cytoplasmic domain blocks virus infectivity, *J Virol 66*, 6616-6625.

15. Kim, S., Pang, H. B., and Kay, M. S. (2008) Peptide mimic of the HIV envelope gp120-gp41 interface, *J Mol Biol 376*, 786-797.

Supplemental Figure

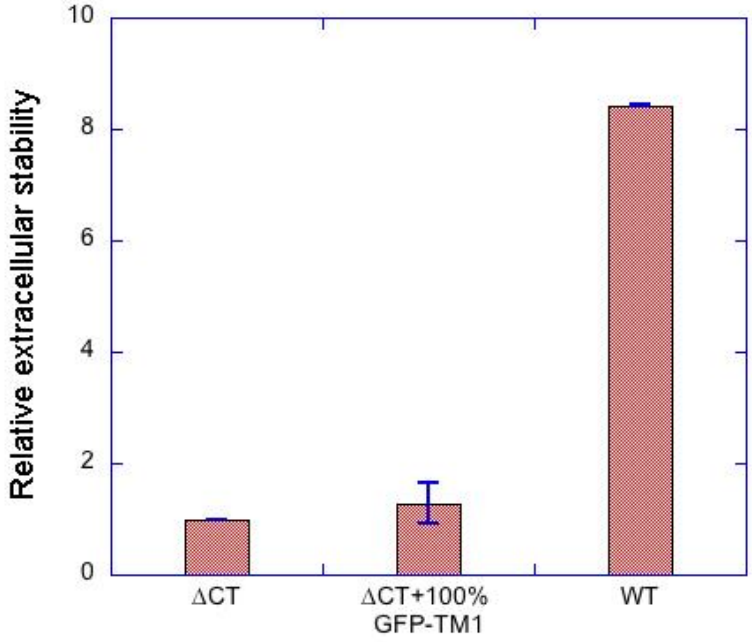

Supplemental Fig B-1. GFP-TM1 does not rescue the extracellular stability of immature ΔCT.
Immature virions bearing both ΔCT and GFP-TM1 were produced as described in Chapter 3. 100% means that the amount of GFP-TM1 plasmid used in transfection is equal to that of ΔCT. Extracellular stability of the above viruses was calculated as relative entry activity of viruses after 50 ℃ 1 h treatment compared to that of 4 ℃ treated. Relative extracellular stability at y-axis was obtained by normalizing the extracellular stability value of each virus to that of immature ΔCT.
Error bars indicate the SEM.